PEOPLE'S DEMOCRATIC REPUBLIC OF ALGERIA

MINESTRY OF HIGHER EDUCATION AND SCIENTIFIC RESEARCH

MOHAMED BOUDIAF UNIVERSITY- M'SILA

FACULTY OF SCIENCES **DOMAIN: Material sciences.**

PHYSICS DEPARTMENT **FIELD: Physics.**

***N°: PH/* MAT/11/2023** **OPTION: Physics of materials.**

Thesis presented for the award of

The Academic Master's Degree

By: MERROUCHE Abir

Title:

Electronic Structure Of 2D Materials

Supported on the: June,24 th,2023 in front of the jury composed of:

BAAZIZ Hakim	M'sila University	Chair
CHARIFI Zoulikha	M'sila University	Supervisor
GHELLAB Torkia	M'sila University	Examiner

Academic year: 2022/2023

In the name of Allah, the most gracious, the most merciful.

« Read: In the name of your Lord, who created »

The Holy Quran

“Clot (96:1)”

First and foremost, praise and gratitude to Allah.

Allah, who is characterized by omnipotence, benevolence, and sovereignty over all creation, has bestowed upon me numerous blessings throughout my existence.

I express my gratitude to Allah being for endowing me with the virtues of fortitude and perseverance throughout my existence, and particularly for enabling me to successfully complete this task.

Expressing gratitude towards Allah who provided unwavering support throughout a challenging period, during which even those closest to oneself were unable to offer assistance.

Acknowledgements

First of all, I would like to thank and describe my gratitude to my supervisor **Professor. CHARIFI Zoulikha** for guiding me through this work.

I would like to extend my sincere thanks to **the jury**:

Professor. BAAZIZ Hakim and **Doctor GHELLAB Torkia** for accepting the assessment of this work.

I would be remiss in not mentioning **Dr. MERROUCHE Djemai** for the efforts he had made to help me to complete my research, for his moral support which inspired me.

And special thanks go to **Dr. OSMANI Nadjet** for her helps and efforts she made for me.

Lastly, I would like to mention my family, especially my mother and my two sisters for their belief in me, has kept my spirits and motivation high during this process. I would also like to thank all those who have contributed in any way to the success of this work.

Dedication

I dedicate this modest work to:

My beloved parents,

My two sisters,

My maternal aunt Darine,

And the whole family.

I dedicate it also to my friends and my classmates.

Finally, I dedicate this thesis to the unknown who will search for the subject of my thesis,

I offer you my search and greetings,

I give you my tiredness, my knowledge and my work,

I offer you the fruit of my effort, hoping that it may be a seed for your scientific project.

Summary

CHAPTER III: RESULTS AND DISCUSSIONS

A. Part One: Studying the properties of h-BN

B. Part Two: Comparative study between Boron-Nitride and Gallium-Nitride

Tables List

List of Figures

List of Abbreviation

Abbreviation	Definition
NMs	Nanomaterials
3D	Three-Dimensions
2D	Two-Dimensions
h-BN	Hexagonal Boron-Nitride
GaN	Gallium-Nitride
CNTs	Carbon Nanotubes
SWNTs	Single-Walled Nanotubes
MWNTs	Multi-Walled Nanotubes
BO	Born-Oppenheimer
HF	Hartree-Fock
DFT	Density Functional Theory
GGA	Generalized Gradient Approximations
LDA	Local Density Approximations
LCAO	Linear Combination of Atomic Orbitals
OPW	Orthogonal Plane Wave
APW	Augmented Plane Wave
LAPW	Linearized Augmented Plane Wave

LMTO	Linearized Muffin-Tin Orbitals
SD	Slater determinant
FP-LAPW	Full Potential Linearized Augmented Plane Wave

General Introduction

Introduction

Welcome to the enthralling domain of solid-state physics, a field that investigates the properties, behaviour, and interactions of solid materials. In this domain, the fundamental building blocks of matter self-organize into intricate structures, giving birth to a plethora of fascinating phenomena and paving the way for technological advances that shape our contemporary world.

Solid state physics, also known as condensed matter physics, is one of the most dynamic and versatile branches of contemporary physics **[1]**. It has developed in response to the technological advancements that have profoundly altered our lives over the past 50 years **[2,3]**. This branch focuses on the study of the properties of solids at the atomic level and above, i.e., the comprehension of how the macroscopic properties of solids result from their microscopic, atomic-scale properties. Nanomaterials is a fascinating subfield of solid-state physics that investigates materials with dimensions on the nanoscale, typically between one and a few hundred nanometers. Due to their diminutive size, increased surface-to-volume ratio, and quantum confinement effects, nanomaterials display properties and behaviours that can differ substantially from their bulk counterparts.

The discipline of nanomaterials has brought about a significant transformation in various fields, including but not limited to electronics, energy, medicine, and environmental science. Quantum dots, which are semiconductor particles at the nanoscale, possess distinctive electronic characteristics that facilitate the development of solar cells with high efficiency, vivid displays, and accurate biomedical imaging. Carbon nanotubes are cylindrical structures composed of carbon atoms that possess remarkable strength and electrical conductivity. As a result, they have significant potential for utilisation in various fields such as electronics, energy storage, and materials reinforcement.

The domains of nanomaterials and 2D materials have surfaced as significant frontiers of exploration and innovation in the constantly evolving landscape of scientific and technological advancements. The exceptional characteristics of nanomaterials at the nanoscale and the remarkable two-dimensional structure of 2D materials have attracted the attention of researchers from various fields. Both domains possess significant potential for transforming diverse industries, including but not

limited to electronics, energy storage, biomedical applications, and environmental sustainability.

Nanomaterials are defined as materials that possess at least one dimension within the nanometer range, which typically spans from 1 to 100 nanometers. The unique characteristics of these materials can be attributed to quantum confinement and surface effects, which distinguish them from their bulk counterparts. Due to their size-dependent behaviour, nanoparticles exhibit exceptional mechanical, electrical, thermal, and optical properties, which render them highly desirable for advanced technological applications. Nanomaterials are a diverse group of materials that comprise nanoparticles, nanowires, nanotubes, and nanocomposites, which are characterised by distinct benefits and potential uses.

On the other hand, 2D materials are a fascinating class of materials that consist of single or few-atom-thick layers. Graphene, which consists of a single layer of carbon atoms arrayed in a honeycomb lattice, is the most prominent example. However, the family of 2D materials also includes transition metal dichalcogenides (TMDs), black phosphorus, and hexagonal boron nitride (h-BN), in addition to graphene. The extraordinary electrical, mechanical, and thermal properties of these materials make them extremely promising for next-generation electronics, optoelectronics, and flexible devices. The atomically thin nature of 2D materials enables unprecedented control over their properties and paves the way for thrilling fundamental scientific investigations.

Nanomaterials and 2D materials, despite their unique attributes, frequently intersect and exhibit complementary properties, resulting in synergistic outcomes and improved efficacy across diverse domains. The amalgamation of nanomaterials with 2D materials or the converse has significant potential for attaining customised functionalities, heightened stability, and improved properties. The convergence of the nanoscale and two-dimensional realms possesses the capability to bring about a significant transformation in domains such as catalysis, sensing, energy conversion, and storage. Additionally, it could facilitate the development of innovative biomedical apparatus and environmental remediation approaches. This has been suggested by recent research.**[4]**.

This preliminary investigation examines the intriguing correlation between nanomaterials and 2D materials, scrutinising their distinctive characteristics, methods

of production, and the potential they hold for advanced technologies. The objective of this study is to explore the potential synergies between nanomaterials and 2D materials, with the aim of identifying novel opportunities that have yet to be fully realised. This convergence has the potential to lead to the development of advanced materials and transformative applications, thereby shaping a future that is enriched with new possibilities.**[5]**.

Hexagonal boron nitride (h-BN) is a two-dimensional layered material that bears a resemblance to graphene and is commonly denoted as "white graphene," as previously stated. The substance in question is classified under the hexagonal crystal system and exhibits a white coloration in either block or powder form. Its layered structure bears resemblance to the graphene lattice constant and shares comparable characteristics. This information has been documented in reference [6]. The fundamental building block of hexagonal boron nitride (h-BN) is a hexagonal lattice comprised of boron and nitrogen atoms arranged in an alternating pattern. Hexagonal boron nitride (H-BN) exhibits distinctive characteristics, including exceptional thermal conductivity, remarkable mechanical robustness, exceptional chemical inertness, and outstanding electrical insulation, rendering it a highly desirable substance for a wide range of applications. The h-BN material exhibits a significantly higher surface optical phonon energy compared to SiO2, by a factor of two orders of magnitude. This characteristic renders it a highly suitable option for serving as a gate insulating layer in graphene-based applications. Hexagonal boron nitride (H-BN) has been employed as a dielectric layer or substrate in the context of two-dimensional electronic devices. In contradistinction to graphene, hexagonal boron nitride (h-BN) is characterised as a wide-bandgap insulator, exhibiting a bandgap of approximately 5-6 eV.

The field of materials science and engineering has witnessed a rapid development in the area of nanoscale materials, which has garnered significant interest. Nanomaterials possess distinct characteristics and tendencies that deviate considerably from their larger-scale equivalents, rendering them exceedingly coveted for a diverse array of purposes. Hexagonal boron nitride (h-BN) has garnered significant interest owing to its exceptional properties and versatility, among the various nano materials available. The two-dimensional material h-BN is comprised of a hexagonal arrangement of boron and nitrogen atoms, which combine to form a honeycomb lattice structure. The material in question exhibits certain structural resemblances to other prominent two-dimensional

substances, including graphene and transition metal dichalcogenides (TMDs). Nevertheless, hexagonal boron nitride (h-BN) exhibits unique properties that distinguish it from other materials, rendering it a fascinating substance for diverse applications. The outstanding dielectric properties of h-BN serve as a notable characteristic that sets it apart from other two-dimensional materials. Hexagonal boron nitride (h-BN) demonstrates a broad bandgap, rendering it a highly proficient insulator. The aforementioned characteristic endows the material with the ability to function as a dielectric in electronic apparatus, thereby conferring electrical insulation and impeding current leakage. Moreover, the exceptional thermal conductivity and chemical stability of h-BN render it a suitable option for applications that necessitate effective heat dissipation and endurance against severe surroundings.

Moreover, the distinctive structural characteristics of h-BN are responsible for its outstanding efficiency. The material exhibits notable mechanical robustness and pliability, enabling it to endure various forms of mechanical stress such as bending, stretching, and deformation. The mechanical durability of the material is especially beneficial in the context of flexible electronics and nanomechanical devices, as these applications require materials to withstand diverse mechanical strains. The amalgamation of h-BN's dielectric characteristics, thermal conductivity, chemical stability, and mechanical robustness renders it a highly promising contender for a diverse array of applications. This material has been utilised in various domains, including but not limited to nanoelectronics, optoelectronics, photonics, thermal management, sensing, and lubrication. Furthermore, the compatibility of h-BN with other two-dimensional materials and its potential to create heterostructures present promising opportunities for designing novel materials with customised properties and functionalities.

To conclude, the distinctive characteristics of hexagonal boron nitride (h-BN) render it an exceptional nanomaterial with vast potential for diverse applications. The material's broad bandgap, dielectric characteristics, robust mechanical properties, and chemical stability render it a highly adaptable substance within the field of nanotechnology. The potential for technological advancements and innovation across various disciplines is held by the exploration and utilisation of h-BN, in combination with other nano materials. In the thesis we are representing consists of three chapters, organized as follows:

In the first chapter, which contains information about nanomaterials and their applications, we have highlighted and provided details about the compound we studied. Modern methods for calculating electronic structures are based on density functional theory (DFT), which is reviewed in the second chapter. Then, we described the Kohn-Sham equations, which provide a new form of the Schrodinger equation, and discussed the various approximations associated with this theory, such as the LDA local density approximation and the generalised gradient approximation (GGA). In the second section of chapter II, we reviewed the linearized augmented plane wave (FP-LAPW) principle and concluded by discussing the Wien2k code representation.

Chapter three of this study is bifurcated into two sections. The first part is dedicated to the exposition and analysis of the outcomes achieved for the structural and electronic characteristics of h-BN compounds in both two-dimensional (2D) and three-dimensional (3D) forms. The subsequent section involved a comparative analysis of Boron nitride and Gallium nitride. The chapter presents a comprehensive examination of the characteristics of said compounds, which were acquired through first-principles computations.

The work concludes with a summary of the most significant findings from the entire investigation.

References

[1] G.W. Luckey, Introduction to Solid State Physics, J. Am. Chem. Soc. 79 (1957) 3299. https://doi.org/10.1021/ja01569a094.

[2] S. Citation, Condensed-Matter and Materials Physics, 1999. https://doi.org/10.17226/6407.

[3] G. Gehring, Solid-state theory, Nature. 277 (1979) 673–674. https://doi.org/10.1038/277673b0.

[4] Y. Chen, Z. Fan, Z. Zhang, W. Niu, C. Li, N. Yang, B. Chen, H. Zhang, Two-Dimensional Metal Nanomaterials: Synthesis, Properties, and Applications, Chem. Rev. 118 (2018) 6409–6455. https://doi.org/10.1021/acs.chemrev.7b00727.

[5] N. Baig, Two-dimensional nanomaterials: A critical review of recent progress, properties, applications, and future directions, Compos. Part A Appl. Sci. Manuf. 165 (2023) 107362. https://doi.org/https://doi.org/10.1016/j.compositesa.2022.107362.

[6] J. Wang, F. Ma, M. Sun, Graphene, hexagonal boron nitride, and their heterostructures: properties and applications, RSC Adv. 7 (2017) 16801–16822. https://doi.org/10.1039/c7ra00260b.

CHAPTER I

Nanomaterials and its Applications

I.1. Introduction

Nanomaterial science have been developed during the last years to become an important research field in solid state physics, chemistry, and engineering due to multiple reasons. One reason is an industrial need for the fabrication of new materials in a very finer scale to optimize the cost and to increase the speed of information transmission and storage. Another reason is that nanomaterial presents novel and enhanced properties compared to traditional materials, which gives opportunities for new technological applications. This is observed on possibilities for tailoring the optical, magnetic, electronic, mechanical, and chemical properties of materials. Nanoscale substances demonstrate innovative material properties, essentially due to the self-assembly of the building blocks into functional structures that may be useful for electronic, photonic, medical, or bioanalytical problems.

The objective of studying nanomaterials and 2D materials is to explore their unique properties and potential applications in various fields, such as water management, energy production/storage, tissue engineering, sensing, catalytic applications, and drug delivery. 2D materials are the thinnest materials and possess the highest surface area of all known materials, making them highly suitable for many applications. They exhibit extraordinary mechanical, chemical, electronic, optical, and magnetic properties that can be tuned for specific applications. The study of 2D nanomaterials aims to understand their fundamental properties and how they can be used to develop high-quality devices and materials for various applications **[64–68]**. In the next sections, we will give a brief description of nanomaterial substances with more focus on their classification and properties that can be offered by uses and applications.

I.2. Definitions

The prefix "nano" comes from the Greek word "nanos," which means "dwarf," and the Latin word "nanus," which also means "dwarf." The term "nano" is used as a prefix to indicate a scale of measurement that is one billionth 10^{-9} of a unit **[3]**.

Nanomaterials are materials that have at least one external dimension measuring between 1 and 100 nanometers (nm), or materials that have internal structure or surface structure features that measure between (1 and 100 nm) **[4],** which is about 1,000 times smaller than the width of a human hair as shown in the Figure**(I.1)**. Within these dimensions and scale level, the properties of materials can differ significantly from their bulk counterparts, leading to unique physical, chemical, and biological properties **[5]**.

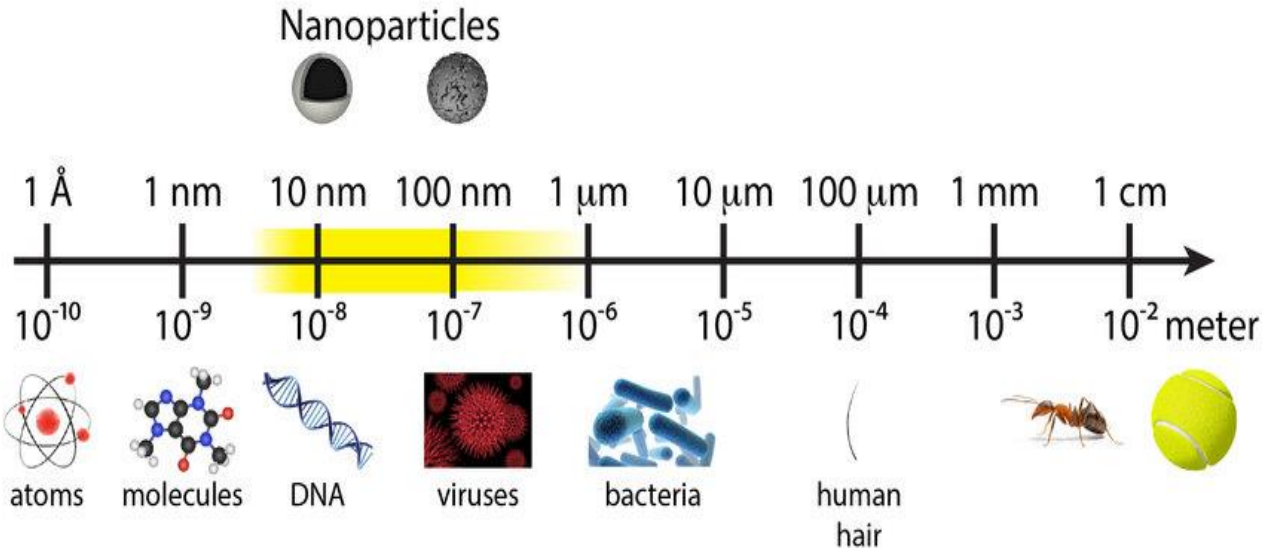

Figure (I.1): Nanomaterials size range. Reprinted from the reference **[6]**.

I.3. Types and classification of nanomaterials

Nanomaterials can be classified based on their four material-based categories, or by their dimension levels **[7]**, as illustrated in Figure **(I.2)**.

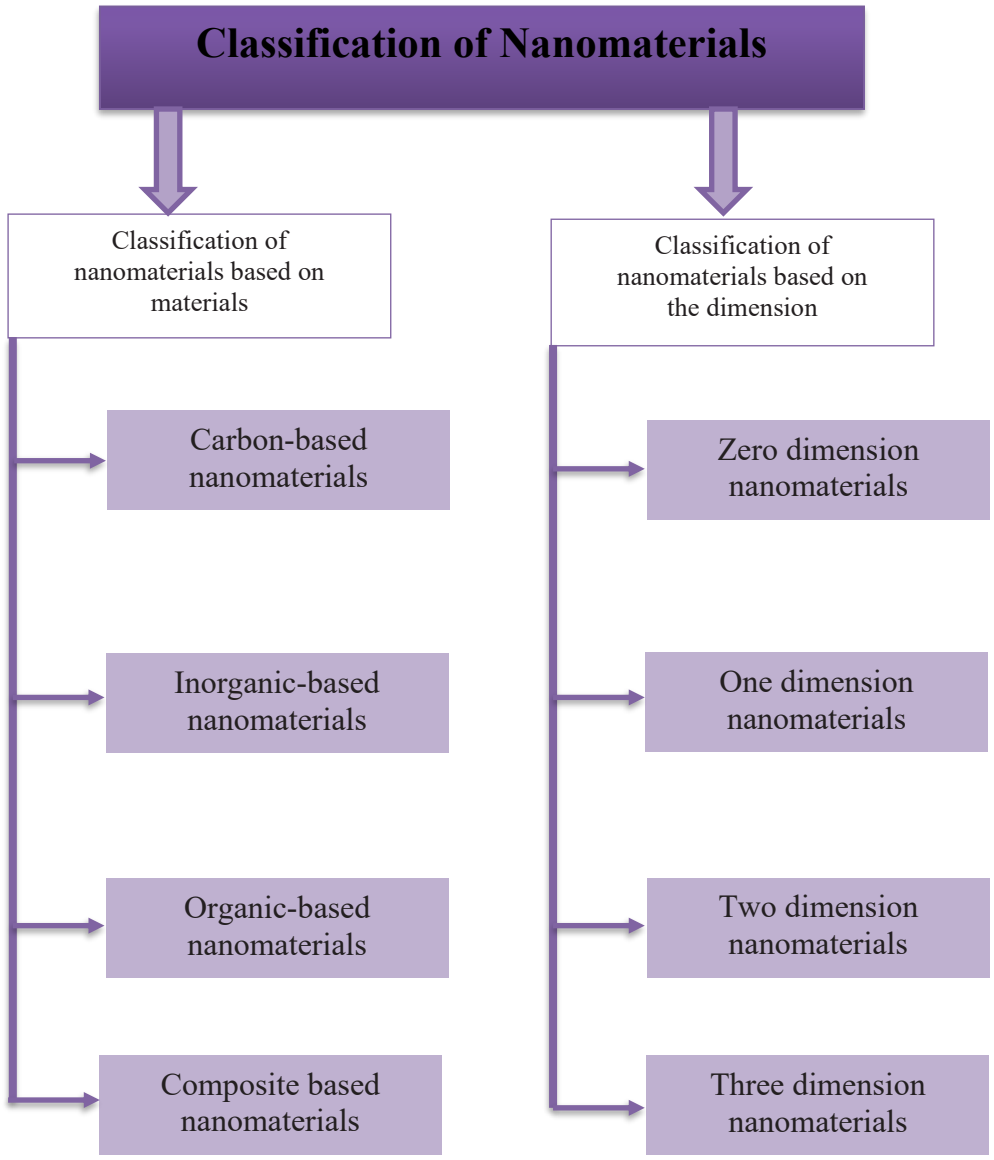

Figure (I.2): Schematic diagram showed the basic classification of nanomaterials.

I.3.1- Classification of nanomaterials based by their materials

Nanomaterials can be classified based on their materials into different categories. The most common classification includes: Carbon-based nanomaterials, Inorganic-based materials, Organic-based materials and Composite-based nanomaterials **[4]**.

I.3.1-1-Carbon-based Nanomaterials

Carbon-based nanomaterials such as **fullerenes (C_{60}), carbon nanotubes (CNTs), carbon nanofibers, carbon black, and graphene (Gr)** are found in various morphologies, such as hollow tubes, ellipsoids, or spheres **[8].** They are manufactured using Laser ablation, arc discharge, and chemical vapor deposition techniques. Carbon nanomaterials possess unique physical and chemical properties compared to bulk materials, and they have various applications in different fields **[9]**.

a. Fullerenes

Fullerenes are a class of hollow molecules composed only of carbon atoms that form a closed cage-like structure or a cylinder. The closed cage-like structure is known as buckminsterfullerene or buckyball **(** C_{60} **)** Figure **(I.3)**, which is composed of 12 pentagonal and 20 hexagonal carbon atoms **[10]**. Fullerenes can have various shapes and sizes, and they are stable but not totally unreactive. Fullerenes are an unusual reactant in many organic reactions, and they have been found to have various applications in different fields **[11]**.

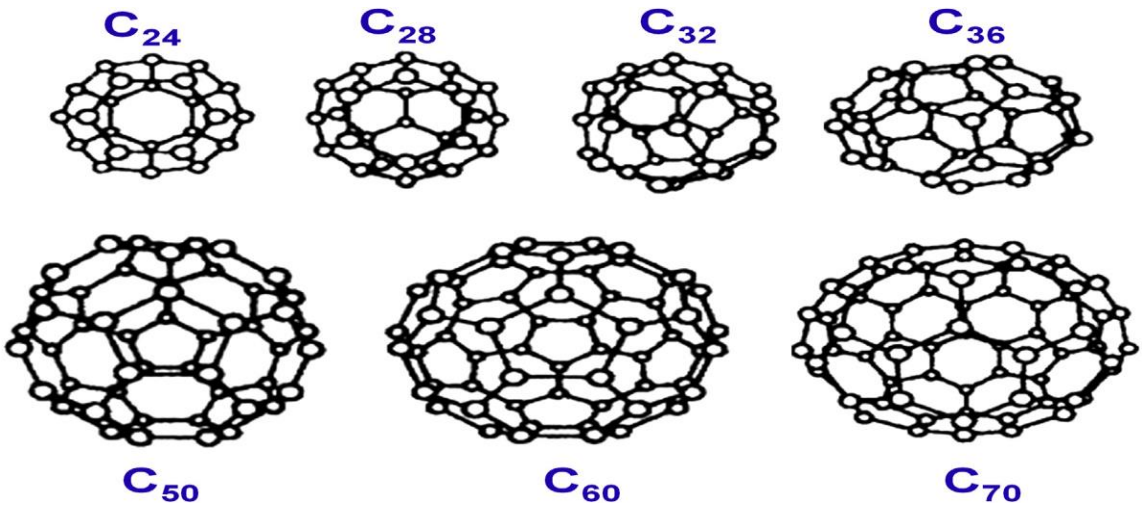

Figure (I.3): Types of Fullerenes. Reprinted from the reference **[11].**

b. Carbon nanotubes (CNTs)

These are nano foils made up of carbon-containing graphene. In this morphology, the carbon atoms are arranged in honeycomb lattice and form hollow cylinders of 0.7 nm diameter for a single-layered CNT and about 100 nm for a multi-layered CNT. The length of CNT varies from a few μm to a few mm **[12]**. There are two types of CNT which are:

1. Single-walled nanotubes (SWNTs) in which we can observe three possibles classes, named: Zigzag, Chiral, and Armchair **[13]**, and
2. Multi-walled carbon nanotubes (MWNTs).

To describe these nanotubes, the chiral vector (Ch) defines the unit cell, which is defined as the circumference of the surface of the tube. The chiral vector is given by **[14]**:

$$\vec{C}_h = n\vec{a}_1 + m\vec{a}_2 \qquad \textbf{(I.1)}$$

Where:

a_1 and a_2 : are unit vectors in the two-dimensional hexagonal lattice.

n and m : are integers.

The chiral index or chirality is determined by the pair of integers (n, m). The chiral angle (θ) can be obtained from the relation **[14]**:

$$\tan\theta = \frac{\sqrt{3}m}{2n+m} \qquad \textbf{(I.2)}$$

Therefore, the three types of CNTs can be determined by the chiral angle and chirality indices, which their values are **[14]**:

- Zigzag if (m =0 or n=0, θ = 30°).
- Armchair if (n =m, θ = 0°).
- Chiral if (0 < |m| < n, 0 < θ < 30◦).

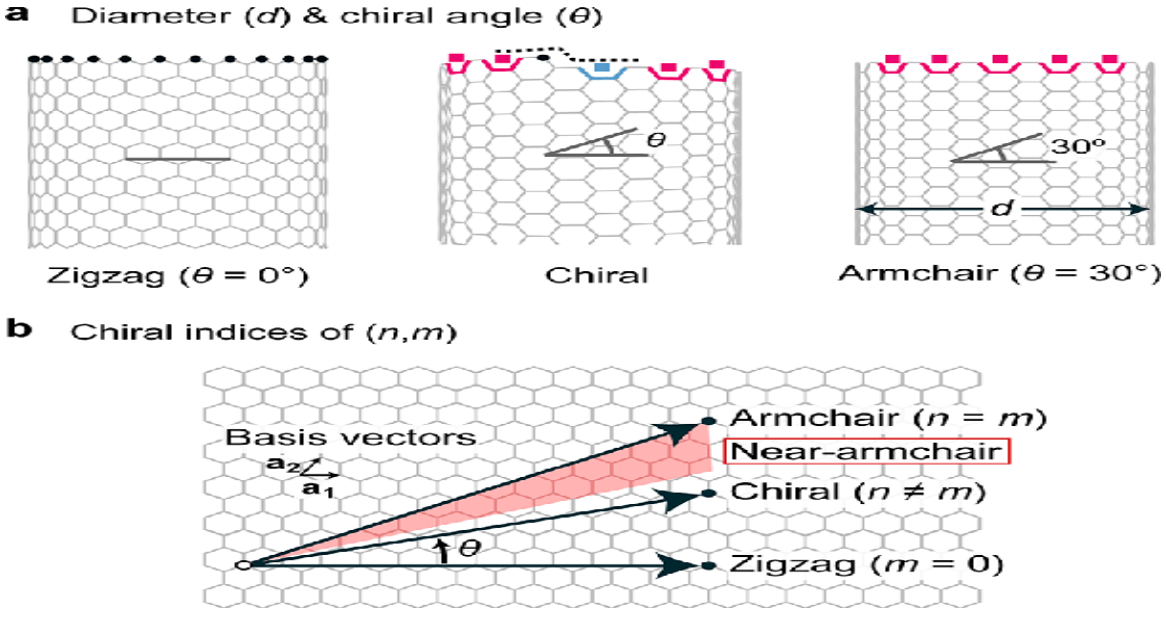

Figure (I.4): Structural classification of single-walled carbon nanotubes **[15]**.

c. Carbon nanofibers

The graphene nanofoils used in the production of carbon nanofibers have a different structure than CNTs, even though they are made of the same graphene. The graphene molecules are arranged in a cone or cup form instead of the regular cylindrical tubes of CNTs **[16,17]**.

d. Carbon black

Carbon black is an amorphous nanomaterial made up of carbon atoms that are arranged in a spherical shape with diameters ranging from 20 to 70 nm. The particle-particle interaction of carbon black is so high that they bind with each other and form aggregates around 500 nm **[12]**.

e. Graphene

Graphene is a two-dimensional (2D) material composed of a single layer of carbon atoms arranged in hexagons resembling a honeycomb structure **[18]**. It has unique properties such as high electron mobility, high thermal and electrical conductivity, and high mechanical strength. Graphene has various applications in different fields such as electrochemiluminescence (ECL) sensor, transistors, water filtration, energy storage, biosensors, solar cells, and photonic devices **[19,20]**.

Graphene can be wrapped up into zero-dimensional (0D) fullerenes, rolled into one-dimensional (1D) nanotubes, or stacked into three-dimensional (3D) graphite **[21,22]**, as depicted in Figure **(I.5)**:

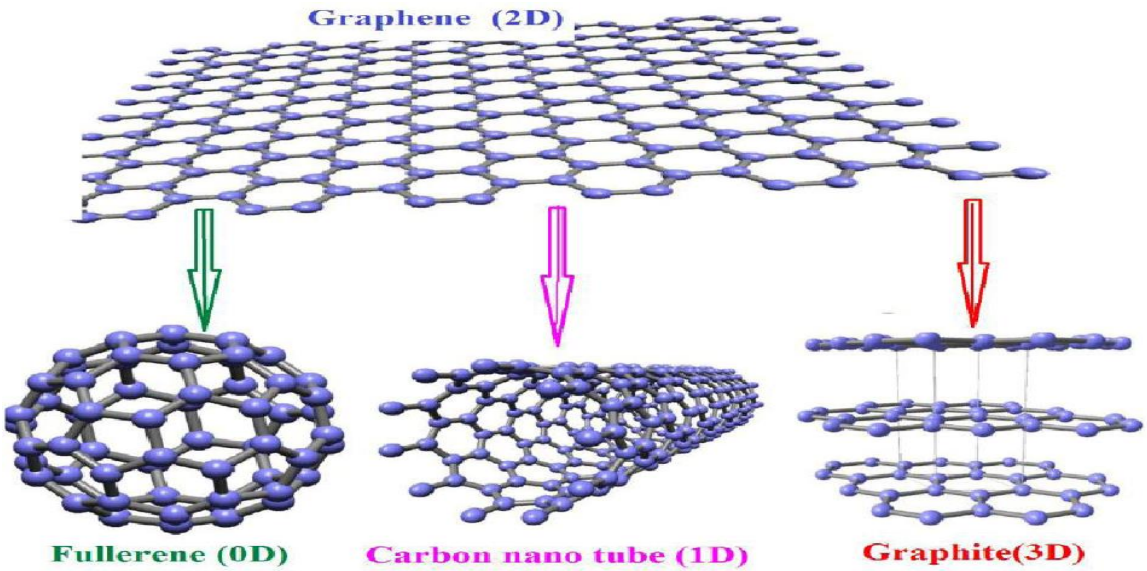

Figure (I.5): Graphene similar structures **[23]**.

I.3.1-2-Inorganic-based Nanomaterials

Metals such as Ag, Au and Fe and metal oxides as TiO2, ZnO, and MnO2, can be synthesized into nanomaterials. In addition, semiconductor nanomaterials can be synthesized from silicon and ceramic materials **[24,25]**.

I.3.1-3-Organic-based Nanomaterials

Organic-based nanomaterials are composed of organic matter other than carbon and inorganic material. These nanomaterials are synthesized through self-assembly or transformation from organic matter into the desired structure, and noncovalent weak interaction applies in these types of materials **[26,27]**.

I.3.1-4-Composite-based Nanomaterials

Composite nanomaterials consist of one or more layers of nanoparticles combined with other nanoparticles, bulk materials, or more complex materials like metal frameworks. These composites may be made up of many types of materials such as metal, ceramic, organic, inorganic, carbon-based, or bulk polymers. The morphologies of these materials depend on the synthesis and required properties for the desired applications **[28,29]**.

I.3.2- Classification of nanomaterials based by their dimensions

Siegel classified nanomaterials into four types: zero-dimensional, one-dimensional, two-dimensional, and three-dimensional nanostructures. The classification of nanomaterials is based on the number of dimensions not confined to the nanoscale range **[30].**

I.3.2-1- Zero-Dimensional materials

Zero-dimensional nanoparticles are nanomaterials with all dimensions in the range of the nanoscale, i.e., no dimensions are larger than 100 nm. These nanoparticles are point-like particles, as small as a point, and are the most common type of nanomaterials. Examples of zero-dimensional nanoparticles include: quantum dots, hollow spheres, and nano lenses. The classification of nanomaterials based on their dimensionality divides nanomaterials into nanoparticles, nanotubes, and nanofilms **[31]**.

I.3.2-2- One-Dimensional materials

One-dimensional nanoparticles are a type of nanomaterials with at least one dimension larger than the nanoscale, while the other dimensions are within the nanoscale. The most common examples of one-dimensional nanoparticles are nanofibers, nanotubes, and

nanorods. Nanotubes, nanorods, and nanowires are examples of one-dimensional structured materials that are in the nanoscale in two dimensions **[32,33]**.

I.3.2-3- Two-Dimension materials

Two-dimensional nanomaterials possess two dimensions larger than the nanoscale (100 nm), while the other dimension is within the nanoscale. The most common examples of this class are nanofilms, nanolayers, and nanocoating. These nanomaterials have plate-like structures such as: (Graphene and Boron Nitride). Nanosheets or nanolayers are included as nano-objects, which are nanoscale only in one dimension **[34]**.

I.3.2-4- Three-Dimensional materials

Three-dimensional nanomaterials are a type of nanomaterials with all three dimensions larger than 100 nm, but their components are below 100 nm in size. Nano range particles come together to form three-dimensional nanomaterials. These materials are generally nonporous in nature and have many applications. The most common examples of three-dimensional nanomaterials are nanocomposites, bundles of nanofibers, and multi nanolayer-type structures **[35]**.

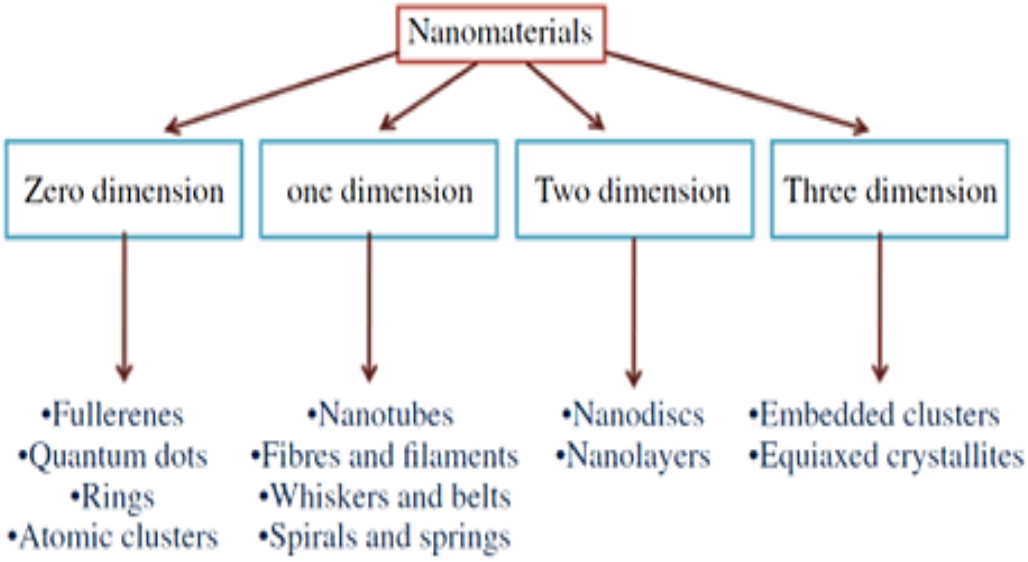

Figure (I.6.a): Classification of nanomaterials on the basis of dimensions **[12]**.

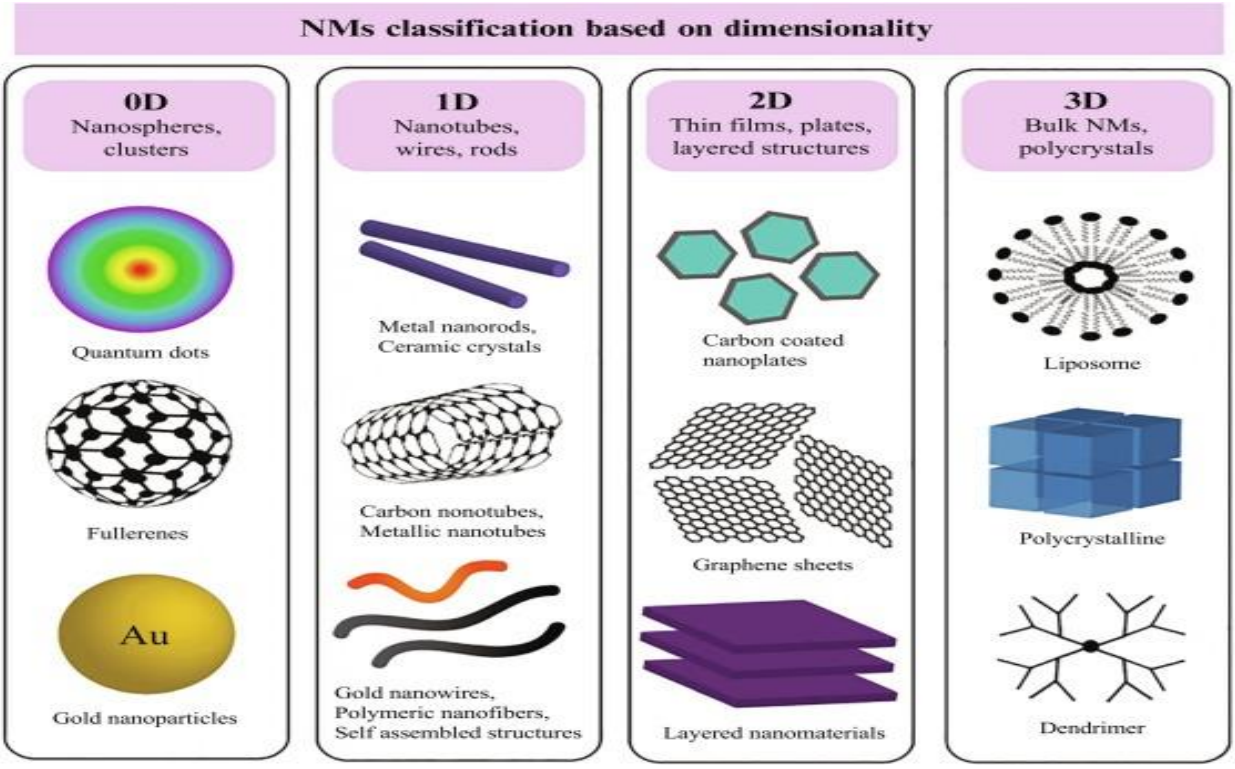

Figure (I.6.b): Nanomaterials classification based on dimensions **[7]**.

I.4.Nanomaterial's Properties

Nanomaterials have more surface area and some specific properties compared with bulk materials due to their small size. The properties of nanomaterials are described in terms of physical and chemical properties **[36]**.

I.4.1-Physical Properties

Some of the physical properties of nanomaterials include optical, mechanical, hydrophilicity, hydrophobicity, suspension, settling, thermal, magnetic, and electrical properties **[37]**. A brief explanation of these properties is given in the next points.

I.4.1-1-Optical Properties

Nanomaterials exhibit unique and interesting optical properties **[38]**. Some of the optical properties of nanomaterials include: color, transparency, absorption, transmission, reflection, and light emission **[39]**.

I.4.1-2-Magnetic and Electrical Properties

The magnetic and electrical properties of nanomaterials are important for various applications in electronics, energy, and many other fields. The electrical properties of nanomaterials include conductivity, resistivity, and dielectric permittivity, which depend significantly on the nanoparticle size and morphology. The electrical conductivity of

nanomaterials may rise in relation to their aspect ratio and ordering. The magnetic properties of nanomaterials include coercivity, magnetization, and magnetic susceptibility, which are affected by the nanoparticle size, shape, and composition. **[40,41]**.

I.4.1-3-Mechanical Properties

Some of the mechanical properties of nanoparticles include elasticity, tensile strength, hardness, and flexibility. These mechanical properties play a key role in the nanomaterials applied in different fields **[12]**. The mechanical strength and modulus of nanomaterials depend strongly on their structure, size, and composition **[42,43]**.

I.4.1-4-Other Properties

Nanomaterials possess some important properties such as hydrophilicity, hydrophobicity, suspension, diffusion, and thermal conductivity. These effects of nanomaterial on properties and possible opportunities relating to the broad area of nanomaterials have created a multitude of innovative applications in the fields of medicine and other areas **[37]**.

I.4-2. Chemical properties

Chemical properties such as : stability and sensitivity, corrosive and anti-corrosive, oxidation, reduction, antifungal, toxicity, antibacterial, and disinfection, are important factors in nanoparticles, mainly in applications related to chemical and biomedical engineering **[12]**. The large numbers of atoms on the surface of nanomaterials result in higher average energy than longer structures, leading to more catalytic activity than bulk materials **[44]**.

I.5. Application of Nanomaterials in Physics

Nanomaterials have a wide range of applications in various fields, including medicine, military applications, paints, food products, and the improvement of nutritional values **[45,46]**. In this paragraph, we are going to cite and address some of the common applications in physics:

Uses of nanomaterials in physics can be in lightweight construction, painting, wear protection for tools and machines, and in the manufacturing of electronic devices. Carbon nanotubes and graphene are close to replace silicon as a material for making smaller, faster, and more efficient microchips and devices, as well as lighter, more conductive, and stronger quantum nanowires. Nanomaterials can also improve energy conversion and storage. They can facilitate the creation of small-scale products and processes at the nanoscale **[47,48]**.

After having an introduction on the classification and properties of nanomaterials, we will shift now our focus on 2D materials, particularly the **hexagonal boron nitride** our selected material and the subject of our study in this thesis. We will extensively explain its morphology and properties governing its uses and applications.

I.6. Boron Nitride nanosheets

I.6.1-definition of Boron Nitride

Boron nitride is a refractory compound of boron and nitrogen with the chemical formula BN. It is a non-toxic thermal and chemical refractory compound with high electrical resistance. Boron nitride exists in various crystalline forms that are isoelectronic to a similarly structured carbon lattice **[49,50]**. The Boron Nitride can experience many forms:

- Amorphous form (a-BN).
- Cubic form (c-BN).
- Hexagonal form (h-BN).
- Wurtzite form (w-BN).

The hexagonal form of boron nitride h-BN corresponding to graphite, is the most stable and soft among the other structures, and whose thickness varies from one layer to a few atomic layers. The h-BN consists of conjugated-sp2 boron and nitrogen atoms that form a honeycomb structure **[50]**. Its geometry is similar to that of all-carbon graphene, as clarified in Figure **(I.7)**.

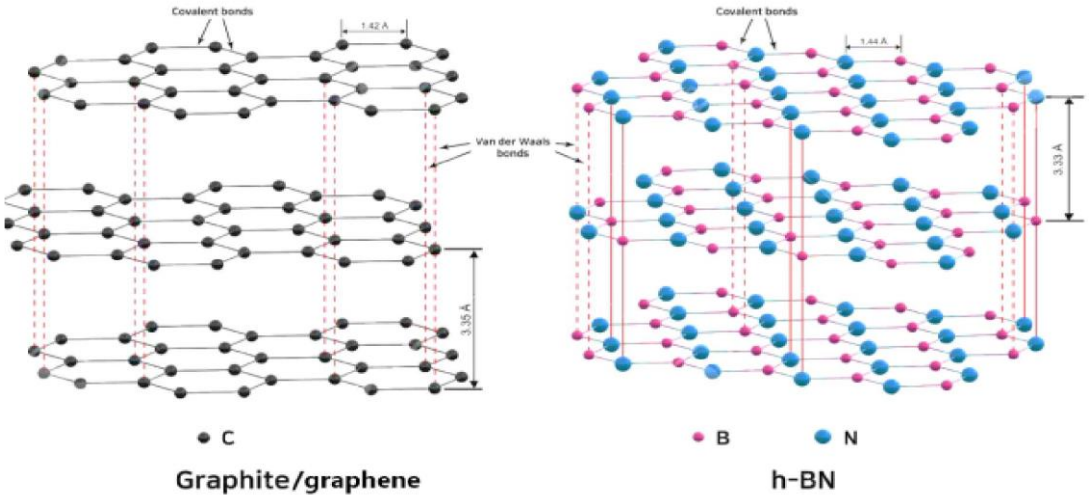

Figure (I.7): Crystal structure of hexagonal boron nitride and carbon graphite**[51]**.

The hexagonal boron nitride h-BN is the only two-dimensional material with a wide band gap of ~5.0 eV, which makes it an insulator. The highest occupied molecular orbital (HOMO) and the lowest unoccupied molecular orbital (LUMO) levels of 2D h-BN are determined by π and π* bands which are located in the nitrogen and boron atoms, respectively, as depicted in Figure **(I.8)**. The h-BN is a layered inorganic synthetic crystal that exhibits high temperature stability, high thermal conductivity, and excellent insulating properties. It is commonly used as an insulator for the production of ultrahigh mobility 2D heterostructures composed of various types of 2D semiconductors **[52,53]**.

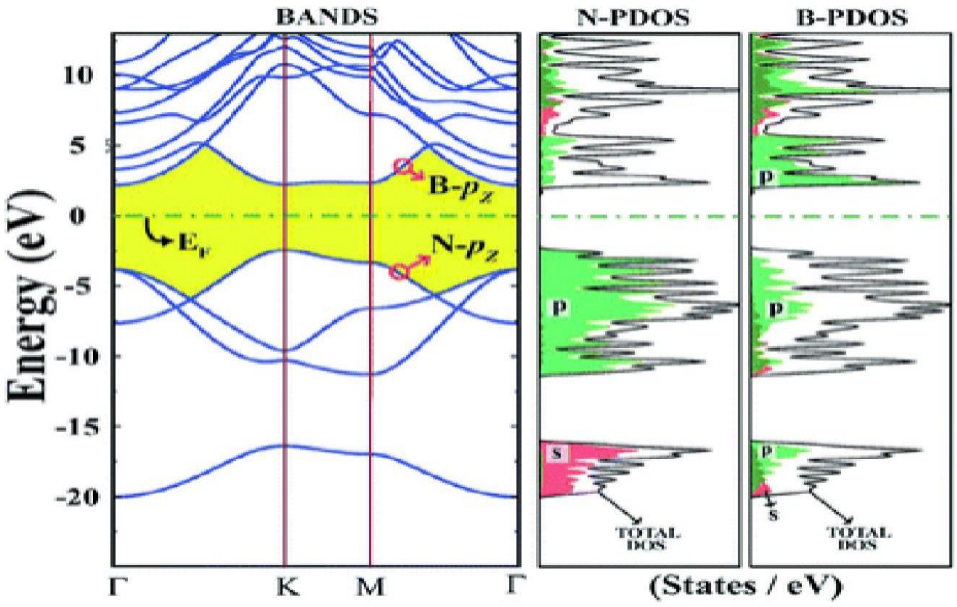

Figure (I.8): Orbital property and electronic structure of h-BN **[54]**.

I.6.2- Properties of Boron Nitride (h-BN)

The hexagonal boron nitride is an insulator with a direct band gap of ~5.0 eV and has a low dielectric constant **[55]**. The h-BN has a plate-like microstructure and a layered lattice structure that give it good lubricating properties. It is resistant to sintering and can be formed by hot pressing. The dielectric constant of h-BN in the out-of-plane direction ranges from 3.29 to 3.76 and shows thickness dependence. The h-BN is used extensively as an insulator for the production of ultrahigh mobility 2D heterostructures composed of various types of 2D semiconductors. It has exotic opto-electronic properties and mechanical robustness **[53]**.

I.6.3- Applications of Boron Nitride (h-BN)

The Hexagonal boron nitride (h-BN) is a multipurpose material and has a wide range of applications. It is used as an insulator for the production of ultrahigh mobility 2D heterostructures composed of various types of 2D semiconductors. The h-BN is also used in metallurgy, cosmetics, and coatings. It has been employed as a temperature-resistant coating for metallurgical, ceramic, or polymer processing machinery **[56–58]**. The h-BN is a ceramic material known for its high thermal conductivity, inertness, and tribological properties**[57]**.

The Hexagonal boron nitride nanoplatelets show high transparency in the UV to IR wavelengths, while the net absorption peak appears in the deep ultraviolet (DUV). It has exotic opto-electronic properties, such as wide bandgap and low dielectric constant, along with mechanical robustness, high thermal conductivity, and strong athodo-luminescence emissions in the DUV range. It could be a promising candidate for application in ultraviolet lasing, photon emission, and DUV detectors. It is also used as an optical and magneto-optical recording media, as well as for optical disc memories. In electronic and optical devices, it is widely used as a dielectric substrate for graphene and other 2D-layered semiconductors. It finds applications in FETs, quantum tunnelling transistors, thermoelectric devices, and many optical areas **[59,60]**.

In nanoelectronics, h-BN has excellent insulating and dielectric properties combined with high thermal conductivity, making it a unique 2D material for the design and manufacture of high-quality devices. It is applied as insulating layers for MISFET semiconductors, as barriers in field tunneling transistors, and as atomically thin insulators for separating metal channels. The h-BN is also used as a substrate for high-performance devices, such as windows in microwaves. Due to its oxidation resistance even at high temperatures and chemical resistance to both acids and bases, h-BN is believed to be a better insulator than other materials. The h-BN material is widely used as a dielectric substrate in electronic and optical devices for graphene and other 2D-layered semiconductors. It finds applications in FETs, quantum tunnelling transistors, thermoelectric devices, and many optical areas **[61–63]**.

Corollary of the chapter

The objective of nanomaterials and 2D materials is to explore their unique properties and potential applications in various fields, such as water management, energy production/storage, tissue engineering, sensing, catalytic applications, and drug delivery. 2D materials are the thinnest materials and possess the highest surface area of all known materials, making them highly suitable for many applications. They exhibit extraordinary mechanical, chemical, electronic, optical, and magnetic properties that can be tuned for specific applications. The study of 2D nanomaterials aims to understand their fundamental properties and how they can be used to develop high-quality devices and materials for various applications **[64–68]**.

References

[1] K. Sharma, (III B . Sc Physics), (n.d.).

[2] S. Bayda, M. Adeel, T. Tuccinardi, M. Cordani, F. Rizzolio, The history of nanoscience and nanotechnology: From chemical-physical applications to nanomedicine, Molecules. 25 (2020) 1–15. https://doi.org/10.3390/molecules25010112.

[3] F. Trotta, A. Mele, Nanomaterials: Cek, Nanosponges. (2019) 1–26.

[4] J. Jeevanandam, A. Barhoum, Y.S. Chan, A. Dufresne, M.K. Danquah, Review on nanoparticles and nanostructured materials: History, sources, toxicity and regulations, Beilstein J. Nanotechnol. 9 (2018) 1050–1074. https://doi.org/10.3762/bjnano.9.98.

[5] OECD International Futures Programme, Small sizes that matter: Opportunities and risks of Nanotechnologies, Allianz. (2007) 46.

[6] M. Bloemen, Immunomagnetic separation of bacteria by iron oxide nanoparticles, Ku Leuven. (2015) 1–157.

[7] İ.M. Alkaç, B. Çerçi, C. Timuralp, F. Şen, 2 - Nanomaterials and their classification, in: F.B.T.-N. for D.A.F.C. Şen (Ed.), Micro Nano Technol., Elsevier, 2021: pp. 17–33. https://doi.org/https://doi.org/10.1016/B978-0-12-821713-9.00011-1.

[8] N. Rao, R. Singh, L. Bashambu, Carbon-based nanomaterials: Synthesis and prospective applications, Mater. Today Proc. 44 (2021) 608–614. https://doi.org/https://doi.org/10.1016/j.matpr.2020.10.593.

[9] A.D. Goswami, D.H. Trivedi, N.L. Jadhav, D. V Pinjari, Sustainable and green synthesis of carbon nanomaterials: A review, J. Environ. Chem. Eng. 9 (2021) 106118. https://doi.org/https://doi.org/10.1016/j.jece.2021.106118.

[10] D.R.. Kroto, Harold W, and Walton, “fullerene,” Encycl. Br. (n.d.). https://www.britannica.com/science/fullerene (accessed May 14, 2023).

[11] B.D. Malhotra, M.A. Ali, Functionalized Carbon Nanomaterials for Biosensors, Nanomater. Biosens. (2018) 75–103. https://doi.org/10.1016/b978-0-323-44923-6.00002-9.

[12] V. Singh, P. Yadav, V. Mishra, Recent Advances on Classification, Properties,

Synthesis, and Characterization of Nanomaterials, Green Synth. Nanomater. Bioenergy Appl. (2020) 83–97. https://doi.org/10.1002/9781119576785.ch3.

[13] H. An, A. Kumamoto, R. Xiang, T. Inoue, K. Otsuka, S. Chiashi, C. Bichara, A. Loiseau, Y. Li, Y. Ikuhara, S. Maruyama, Atomic-scale structural identification and evolution of Co-W-C ternary SWCNT catalytic nanoparticles: High-resolution STEM imaging on SiO2, Sci. Adv. 5 (2023) eaat9459. https://doi.org/10.1126/sciadv.aat9459.

[14] A. Aqel, K.M.M.A. El-Nour, R.A.A. Ammar, A. Al-Warthan, Carbon nanotubes, science and technology part (I) structure, synthesis and characterisation, Arab. J. Chem. 5 (2012) 1–23. https://doi.org/https://doi.org/10.1016/j.arabjc.2010.08.022.

[15] T. Nishihara, A. Takakura, K. Matsui, K. Itami, Y. Miyauchi, Statistical Verification of Anomaly in Chiral Angle Distribution of Air-Suspended Carbon Nanotubes, Nano Lett. 22 (2022). https://doi.org/10.1021/acs.nanolett.2c01473.

[16] I. Ijaz, E. Gilani, A. Nazir, A. Bukhari, Detail review on chemical, physical and green synthesis, classification, characterizations and applications of nanoparticles, Green Chem. Lett. Rev. 13 (2020) 223–245. https://doi.org/10.1080/17518253.2020.1802517.

[17] D. Torres, S. Pérez-Rodríguez, D. Sebastián, J.L. Pinilla, M.J. Lázaro, I. Suelves, Graphene oxide nanofibers: A nanocarbon material with tuneable electrochemical properties, Appl. Surf. Sci. 509 (2020) 144774. https://doi.org/https://doi.org/10.1016/j.apsusc.2019.144774.

[18] V.B. Mbayachi, E. Ndayiragije, T. Sammani, S. Taj, E.R. Mbuta, A. ullah khan, Graphene synthesis, characterization and its applications: A review, Results Chem. 3 (2021) 100163. https://doi.org/https://doi.org/10.1016/j.rechem.2021.100163.

[19] A.R. Urade, I. Lahiri, K.S. Suresh, Graphene Properties, Synthesis and Applications: A Review, JOM. 75 (2023) 614–630. https://doi.org/10.1007/s11837-022-05505-8.

[20] S. Muley, N.M. Ravindra, Graphene: Properties, Synthesis, and Applications BT - Semiconductors: Synthesis, Properties and Applications, in: M.I. Pech-Canul, N.M. Ravindra (Eds.), Springer International Publishing, Cham, 2019: pp. 219–332. https://doi.org/10.1007/978-3-030-02171-9_5.

[21] Y. Chen, Y. Xie, X. Yan, M.L. Cohen, S. Zhang, Topological carbon materials: A new perspective, Phys. Rep. 868 (2020) 1–32. https://doi.org/https://doi.org/10.1016/j.physrep.2020.05.003.

[22] N. Choudhary, S. Hwang, W. Choi, Carbon Nanomaterials: A Review BT - Handbook of Nanomaterials Properties, in: B. Bhushan, D. Luo, S.R. Schricker, W. Sigmund, S. Zauscher (Eds.), Springer Berlin Heidelberg, Berlin, Heidelberg, 2014: pp. 709–769. https://doi.org/10.1007/978-3-642-31107-9_37.

[23] S. Kamel, M.A. El-Sakhawy, B. Anis, H.-A.S. Tohamy, Graphene: Structure, Synthesis, and Characterization; a brief review, Egypt. J. Chem. (2019).

[24] A.A. Yaqoob, H. Ahmad, T. Parveen, A. Ahmad, M. Oves, Recent Advances in Metal Decorated Nanomaterials and Their Various Biological Applications : A Review, 8 (2020) 1–23. https://doi.org/10.3389/fchem.2020.00341.

[25] Y. Yoon, P.L. Truong, D. Lee, S.H. Ko, Metal-Oxide Nanomaterials Synthesis and Applications in Flexible and Wearable Sensors, ACS Nanosci. Au. 2 (2022) 64–92. https://doi.org/10.1021/acsnanoscienceau.1c00029.

[26] Z.U.R. Farooqi, A. Qadeer, M.M. Hussain, N. Zeeshan, P. Ilic, Chapter 5 - Characterization and physicochemical properties of nanomaterials, in: M.B. Tahir, M. Sagir, A.M.B.T.-N.S. Asiri Characterization, Hazards and Safety (Eds.), Micro Nano Technol., Elsevier, 2021: pp. 97–121. https://doi.org/https://doi.org/10.1016/B978-0-12-823823-3.00005-7.

[27] H. Dong, W. Hu, Organic Nanomaterials BT - Springer Handbook of Nanomaterials, in: R. Vajtai (Ed.), Springer Berlin Heidelberg, Berlin, Heidelberg, 2013: pp. 905–940. https://doi.org/10.1007/978-3-642-20595-8_25.

[28] D. Sannino, Types and Classification of Nanomaterials BT - Nanotechnology: Trends and Future Applications, in: M.B. Tahir, M. Rafique, M. Sagir (Eds.), Springer Singapore, Singapore, 2021: pp. 15–38. https://doi.org/10.1007/978-981-15-9437-3_2.

[29] M. Rizwan, A. Shoukat, A. Ayub, B. Razzaq, M.B. Tahir, Chapter 3 - Types and classification of nanomaterials, in: M.B. Tahir, M. Sagir, A.M.B.T.-N.S. Asiri Characterization, Hazards and Safety (Eds.), Micro Nano Technol., Elsevier, 2021: pp. 31–54. https://doi.org/https://doi.org/10.1016/B978-0-12-823823-3.00001-X.

[30] J. Jeevanandam, A. Barhoum, Y.S. Chan, A. Dufresne, M.K. Danquah, Review

on nanoparticles and nanostructured materials: history, sources, toxicity and regulations., Beilstein J. Nanotechnol. 9 (2018) 1050–1074. https://doi.org/10.3762/bjnano.9.98.

[31] I. Khan, K. Saeed, I. Khan, Nanoparticles: Properties, applications and toxicities, Arab. J. Chem. 12 (2019) 908–931. https://doi.org/10.1016/j.arabjc.2017.05.011.

[32] S. Bashir, J.L. Liu, Nanomaterials and Their Application, Adv. Nanomater. Their Appl. Renew. Energy. (2015) 1–50. https://doi.org/10.1016/B978-0-12-801528-5.00001-4.

[33] J. Abraham, A. Rehghunadhan, K.C. Nimitha, S. George, S. Thomas, One-dimensional (1D) nanomaterials: Nanorods and nanowires; nanoscale processing, in: 2021: pp. 71–101. https://doi.org/10.1016/B978-0-12-820569-3.00003-7.

[34] Z. Rafiei-Sarmazdeh, S.M. Zahedi-Dizaji, A.K. Kang, Two-Dimensional Nanomaterials, in: S. Ameen, M.S. Akhtar, H.-S. Shin (Eds.), IntechOpen, Rijeka, 2019: p. Ch. 3. https://doi.org/10.5772/intechopen.85263.

[35] A. Mandal, E. Ray Banerjee, Introduction to Nanoscience, Nanotechnology and Nanoparticles BT - Nanomaterials and Biomedicine: Therapeutic and Diagnostic Approach, in: E. Ray Banerjee (Ed.), Springer Singapore, Singapore, 2020: pp. 1–39. https://doi.org/10.1007/978-981-15-5274-8_1.

[36] W.L.F. Armarego, Nanomaterials, Purif. Lab. Chem. (2022) 586–630. https://doi.org/10.1016/B978-0-323-90968-6.50005-9.

[37] N. Čitaković, Physical properties of nanomaterials, Vojnoteh. Glas. 67 (2019) 159–171. https://doi.org/10.5937/vojtehg67-18251.

[38] V.M. Rodriguez, H.A. Abhyankar, Optical Properties of Nanomaterials, Nanocomposite Mater. (2016) 81–103. https://doi.org/10.1201/9781315372310-5.

[39] B. Wiley, Introduction: Chemical, physical and mechanical properties of nanomaterials, Encycl. Nanomater. (2023) 382. https://doi.org/10.1016/B978-0-12-822425-0.00115-9.

[40] G.Y. Yurkov, A.S. Fionov, Y.A. Koksharov, V. V. Koleso, S.P. Gubin, Electrical and magnetic properties of nanomaterials containing iron or cobalt nanoparticles, Inorg. Mater. 43 (2007) 834–844.

[41] A. Barhoum, M. Luisa García-Betancourt, Chapter 10 - Physicochemical characterization of nanomaterials: size, morphology, optical, magnetic, and electrical properties, in: A. Barhoum, A.S.H.B.T.-E.A. of N. and A.N. Makhlouf (Eds.), Micro Nano Technol., Elsevier, 2018: pp. 279–304. https://doi.org/https://doi.org/10.1016/B978-0-323-51254-1.00010-5.

[42] N. Joudeh, D. Linke, Nanoparticle classification, physicochemical properties, characterization, and applications: a comprehensive review for biologists., J. Nanobiotechnology. 20 (2022) 262. https://doi.org/10.1186/s12951-022-01477-8.

[43] Y. Hui, X. Yi, F. Hou, D. Wibowo, F. Zhang, D. Zhao, H. Gao, C.-X. Zhao, Role of Nanoparticle Mechanical Properties in Cancer Drug Delivery, ACS Nano. 13 (2019) 7410–7424. https://doi.org/10.1021/acsnano.9b03924.

[44] A.M. Ealias, M.P. Saravanakumar, A review on the classification, characterisation, synthesis of nanoparticles and their application, IOP Conf. Ser. Mater. Sci. Eng. 263 (2017). https://doi.org/10.1088/1757-899X/263/3/032019.

[45] H.S. Hussein, The state of the art of nanomaterials and its applications in energy saving, Bull. Natl. Res. Cent. 47 (2023) 7. https://doi.org/10.1186/s42269-023-00984-4.

[46] M. Shafiq, S. Anjum, C. Hano, I. Anjum, B.H. Abbasi, An Overview of the Applications of Nanomaterials and Nanodevices in the Food Industry., Foods (Basel, Switzerland). 9 (2020). https://doi.org/10.3390/foods9020148.

[47] H.P.S. Abdul Khalil, R. Dungani, M.S. Hossain, N.L.M. Suraya, S. Aprilia, A.A. Astimar, Z. Nahrul Hayawin, Y. Davoudpour, Mechanical properties of oil palm biocomposites enhanced with micro to nanobiofillers, Biocomposites Des. Mech. Perform. (2015) 401–435. https://doi.org/10.1016/B978-1-78242-373-7.00026-3.

[48] A.S. Ali, Application of Nanomaterials in Environmental Improvement, in: M. Sen (Ed.), IntechOpen, Rijeka, 2020: p. Ch. 2. https://doi.org/10.5772/intechopen.91438.

[49] The Editors of Encyclopaedia, Britannica, “boron Nitride.” (2013). https://www.britannica.com/science/boron-nitride (accessed May 16, 2023).

[50] G.R. Bhimanapati, N.R. Glavin, J.A. Robinson, Chapter Three - 2D Boron Nitride: Synthesis and Applications, in: F. Iacopi, J.J. Boeckl, C.B.T.-S. and S. Jagadish

(Eds.), 2D Mater., Elsevier, 2016: pp. 101–147. https://doi.org/https://doi.org/10.1016/bs.semsem.2016.04.004.

[51] P.K. Nayak, ed., Two-dimensional Materials, (2016). https://doi.org/10.5772/64760.

[52] G.R. Bhimanapati, N.R. Glavin, J.A. Robinson, 2D Boron Nitride: Synthesis and Applications, Semicond. Semimetals. 95 (2016) 101–147. https://doi.org/10.1016/bs.semsem.2016.04.004.

[53] S. Angizi, M. Khalaj, S.A.A. Alem, A. Pakdel, M. Willander, A. Hatamie, A. Simchi, Review—Towards the Two-Dimensional Hexagonal Boron Nitride (2D h-BN) Electrochemical Sensing Platforms, J. Electrochem. Soc. 167 (2020) 126513. https://doi.org/10.1149/1945-7111/abaf29.

[54] M. Topsakal, E. Aktürk, S. Ciraci, First-principles study of two- and one-dimensional honeycomb structures of boron nitride, Phys. Rev. B. 79 (2009) 115442. https://doi.org/10.1103/PhysRevB.79.115442.

[55] A. Laturia, M.L. Van de Put, W.G. Vandenberghe, Dielectric properties of hexagonal boron nitride and transition metal dichalcogenides: from monolayer to bulk, Npj 2D Mater. Appl. 2 (2018) 6. https://doi.org/10.1038/s41699-018-0050-x.

[56] A.F. Rigosi, A.L. Levy, M.R. Snure, N.R. Glavin, Turn of the decade: versatility of 2D hexagonal boron nitride., JPhys Mater. 4 (2021). https://doi.org/10.1088/2515-7639/abf1ab.

[57] M. Engler, B. Ruisinger, Anwendungen von Metallurgie bis Kosmetik, Ceram. Forum Int. 12 (2016) 25–29.

[58] S. Roy, X. Zhang, A.B. Puthirath, A. Meiyazhagan, S. Bhattacharyya, M.M. Rahman, G. Babu, S. Susarla, S.K. Saju, M.K. Tran, L.M. Sassi, M.A.S.R. Saadi, J. Lai, O. Sahin, S.M. Sajadi, B. Dharmarajan, D. Salpekar, N. Chakingal, A. Baburaj, X. Shuai, A. Adumbumkulath, K.A. Miller, J.M. Gayle, A. Ajnsztajn, T. Prasankumar, V.V.J. Harikrishnan, V. Ojha, H. Kannan, A.Z. Khater, Z. Zhu, S.A. Iyengar, P.A. da S. Autreto, E.F. Oliveira, G. Gao, A.G. Birdwell, M.R. Neupane, T.G. Ivanov, J. Taha-Tijerina, R.M. Yadav, S. Arepalli, R. Vajtai, P.M. Ajayan, Structure, Properties and Applications of Two-Dimensional Hexagonal Boron Nitride, Adv. Mater. 33 (2021) 2101589.

[59] Y. Feng, F. Wang, Z. Yang, J. Wang, Two dimensional hexagonal boron nitride (2D-hBN): Synthesis, properties and applications, J. Mater. Chem. C. 5 (2017). https://doi.org/10.1039/C7TC04300G.

[60] M. Zhao, Y. Hao, C. Zhang, R. Zhai, B. Liu, W. Liu, C. Wang, S.H.M. Jafri, A. Razaq, R. Papadakis, J. Liu, X. Ye, X. Zheng, H. Li, Advances in Two-Dimensional Materials for Optoelectronics Applications, Crystals. 12 (2022). https://doi.org/10.3390/cryst12081087.

[61] S. Gupta, P. Joshi, R. Sachan, Fabricating Graphene Oxide / h-BN Metal Insulator Semiconductor Diodes by Nanosecond Laser Irradiation, (2022).

[62] Q. Weng, X. Wang, X. Wang, Y. Bando, D. Golberg, Functionalized hexagonal boron nitride nanomaterials: Emerging properties and applications, Chem. Soc. Rev. 45 (2016) 3989–4012. https://doi.org/10.1039/c5cs00869g.

[63] S.K. Jang, J. Youn, Y.J. Song, S. Lee, Synthesis and Characterization of Hexagonal Boron Nitride as a Gate Dielectric, Sci. Rep. 6 (2016) 30449. https://doi.org/10.1038/srep30449.

[64] P. Accessible, P. Dissertations, D. Er, ScholarlyCommons 2d Materials For Energy Applications 2d Materials For Energy Applications, (2018).

[65] H. Zhang, T. Fan, W. Chen, Y. Li, B. Wang, Recent advances of two-dimensional materials in smart drug delivery nano-systems., Bioact. Mater. 5 (2020) 1071–1086. https://doi.org/10.1016/j.bioactmat.2020.06.012.

[66] R. Mohanty, A. Mishra, J. Khatei, Two-Dimensional Nanostructures for Advanced Applications, ACS Symp. Ser. 1353 (2020) 1–31. https://doi.org/10.1021/bk-2020-1353.ch001.

[67] J. Fatima, A.N. Shah, M.B. Tahir, T. Mehmood, A.A. Shah, M. Tanveer, R. Nazir, B.L. Jan, S. Alansi, Tunable 2D Nanomaterials; Their Key Roles and Mechanisms in Water Purification and Monitoring, Front. Environ. Sci. 10 (2022) 1–23. https://doi.org/10.3389/fenvs.2022.766743.

[68] N. Baig, Two-dimensional nanomaterials: A critical review of recent progress, properties, applications, and future directions, Compos. Part A Appl. Sci. Manuf. 165 (2023) 107362.

CHAPTER II

- Calculation approach -

Density Functional Theory (DFT)

And the augmented plane wave method (FP-LAPW)

II.1. Introduction

Studying the properties of materials involves examining the unique characteristics of each material **[1,2].** And these characteristics can be done experimentally or through simulation.

Experimental characterization refers to the process of determining the material properties through tests conducted on suitably designed specimens. This process is fundamental in the field of materials science, without which no scientific understanding of engineering materials could be ascertained. However, with the advancement of technology, simulation and modeling have become increasingly important in materials science. Modeling and simulation allow for the understanding and prediction of material behavior at scales from atomistic to macroscopic, which is difficult to achieve through experimental characterization alone. The microscopic arrangement of atoms and molecules is the determining factor in how materials behave and perform in chemical and physical applications, and the structure, specifically the electronic structure, can be differentiated to calculate any physical property of a material **[1,3]**.

So, the question is how can we use simulation to get the properties we want? The answer will be easy by calculation codes. This calculation codes (in our case we used **WIEN2K**) are based on the density functional theory (DFT) **[4]**, which is a computational quantum mechanical modeling method used in physics, chemistry, and materials science to investigate the electronic structure (or nuclear structure) of many-body systems, in particular atoms, molecules, and the condensed phases **[5–7]**. Density functional theory (DFT) has its origins in the model developed by Thomas and Fermi in the late 1920s. However, it was not until the mid-1960s that the contributions of Hohenberg and Kohn on the one hand and Kohn and Sham on the other established the theoretical formalism on which the current method is based. DFT has been very popular for calculations in solid-state physics since the 1970s and has become one of the most important methods to solve the Schrödinger and Dirac equations approximately **[8,9]**.

In other words, we can say that DFT is a powerful approach for the treatment of the many-body problem. However, the choice of wave function basis is crucial for the solution of the Khon-Sham equations. There are several methods for solving the Schrödinger equation, which differ in the form of the potential used and in the wave functions taken as a basis. Among them are the methods based on a linear combination of atomic orbitals (LCAO), orthogonal plane wave (OPW) methods, cellular methods

of the augmented plane wave (APW) type, and linearized methods developed by Andersen, such as Linearized Augmented Plane Waves (LAPW) and Linearized Muffin-Tin Orbitals (LMTO). These methods save several orders of magnitude in computing time and allow the treatment of transition metals and conduction bands of "s-p" character of single metals **[10]**.

In the end we can say that in this chapter, the foundations of Density Functional Theory (DFT) will be briefly outlined. The different levels of approximation involved in its practical implementation will then be detailed, then we are going to explain the different method of the wave function that used to solve the Kohn-Sham equations. Finally, we will present the organization chart of the code WIEN2K programs.

II.2. Schrödinger's Equation and the N-body problem

II.2.1-Schrödinger's Equation

In quantum mechanics, the Schrödinger equation is a partial differential equation that describes how the quantum state of a physical system changes with time. This equation describes the time-dependent states of quantum systems. The Schrödinger equation is of particular importance in quantum mechanics because it is considered the second law of motion in classical physics, similar to Newton's laws of motion **[11]**.

The Schrödinger equation is used extensively in atomic, nuclear, and solid-state physics, which is written in the form:

$$H\Psi = E\Psi$$

Where:

H : Hamiltonian.

Ψ : Wave function.

E : Total energy of the system.

The Hamiltonian is a mathematical operator that represents the total energy of quantum-mechanical system. The exact Hamiltonian of a crystal results from the presence of electrostatic forces of interaction: which can be either repulsive or attractive depending on the charge of the particles, such as ions, electrons, and nuclei [12]**.**

And it is given by the general relation:

$$H_T = T_n + T_e + V_{n-e} + V_{e-e} + V_{n-n} \quad \text{(II.1)}$$

In which the terms $T_e, T_n, V_{n-n}, V_{e-e}, V_{n-e}$ correspond respectively to the following terms:

- The kinetic energy of electrons their mass m_e :

$$T_e = -\frac{\hbar^2}{2}\sum_i \frac{\nabla^2_{\vec{r_i}}}{m_e} \quad \text{(II.2)}$$

- The kinetic energy of nuclei their mass M_n:

$$T_n = -\frac{\hbar^2}{2}\sum_i \frac{\nabla^2_{\vec{R_I}}}{M_n} \quad \text{(II.3)}$$

- The repulsive Coulomb interaction (electron-electron):

$$V_{e-e} = \frac{1}{8\pi\varepsilon_0}\sum_{i\neq j}\frac{e^2}{|\vec{r_i}-\vec{r_j}|} \quad \text{(II.4)}$$

- The repulsive Coulomb interaction (nucleus-nucleus):

$$V_{n-n} = \frac{1}{8\pi\varepsilon_0}\sum_{i\neq j}\frac{e^2 Z_i Z_j}{|\vec{R_i}-\vec{R_j}|} \quad \text{(II.5)}$$

- The attractive Coulomb interaction (nucleus-electron):

$$V_{n-e} = -\frac{1}{4\pi\varepsilon_0}\sum_{i,j}\frac{e^2 Z_i}{|\vec{R_i}-\vec{r_j}|} \quad \text{(II.6)}$$

So, Schrödinger's equation is writing as the following form:

$$\left[-\frac{\hbar^2}{2}\sum_i\frac{\nabla^2_{\vec{r_i}}}{m_e} - \frac{\hbar^2}{2}\sum_i\frac{\nabla^2_{\vec{R_I}}}{M_n} + \frac{1}{8\pi\varepsilon_0}\sum_{i\neq j}\frac{e^2}{|\vec{r_i}-\vec{r_j}|} + \frac{1}{8\pi\varepsilon_0}\sum_{i\neq j}\frac{e^2 Z_i Z_j}{|\vec{R_i}-\vec{R_j}|} - \frac{1}{4\pi\varepsilon_0}\sum_{i,j}\frac{e^2 Z_i}{|\vec{r_i}-\vec{R_j}|}\right]\Psi = E\Psi \quad \text{(II.7)}$$

II.2.2-The N-body problem

The wave function of N electrons depends on 3N spatial coordinates and N spin coordinates. For example, taking atom of oxygen with Z=8 electrons.

$$\psi(\vec{X}_1, \vec{X}_2, ..., \vec{X}_7, \vec{X}_8) \quad \text{(II.8)}$$

Thus, the wave function contains 4x8=32 variables. To store this function on an array of 10 values per coordinate of the 8 electrons, it would require 101x4x8=1032 bytes, or 1020 terabytes if each value is stored on 1 byte. Even with a futuristic storage device

with a data transfer rate of 1 terabyte per second, it would still take 3.169 billion years to write the wave function (assuming the universe is about 13.7 billion years old!)[13].

In this case the equation of Schrödinger is too complex to be solved analytically, so there are different levels of approximation must be considered when simplifying mathematical expressions. The three main levels of simplification generally used are:

- The Born-Oppenheimer approximation.
- The Hartree-Fock approximation.
- Formalism of the density functional theory.

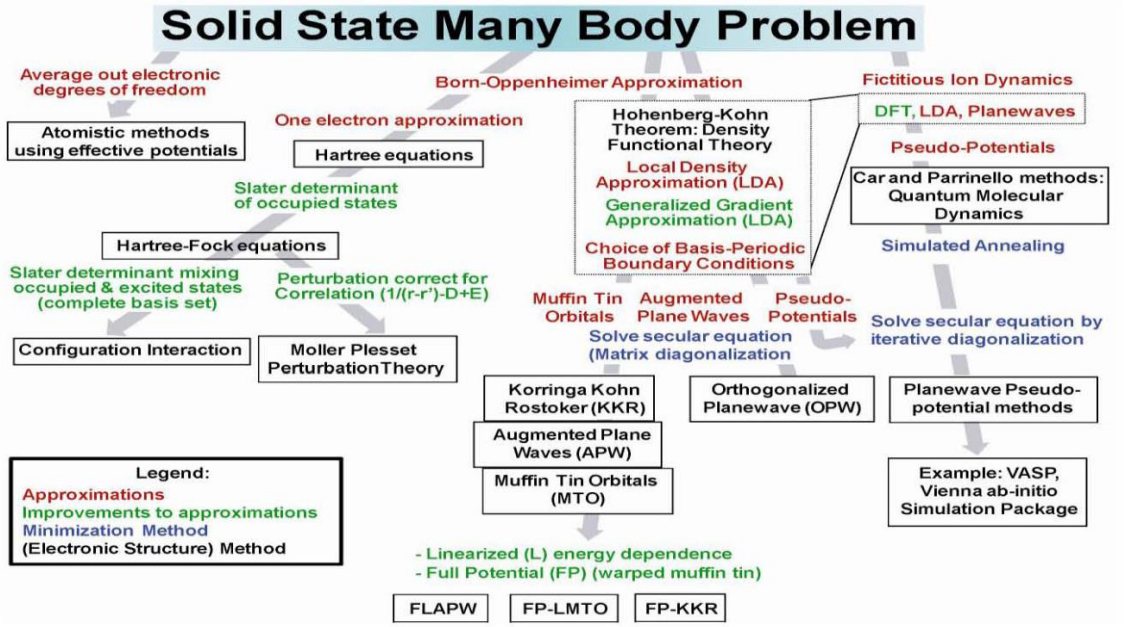

Figure (II.1): Schematic of the methods developed by the chemistry and physics communities to solve the materials many body problem**[14].**

II.3. Born-Oppenheimer approximation

To simplify the solution of the Schrödinger equation, (Max Born et Robert Oppenheimer) the authors of the approximation of Born-Oppenheimer (BO) assume that the treatment of electrons and nuclei in a separate way is possibility that allows the simplification of N-body problem this problem which is the solution of Schrödinger's equation, that is, there will be two parties nuclear part and an electronic part. Therefore, the system wave function is written as:

$$\Psi(\vec{r},\vec{R}) = \Psi_n(\vec{R})\Psi_e(\vec{r}) \qquad \text{(II.9)}$$

With:

Ψ_n **:** the nuclear wave function.

Ψ_e **:** the electronic wave function.

This approximation based on the fact that the mass of an atomic nucleus in a molecule is much larger than the mass of an electron about 1836 times **[15],** so we can neglect the movement of nucleus and consider only the movement of the electrons.

Hence, the motion of the nuclei is negligible **(**$T_n \approx 0$**)** and the potential energy of interaction between the nucleus becomes constant $(V_{n-n} = C^{ste})$ **[16]**. This approach leads to a Hamiltonian for which the electrons move in a field created by a static configuration of the nuclei **[17]**.

The electronic Hamiltonian became as the following:

$$H_e = T_e + V_{e-e} + V_{e-n} \qquad \textbf{(II.10)}$$

With:

T_e : the kinetic energy of electrons.

V_{e-e} : The repulsive Coulomb interaction (electron-electron).

V_{e-n} : The attractive Coulomb interaction (electron-nucleus).

And the Schrödinger's equation can be written as:

$$H_e \Psi_e = E_e \Psi_e \qquad \textbf{(II.11)}$$

$$\left[-\frac{\hbar^2}{2}\sum_i \frac{\nabla^2_{\vec{r_i}}}{m_e} + \frac{1}{8\pi\varepsilon_0}\sum_{i\neq j}\frac{e^2}{|\vec{r_i}-\vec{r_j}|} - \frac{1}{4\pi\varepsilon_0}\sum_{i,j}\frac{e^2 Z_i}{|\vec{r_i}-\vec{R_j}|}\right]\Psi_e = E_e \Psi_e \qquad \textbf{(II.12)}$$

Where:

E_e : Represents the energy of electrons moving in the field created by fixed nuclei.

The Born-Oppenheimer approximation simplifies the Schrödinger equation for multi-electron systems, resulting in a simpler equation **(II.12).** However, the resulting equation still describes an N-body problem that is hard to solve due to the complexity of electron-electron interactions**[18].** Even with the simplification of the approximation of BO the Schrödinger equation still complicated, so another approach was reached by

Hartree and Fock to simplify this equation for multi-electron systems. This successful approximation (Hartree-Fock approximation) reduces equation **(II.12)** to a one-body problem, which is a simpler problem to solve.

II.4. Hartree-Fock approximation

Hartree-Fock (HF) theory is an approximation appeared in the 1920s and 1930s. The HF theory is an approximation method developed in the 1920s and 1930s to determine the wavefunction and energy of a quantum many-body system in a stationary state. The HF theory makes use of a simple guess for the structure of a many-body wavefunction and then uses the variation principle to find an approximation of the actual wavefunction. The theory assumes that all electrons in the system are non-interacting, and the wavefunction would then just be a combination of single-electron wavefunctions. However, simply multiplying single-electron wavefunctions together would not produce the anti-symmetry required for wavefunctions of fermions, so the appropriate from is a SD **[19]**:

$$\Psi_{SD}(X_1,\ldots,X_n)=\frac{1}{\sqrt{n!}}\begin{pmatrix}\psi_1(x_1) & \cdots & \psi_n(x_1)\\ \vdots & \ddots & \vdots\\ \psi_1(x_n) & \cdots & \psi_n(x_n)\end{pmatrix} \qquad \textbf{(II.13)}$$

$\frac{1}{\sqrt{n!}}$ **:** is a normalization factor.

The Hartree-Fock equations can be obtained by applying the variational principle to the problem of minimizing the total energy with respect to the monoelectronic wave function Ψ_i **.**

The equations are given by the following forms:

$$\left[-\frac{\hbar^2}{2m_e}\overrightarrow{\nabla^2}+V_{ext}(\vec{r})+V_H(\vec{r})+V_X(\vec{r})\right]\Psi_i(\vec{r})=E\Psi_i(\vec{r}) \qquad \textbf{(II.14)}$$

Where:

$V_{ext}(\vec{r})$: Represents the attractive interaction between the electron and the nuclei of coordinate $\vec{R}$.

$$V_{ext}(\vec{r}) = -\sum_i \frac{Z_i e^2}{|\vec{r_i}-\vec{R_J}|} \qquad \textbf{(II.15)}$$

$V_H(\vec{r})$: is the Hartree potential arising from the repulsive coulombic interaction between an electron of coordinate $\vec{r}_i$ longe in the mean field of the other electrons of coordinate $\vec{r}_j$.

$$V_H(\vec{r}) = -\int d\vec{r'}\rho(\vec{r'})\frac{1}{|\vec{r_i}-\vec{r'}|} \quad \text{(II.16)}$$

$V_X(\vec{r})$: The Fock term defined by its action on a wave function $\Psi_i(\vec{r})$. The Hartree-Fock equations differ from the Hartree equations by the exchange term:

$$V_X(\vec{r})\Psi(r) = -\sum_{i\neq j}\int dr \frac{\Psi_j^*(r')\Psi_i^*(r')}{|\vec{r}-\vec{r'}|}\Psi_j(r) \quad \text{(II.17)}$$

The HF method is typically used to solve the time-independent Schrödinger equation for a multi-electron atom or molecule as described in the Born-Oppenheimer approximation. However, the HF method has limitations, and it can only deal with systems with few electrons like small molecules. This is because the HF method does not take into account the effects of electronic correlations **[20]**, which become more important as the number of electrons increases. Therefore, the HF method is not suitable for describing the electronic properties of large molecules or materials.

II.5. Density Functional Theory

II.5.1-what is Density Functional Theory?

Density-functional theory (DFT) is a computational quantum mechanical modelling method used in physics, chemistry, and materials science to investigate the electronic structure of many-body systems, in particular atoms, molecules, and the condensed matter. DFT is one of the most popular and successful quantum mechanical approaches to matter. It is routinely applied for calculating the binding energy of molecules in chemistry and the band structure of solids in physics. DFT has been used to study superconductivity, atoms in the focus of strong laser pulses, relativistic effects in heavy elements and in atomic nuclei, classical liquids, and magnetic properties of alloys **[10].**

II.5.2-Origin of Density Functional Theory (DFT)

The origins of density-functional theory (DFT) can be traced back to 1927 when Thomas and Fermi proposed the DFT of quantum systems **[21].** The approach proposed

by Thomas and Fermi shows how DFT works, but it is not exact enough to be applied to modern-day electronic structure calculations. They proposed a method where the kinetic energy is expressed as a functional of the electron density, taking into account electron-electron interaction through mean-field potential. Their method was proposed in analogy with the methods proposed by Hartree and Fock, but they neglected the exchange-correlation in their method. Dirac proposed the local approximation for exchange, which is still in use today, but it has not significantly improved the method. And nowadays Hohenberg, Kohn, and Sham proposed and developed the modern-day DFT formulation, which uses the particle density as a basic variable to describe any kind of many-electron system. In other words, we can say that the modern DFT is based on the theorems of Hohenberg and Kohn **[22]**.

II.5.3-Hohenberg-Kohn Theorems

II.5.3-1-First Theorem

Hohenberg and Kohn's first theorem states that the external potential is a unique functional of the ground-state electron density, which means that any ground state configuration of electrons is uniquely determined by the external potential**[19].**

$$\left[\frac{\partial E[\rho(\vec{r})]}{\partial \rho(\vec{r})}\right]_{\rho(\vec{r})+\rho_0(\vec{r})} = 0 \qquad \text{(II.18)}$$

The Hohenberg-Kohn theorem does not provide any indication o the form of the universal functional $E\left[\rho(\vec{r})\right]$, which is a crucial element in the density functional theory. However, the theorem states that the functional $E\left[\rho(\vec{r})\right]$is universal for any system with several electrons, and if the functional $E\left[\rho(\vec{r})\right]$is known, then it will be relatively easy to use the principle for a given external potential**[23].**

II.5.3-2-Second Theorem

This theorem states that there is a universal functional E(ρ) expressing energy as a function of electron density $\rho(\vec{r})$, which is valid for any external potential V_{ext} . For a given potential V_{ext} and number of electrons N, the ground state energy of the system is the value that minimizes this functional, and the density $\rho(\vec{r})$ associated with it corresponds to the exact density $\rho_0(\vec{r})$ of the ground state. This means that the

electronic density of the ground-state uniquely determines the external potential V_{ext} (r) up to a constant **[23].**

$$\left.\frac{\partial E[\rho(r)]}{\partial \rho(r)}\right|_{\rho=\rho_0} = 0 \Longrightarrow E(\rho_0) = \text{MIN E}(\rho) \qquad \textbf{(II.19)}$$

ρ_0 : the density of the ground state.

Hence, the total energy functional of the ground state is written as follows:

$$E\left[\rho(\vec{r})\right] = F_{HK}\left[\rho(\vec{r})\right] + \int V_{ext}(\vec{r})\rho(\vec{r})d\vec{r} \qquad \textbf{(II.20)}$$

$F_{HK}\left[\rho(\vec{r})\right]$: The universal functional of Hohenberg and Kohn for any system has several electrons.

$V_{ext}(\vec{r})$:is the external potential acting on these particles.

$$F_{HK}\left[\rho(\vec{r})\right] = T_e\left[\rho(\vec{r})\right] + V_{e-e}\left[\rho(\vec{r})\right] \qquad \textbf{(II.21)}$$

With:

$\left[\rho(\vec{r})\right]$: the density functional for kinetic energy.

$V_{e-e}\left[\rho(\vec{r})\right]$: the density functional for electron-electron interaction.

The Hohenberg-Kohn theorem provides a way to calculate the electron-nucleus interaction from the electron density $\rho(\vec{r})$, but the kinetic energy and the electron-electron interaction potential cannot be directly calculated from the electron density, due to the form of the energy functional $F_{HK}\left[\rho(\vec{r})\right]$that it is unknown **[19].** This inconvenient of the unknown form of the functional $F_{HK}\left[\rho(\vec{r})\right]$ in the Hohenberg-Kohn theorem ca be resolved by using the Kohn-Sham approximation.

II.5.4- Kohn-Sham's equations

The Kohn-Sham theorem introduces a set of auxiliary non-interacting particles that have the same electron density as the original system. The kinetic energy and electron-electron interaction potential are calculated for these particles, and the total energy of the system is then calculated as the sum of the kinetic energy, electron-electron

interaction potential, and electron-nucleus interaction potential. The Kohn-Sham equations are a set of one-particle equations whose solutions are the Kohn-Sham orbitals. The Kohn-Sham potential is a local effective external potential in which the non-interacting particles move, and it is defined by the charge density of the system given by the form**[19]:**

$$\rho(\vec{r}) = \sum_{i}^{n} |\Psi_i(\vec{r})|^2 \qquad \textbf{(II.22)}$$

The ground state energy and density of a system of interacting electrons can be obtained using the variational principle. The energetic functional is then written by following:

$$E_{V_{ext}}[\rho(\vec{r})] = T_0[\rho(\vec{r})] + V_H[\rho(\vec{r})] + V_{XC}[\rho(\vec{r})] + V_{ext}[\rho(\vec{r})] \qquad \textbf{(II.23)}$$

Hence:

T_0 : the kinetic energy of the system without interaction.

V_H : the Hartree term (the classical Coulomb interaction between electrons).

V_{XC} : the term that refers the effects of exchange and correlation.

V_{ext} : includes the coulombic interaction of electrons with nuclei and nuclei with each other.

The Hartree term and the kinetic energy term are important in the description of free electron states and play a crucial role in the treatment of electron interaction. The difference between the real kinetic energy and that of the non-interacting electrons, as well as the difference between the real interaction energy and the Hartree energy, are taken into account in the exchange and correlation energy. The Hartree-Fock approximation is one of the most important ways to tackle the kinetic energy of the electrons. The Kohn-Sham equations include the non-interacting kinetic energy, the long-range Hartree term, the external potential, and the exchange-correlation energy. therefor the Schrödinger equation can be written as**[24]:**

$$\left[-\frac{\hbar^2}{2m_e}\nabla_i^2 + V_H(\rho(\vec{r})) + V_{XC}(\rho(\vec{r})) + V_{ext}(\rho(\vec{r}))\right]\Psi_i(\vec{r}) = E_i\Psi_i(\vec{r}) \qquad \textbf{(II.24)}$$

The exchange and correlation potential of the Kohn-Sham density-functional is given by the derived functional:

$$V_{XC}(\vec{r}) = \frac{\partial E_{XC}}{\partial \rho(\vec{r})} \qquad \textbf{(II.25)}$$

The Kohn-Sham equation is a non-interacting Schrödinger equation of a fictitious system of non-interacting particles that generate the same density as a real system of interacting electrons. The Kohn-Sham equation is defined by a local effective external potential in which the non-interacting particles move, typically denoted as $V_{eff}(\vec{r})$, which is the summation of the three terms $V_H(\vec{r}), V_{ext}(\vec{r})$ and $V_{XC}(\vec{r})$:

$$V_{eff}(\vec{r}) = V_H(\vec{r}) + V_{ext}(\vec{r}) + V_{XC}(\vec{r}) \quad \textbf{(II.26)}$$

Then the Kohn-Sham equation is as follows:

$$\left[-\frac{\hbar^2}{2m_e}\nabla_i^2 + V_{eff}(\vec{r})\right]\Psi_i(\vec{r}) = E_i\Psi_i(\vec{r}) \quad \textbf{(II.27)}$$

II.6. Self-Consistent Procedure

The self-consistent cycle involves the solving of the equation **(II.27)** iteratively. The procedure starts by defining the initial electron density ρ_{in} (which is usually constructed from a superposition of atomic densities $\rho_{in} = \rho_{cristal} = \sum_{at}\rho_{at}$)[25], after assuming the initial electron density, the next step is to diagonalize the secular equation:

$$(H - E_i S)C_i = 0 \quad \textbf{(II.28)}$$

Where:

H : is the Hamiltonian matrix.

S : represents the recovery matrix.

Then we get the solution of new density ρ_{out} , if the calculations do not converge, the charge densities ρ_{in} and ρ_{out} are mixed as follows:

$$\rho^{i+1}{}_{in} = (1-\alpha)\rho^{i}_{in} + \alpha\rho^{i}{}_{out} \quad \textbf{(II.29)}$$

i : represents the i-th iteration.

α : mixing parameter.

The iterative procedure is continued until convergence is achieved, which can be tested on energy and/or loads. Self-consistent procedure is illustrated in the general scheme illustrated in Figure **(II.2) [25].**

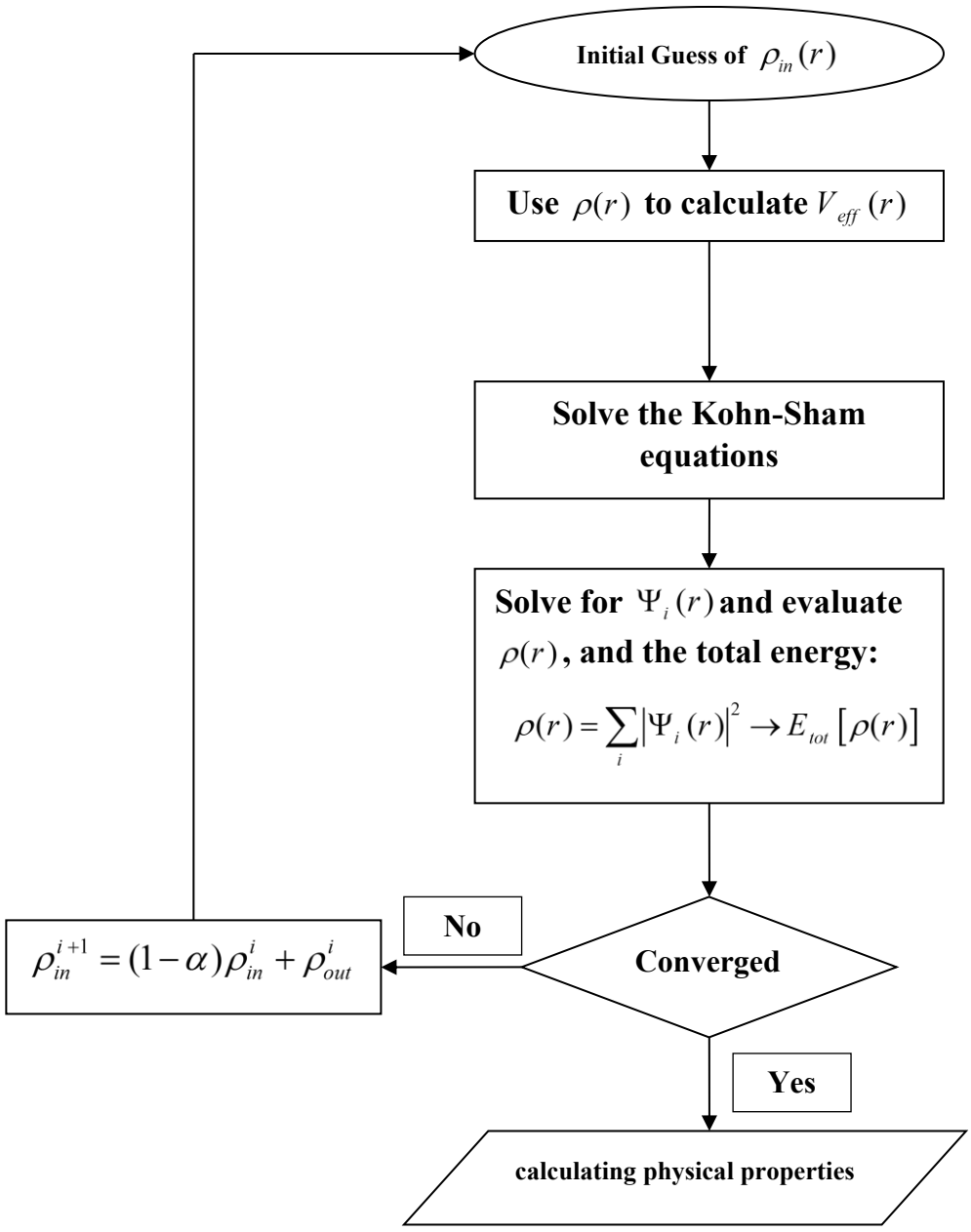

Figure (II.2): A general self-consistent scheme of Density Functional Theory.

II.7. The different types of functionalities

One of the great something that DFT can do regularly is to create an improvement for the approximation of the exchange-correlation energy $E_{XC}[\rho]$ **[19],** for this the two main approximations classes are:

Local-density approximations (LDA) and generalized gradient approximations (GGA).

II.7.1- Local Density Approximations LDA

The local density approximation (LDA) is a simple approximation to the exchange-correlation functional, where the exchange-correlation energy at each point in real space is approximated by the exchange-correlation energy of the homogeneous electron gas of density. The LDA replaces the exchange-correlation potential at each point with that of a homogeneous electron gas.

$$E_{XC}^{LDA}\left[\rho(\vec{r})\right]=\int \rho(\vec{r})\varepsilon_{XC}^{LDA}\left[\rho(\vec{r})\right]d^{3}\vec{r} \qquad \textbf{(II.30)}$$

Where $E_{XC}^{LDA}\left[\rho(\vec{r})\right]$ represents the exchange-correlation energy for a homogeneous gas of electrons of density ρ.

the corresponding exchange-correlation potential is:

$$V_{XC}^{LDA}(\vec{r})=\frac{\delta(\rho(\vec{r})\varepsilon_{XC}^{LDA}\left[\rho(\vec{r})\right])}{\delta\rho(\vec{r})} \qquad \textbf{(II.31)}$$

Finally, the term $E_{XC}^{LDA}\left[\rho(\vec{r})\right]$ of the relation **(II.30)** can be approximated by a sum of two contributions, so:

$$E_{XC}^{LDA}\rho(\vec{r})=\varepsilon_{X}^{LDA}\left[\rho(\vec{r})\right]+\varepsilon_{C}^{LDA}\left[\rho(\vec{r})\right] \qquad \textbf{(II.32)}$$

$\varepsilon_{X}^{LDA}\left[\rho(\vec{r})\right]$: functional exchange.

$\varepsilon_{C}^{LDA}\left[\rho(\vec{r})\right]$: correlation functional.

Or the exchange term, the so-called "Dirac exchange term" is given by:

$$\varepsilon_{XC}^{LDA}\left[\rho(\vec{r})\right]=-\frac{3}{4}\left(\frac{3}{\pi}\rho(\vec{r})\right)^{\frac{1}{3}} \qquad \textbf{(II.33)}$$

II.7.2- Generalized Gradient Approximations GGA

The generalized gradient approximation (GGA) is a type of exchange-correlation functional that seeks to improve upon the accuracy of the local density approximation (LDA) in electronic-structure calculations. The modification made in the generalized gradient approximation (GGA) makes the exchange-correlation energy functional E_{XC} account for the non-uniform character of the electron gas by depending not only on the electron density but also on its gradient**[26]**, Then we can write the exchange-correlation energy as:

$$E_{XC}^{GGA}\left[\rho(\vec{r})\right]=\int \rho(\vec{r})\varepsilon_{XC}\left[\rho(\vec{r}).\nabla\rho(\vec{r})\right]d^{3}\vec{r} \qquad \textbf{(II.34)}$$

$\varepsilon_{XC}\left[\rho(\vec{r}).\nabla\rho(\vec{r})\right]$: represents the exchange-correlation energy by electron in a system of electrons mutual interaction of non-uniform tensity.

The Linearized Augmented Plane Wave (LAPW) method is an implementation of Kohn-Sham density functional theory (DFT) adapted to periodic materials. It is a highly accurate method for performing electronic structure calculations for crystals**[27]**. The LAPW method treats both valence and core electrons on the same footing in the context of DFT and the treatment of the full potential and charge density without any approximations. The central design aspect of the LAPW method is the use of the LAPW basis set to represent the valence electron orbitals. The LAPW method is an extension of the Augmented Plane Wave (APW) method, which uses the radial solution to the spherically averaged potential for the augmentation in the Muffin-Tin spheres **[28]**.

II.8. The Augmented Plane Wave (APW) Method

The Augmented Plane Wave (APW) method was introduced by Slater in 1937 **[29]**. The APW is a method that uses the muffin-tin approximation to describe the crystal potential, and the basic approximation lies in the potential in which the potential is assumed to be spherically symmetric in the muffin-tin region and constant in the interstitial region as shown in Figure **(II.3).**

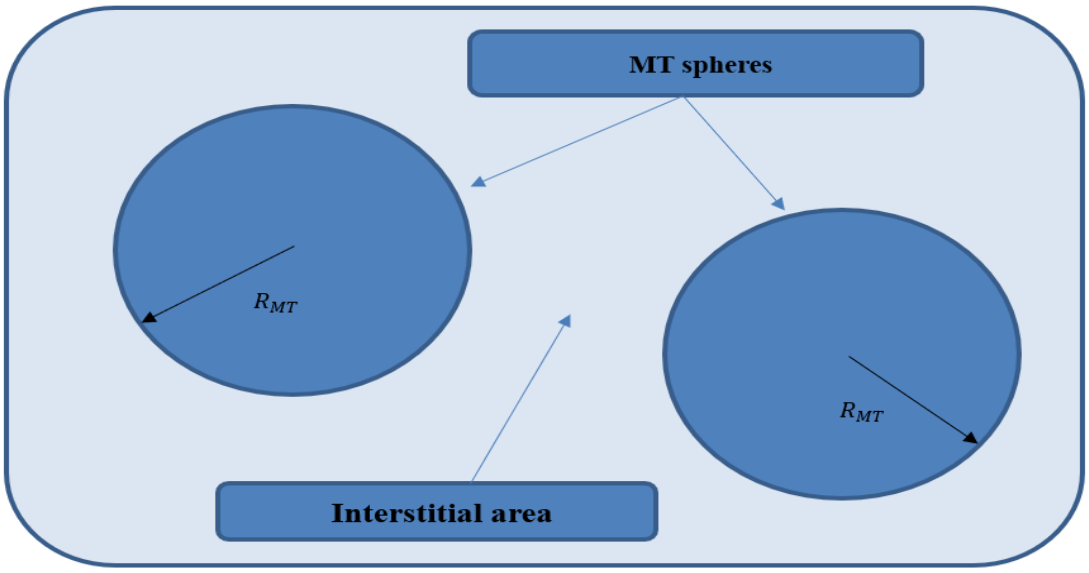

Figure (II.3): Representation of the partition of space according to the Muffin-Tin approximation.

The muffin-tin region is divided into two regions. The first region is near the atomic nuclei, where the potential and the wave function are similar to those of an isolated atom, i.e., they vary strongly, according to spherical symmetry in Muffin-Tin (MT) spheres. The second region is the interstitial region, where the potential is constant **[30].** The wave functions of the crystal are then developed in different bases depending on the region considered:

- inside the sphere of radius R_{MT}, we have a base constituted by a linear combination of the radial of radial functions multiplied by spherical harmonics.
- Plane waves in the interstitial area.

The wave function $\phi(r)$ is then of the form:

$$\phi(r)\begin{cases}\frac{1}{\Omega^{1/2}}\sum_G C_G e^{i(G+K)r} & \mathbf{r} > R_{MT}\\ \sum_{lm} A_{lm}U_l(r)Y_{lm}(r) & \mathbf{r} < R_{MT}\end{cases} \qquad \textbf{(II.35)}$$

Where:

R_{MT} : The radius of the sphere.

Ω : The volume of the unit cell.

A_{lm}, C_G : The development coefficients.

Y_{lm} : The spherical harmonics.

$U_l(r)$: is the regular solution of the Schrödinger equation for the radial part given by:

$$\left\{-\frac{d^2}{dr^2}+\frac{l(l+1)}{r^2}+V(r)-E_l\right\}rU(r)=0 \qquad \textbf{(II.36)}$$

Hence:

$V(r)$: represents the Muffin-Tin potential, it is the spherical component of the potential in the sphere.

E_l : is the linearization energy.

In the muffin-tin approximation, the radial functions defined by **(II.35)** are orthogonal to any eigenstate of the core. However, this orthogonality disappears in the sphere boundary **[31]**, as shown by the following Schrödinger equation:

$$(E_2-E_1)rU_1U_2 = U_2\frac{d^2rU_1}{dr^2}-U_1\frac{d^2rU_2}{dr^2} \qquad \textbf{(II.37)}$$

Where U_1 and U_2 are the radial solutions for the energies E_1 and E_2.

In this method, Slater made a particular choice for the wave functions, he shows that plane waves are the solutions of the Schrödinger equation in a constant potential. Whereas, the radial functions are the solution in the case of the spherical potential. Therefore, it proves that E_l is equal to the eigenvalue E. This approximation is very good for materials with face-centred cubic structure, and less satisfactory with the decrease of symmetry of the material.

To ensure the continuity of the function Φ(r) on the surface of the MT sphere, the coefficients A_{lm} have to be developed in terms of the coefficients C_G of the existing plane waves in the interstitial regions. Thus, after some algebraic calculations, we find that:

$$A_{lm} = \frac{4\pi_i^l}{\Omega^{1/2} U_l(R_\alpha)} \sum_G C_G J_l(|k+g|R_\alpha) Y_{lm}^*(K+G) \qquad \textbf{(II.38)}$$

In the APW method, the origin is taken to be the center of the sphere, and the coefficients A_{lm} are determined from those of the C_G plane waves. The energy parameters E_l are referred to as the variational coefficients of the APW method. The individual functions labeled by G are made compatible with the radial functions in the spheres, resulting in augmented plane waves (APW). The APW functions are solutions of the Schrodinger equation in spheres, but only for the energy E_l. Therefore, the energy E_l must be equal to that of the index band G. This means that the energy bands (for a point k) cannot be obtained by a simple diagonalization, and it is necessary to treat the secular determinant as a function of the energy**.**

The APW method can experience difficulties related to the function $U_l(R_\alpha)$ which appears in the denominator of equation **(II.37)**. Depending on the parameter E_l **,** the value of $U_\alpha(R_\alpha)$can become zero at the surface of the M.T. sphere, leading to a separation of the radial functions from the plane wave functions. To overcome this problem, several modifications to the APW method have been proposed, notably those by Koelling and by Andersen **[32]**.

II.9. Principle of LAPW Method

The LAPW method is among the most accurate methods for performing electronic structure calculations for crystals. As previously mentioned, the LAPW method is an improvement of the APW method developed by Andersen, Koelling, and Arbman based on Marcus' idea. The APW method uses the muffin-tin potential description, and the augmenting function corresponds to the exact muffin-tin potential eigenstate of eigenenergy. The LAPW method is a modification of the APW method that linearizes the basic functions inside the muffin-tin, leading to a better description of the eigenstate and a smaller basis set size to reach the same accuracy **[32,33]**.

The basic functions in the Muffin-Tin (MT) in the LAPW method are linear combinations of the radial functions $U_l(r)Y_{lm}$ and their derivatives $U_l'(r)Y_{lm}$ with respect to energy. The U_l functions are defined as in the APW method equation **(II.36)**, and the $U_l(r)Y_{lm}$ function must satisfy the condition of having both zero value and zero slope at the MT boundary and be normalized:

$$\left\{-\frac{d^2}{dr^2}+\frac{l(l+1)}{r^2}+V(r)-E_l\right\}rU'_l(r)=0 \qquad \textbf{(II.39)}$$

The radial functions $U'_l(r)$ and $U_l(r)$ ensure continuity with plane waves at the surface of the Muffin-Tin (MT) sphere. The basic functions of the LAPW method have an explicit form**:**

$$\phi(r)=\begin{cases}\frac{1}{\Omega^{1/2}}\sum_G C_G e^{i(G+K)r} & r > R_{MT}\\ \sum_{lm}\left[A_{lm}U_l(r,E_0)+B_{lm}U'_l(r,E_0)\right]Y_{lm}(r) & r < R_{MT}\end{cases} \qquad \textbf{(II.40)}$$

The coefficients B_{lm} correspond to the function $U'_l(r)$ and have the same nature as the coefficients A_{lm} . The linearization energy E_l is used in the LAPW method, and the coefficients A_{lm} are determined to ensure the continuity of the potential on the surface of the "Muffin-Tin" (MT) sphere. The LAPW method is more flexible than the APW method because the radial function can be obtained by a Taylor expansion for any linearization energy that differs only slightly from the real eigenenergy **[32]**. where the function $U_l(r)$ be developed as a function of derivative $U'_l(r)$ and energy E_l :

$$U_l(r,E)=U_l(r,E_l)+(E+E_0)U'_l(r,E_0)+0((E-E_0)^2) \qquad \textbf{(II.41)}$$

Where:

$U'_l(r,E_0)=\frac{dU_l}{dE}$

And $0((E-E_0)^2)$: Represents the energy squared error.

The LAPW method ensures the continuity of the wave function on the surface of the Muffin-Tin (MT) sphere, but with a loss of accuracy compared to the APW method. The LAPW method leads to an error on the wave functions of the order of $(E-E_0)^2$ and another on the band energies of the order of $(E-E_0)^4$. Despite this order of error, the LAPW functions form a good basis for obtaining all valence bands in a large energy region with a single value of E_l. However, if U_l is zero at the surface of the sphere, its derivative U'_l will be non-zero.

II.10. The roles of linearization energies

To obtain a good result, one should choose a parameter close to the center of the band, where the errors in the wave function (charge density) are of the order of $(E-E_0)^2$ and in the energy bands of the order of $(E-E_0)^4$. The choice of the parameter E_l can be optimized by calculating the total energy of the system for several values of E_l and selecting the set that gives the lowest energy. However, these strategies may fail in many cases.

The failure of the strategies mentioned earlier is due to the presence and extent of the core state, known as the semi-core state, in several elements, particularly alkali metals, rare earths, recently transition metals, and actinides. The augmented functions $U_l(r)Y_{lm}(r)$ and $U'_l(r)Y_{lm}(r)$ are orthogonal for each core state, but this condition is never satisfied exactly except for the case where the core states would not possess the same l **[34]**.

In the FP-LAPW method, the inaccurate orthogonality to core states has effects that are sensitive to the choices of l. The most critical case is when there is an overlap between the FP-LAPW bases and the core states, which introduces false core states into the energy spectrum known as ghost bands. These ghost bands are easily identified, have a very small dispersion, are highly localized in the sphere, and have a character of

the core state. To eliminate ghost bands from the spectrum, the energy parameter E_l can be set equal to the energy of the core state.

II.11. Development in local orbitals

The Linearized Augmented Plane Wave (LAPW) method aims to obtain precise band energies in the vicinity of the linearization energies E_l. In most materials, it is sufficient to choose these energies in the vicinity of the band centers. However, there are materials, such as those with 4f orbitals and transition metals, for which the choice of a single value of E_l is not sufficient to calculate all the band energies. This is known as the fundamental problem of the semi core state, which is intermediate between the valence and core states **[35,36]**.

To obtain precise band energies in the vicinity of the linearization energies E_l, the use of multiple energy windows or the use of a development in local orbitals can be employed as shown in Figure **(II.4)**. Multiple energy windows can be used when the choice of a single value of E_l is not sufficient to calculate all the band energies, such as in materials with 4f orbitals and transition metals **[36]**.

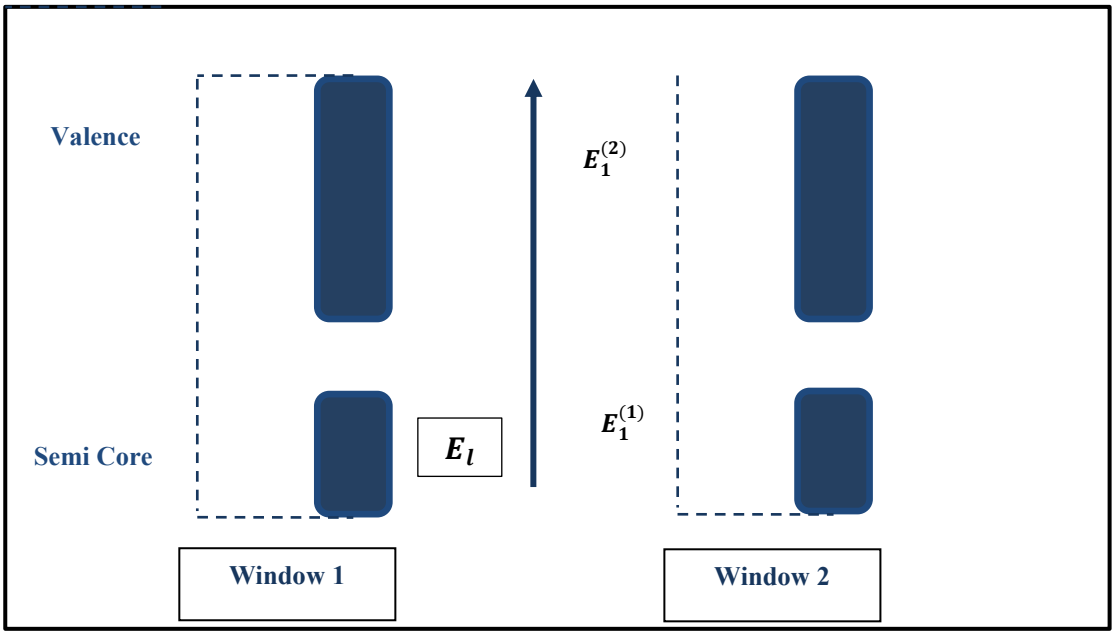

Figure (II.4): Multiple energy windows.

II.11.1- LAPW+lo method

Singh proposed "LO" orbitals as a linear combination of two radial functions, each corresponding to a different energy level, and the derivative of one of these functions with respect to energy. This approach is used in the LAPW method to avoid the use of multiple energy windows and to treat all bands from a single energy window. The LO method can be implemented using the second energy derivative radial functional **[37]**.

$$\phi(r) = \begin{cases} 0 & r > R_{MT} \\ \left[A_{lm}U_l(r,E_l) + B_{lm}U'(r,E_l)C_{lm}U_l(r,E_l)\right]Y_{lm}(r) & r < R_{MT} \end{cases} \quad \text{(II.42)}$$

Where the C_{lm} coefficients are of the same nature as the A_{lm} and B_{lm} coefficients defined above.

Local orbitals are defined for a given 'l' and 'm' and for a given atom in the unit cell, including all atoms and not just the inequivalent ones. These orbitals can be used beyond the treatment of the semi core states to improve the basis for the conduction bands. The implementation of local orbitals using the second energy derivative radial functional can be used to calculate the geometrical and electronic properties.

The LAPW-based linearization method has been successful due to the improvement of the LAPW method, which allows it to be extended to a wider class of compounds **[36,38]**.

The APW method encountered a problem with the energy dependence of the basis functions, which was resolved in the LAPW+LO method. However, this solution resulted in a larger basis size, which limited both the APW and LAPW+LO methods. The energy dependence of the basis functions led to a linearization error in the APW/LAPW basis set, which affected the calculated total energy and its volume dependence. The LAPW and APW+LO methods solved most of the problems associated with the APW method, but required a larger basis set size**[37,39]**.

Sjösted, Nordström, and Singh [29] developed a basis that combines the advantages of the APW method with those of the LAPW+LO method. This method is called "APW+lo" and corresponds to an energy-independent basis, which requires only a very small amount of plane wave cut-off energy compared to the APW method. The APW+lo method solves most of the problems associated with the APW method, such as the energy dependence of the basis functions, while also avoiding the larger basis set size required by the LAPW+LO method. The APW+lo method allows the use of the

LAPW, APW+lo, and LO types of orbitals simultaneously in the full potential augmented plane wave method **[37].**

The method involves using a standard APW basis but considering $U_l(r)$ for a fixed energy E_l to maintain the advantage brought by the linearization of the eigenvalue problem. However, a fixed energy basis does not provide a satisfactory description of the eigenfunctions. To ensure variational flexibility in the radial basis functions, local orbitals are added to the basis set. This method is called "APW+lo" and corresponds to an energy-independent basis that requires only a very small amount of plane wave cut-off energy compared to the APW method. The APW+lo method allows the use of the LAPW, APW+lo, and LO types of orbitals simultaneously in the full potential augmented plane wave method **[40].**

II.11.2- APW+lo method

An "APW+lo" base is defined by the combination of the following two types of wave functions:

- APW plane waves with a set of fixed E_l energies:

$$\phi(r)=\begin{cases}\frac{1}{\Omega^{1/2}}\sum_G C_G e^{i(G+K)r} & r > R_{MT}\\ \sum_{lm} A_{lm}U_l(r)Y_{lm}(r) & r < R_{MT}\end{cases} \qquad \text{(II.43)}$$

- Local orbitals different from those of the LAPW+LO method defined by:

$$\phi(r)=\begin{cases}0 & \mathbf{r} > R_{MT}\\ \left[A_{lm}U_l(r,E_l)+B_{lm}U'_l(r,E_l)\right]Y_{lm}(r) & \mathbf{r} > R_{MT}\end{cases} \qquad \text{(II.44)}$$

In a calculation, a mixed LAPW and APW+lo basis can be used for different atoms and even for different values of the l number. The APW+lo basis is typically used to describe orbitals that converge more slowly with the plane wave number, such as the 3d states of transition metals, or atoms with a small sphere size. The rest of the atoms are described with a LAPW basis. The LAPW and APW+lo methods can be employed simultaneously in the full potential augmented plane wave method **[38].**

II.12. FP-LAPW method

II.12.1- Principle of the FP-LAPW method

The linearized augmented plane wave method with total potential, as implemented in the wien2k code [38], involves using a mixed LAPW and APW+lo basis set. The LAPW basis is given by equation **(II.39)**, and the APW+lo basis is given by equations **(II.43)**. These bases are used according to the nature of the electronic states of the system under study. The APW+lo basis is typically used to describe orbitals that converge more slowly with the plane wave number, such as the **3d** states of transition metals, or atoms with a small sphere size. The rest of the atoms are described with a LAPW basis. No approximation is made for the form of the potential or the charge density. The potential describing the interactions between nuclei and electrons can be treated differently depending on whether one is inside or outside the Muffin-Tin sphere. It is developed in harmonics (in each spherical Muffin-Tin atom) and in Fourier series (in the interstitial regions):

$$V(r)=\begin{cases}\sum_{lm} v_{lm}(r) Y_{lm}(r) & \text{inside the sphere}\\ \sum_{k} v_{k} e^{ikr} & \text{outside the sphere}\end{cases} \qquad \textbf{(II.45)}$$

In the LAPW method, the potential has an angular dependence inside the Muffin-Tin sphere due to the intervention of spherical harmonics. The introduction of a potential of this type gives the LAPW method the characteristic "full potential" because it takes into account the angular dependence in the whole space.

II.12.2- Some advantages of the FP-LAPW method over the APW method

The full potential linearized augmented plane wave (FP-LAPW) method has some advantages over the augmented plane wave (APW) method. The FP-LAPW method enables accurate calculations of electronic and magnetic properties of materials, including the effects of spin-orbit coupling, and can treat **d** bands, which the APW method cannot. The FP-LAPW method also has a higher degree of accuracy than the APW method, especially for systems with large core states. Additionally, the FP-LAPW method does not require the use of pseudopotentials, which can introduce errors in the calculation **[41]**.

II.13. WIEN2k calculation code

WIEN2k is a computer program written in **Fortran** that allows for quantum mechanical calculations on periodic solids. It uses the full-potential (linearized) augmented plane-wave and local-orbitals method **[FP-LAPW+lo]** to solve the Kohn-Sham equations of density functional theory **[38]**. **WIEN2k** was developed by Peter Blaha and Karlheinz Schwarz from the Institute of Materials Chemistry of the Technical University of Vienna (Austria) and was first released in 1990 **[42]**. It has since been updated with subsequent releases, including **WIEN93**, **WIEN97**, and **WIEN2K**. The latest version, **WIEN2k_21.1**, was released on April 14, 2021. **WIEN2k** is widely used for solid-state calculations and has been licensed by more than 3400 user groups and has about 16000 citations on Google Scholar **[43]**.

➢ The different programs in WIEN2k and their flow are illustrated in Figure **(II.5).** The first step in the calculation process is initialization, which involves running a series of small auxiliary programs that produce inputs for the main programs.

NN: calculates the nearest neighbors up to a specified distance and thus helps to determine the atomic sphere radius.

LSTART: generates atomic densities and determines how the orbitals are treated in the band structure calculations (i.e., as core or band states, with or without local orbitals).

SYMMETRY: generates from a raw **case. Struct** file the space group symmetry operations, determines the point group of the individual atomic sites.

KGEN: generates a k-mesh in the Brillouin zone (BZ).

DSTART: generates a starting density for the SCF cycle by superposition of atomic densities generated in **lstart**.

LAPW0: (POTENTIAL) generates potential from density

LAPW1: (BANDS) calculates valence bands (eigenvalues and eigenvectors).

LAPW2: (RHO) computes valence densities from eigenvectors.

LCORE: computes core states and densities.

MIXER: mixes input and output densities.

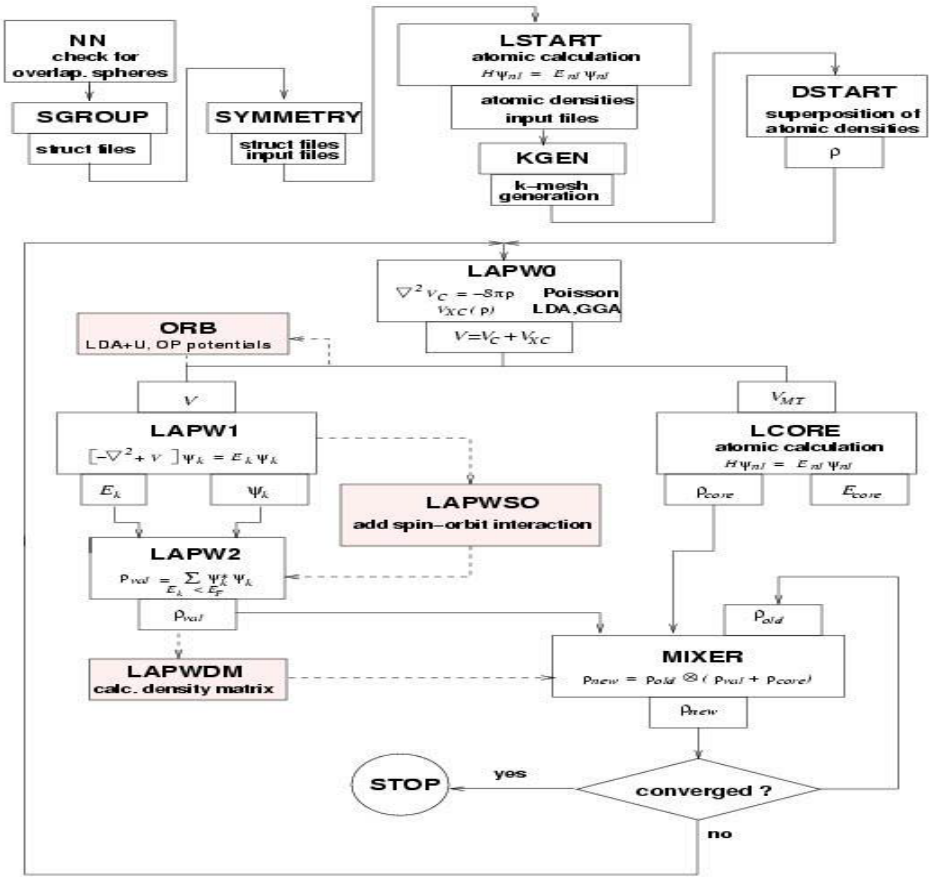

Figure (II.5): The Wien2k code program flowchart **[44]**.

Corollary of the chapter

At the end of this chapter, we conclude that DFT based on the FP-LAPW method is a powerful tool that helps us to solve and simplify the Schrodinger equation, providing a quantum-mechanical treatment of the electronic structure of atoms, molecules, and solids. This method allows us to study the properties of materials and how atoms interact with each other. The LAPW method is based on a partitioning of the material's unit cell into non-overlapping muffin-tin spheres, centered at the atomic nuclei, and an interstitial region. The LAPW basis set is used to represent the valence electron orbitals, leading to a faster convergence of the DFT calculations. The FP-LAPW method is widely used in solid-state physics and materials science, providing a benchmark for other methods and contributing to the development of more accurate DFT functionals **[44,45]**.

References

[1] S.J. Park, M.K. Seo, Composite Characterization, Interface Sci. Technol. 18 (2011) 631–738. https://doi.org/10.1016/B978-0-12-375049-5.00008-6.

[2] M.A. Meyers, K.K. Chawla, Chapter 1 Materials : Structure , Properties , and Performance, (n.d.).

[3] M.A. Martinez Page, S. Hartmann, Experimental characterization, material modeling, identification and finite element simulation of the thermo-mechanical behavior of a zinc die-casting alloy, Int. J. Plast. 101 (2018) 74–105. https://doi.org/https://doi.org/10.1016/j.ijplas.2017.10.010.

[4] L. Chen, C. Lan, B. Xu, K. Bi, Progress on material characterization methods under big data environment, Adv. Compos. Hybrid Mater. 4 (2021) 235–247. https://doi.org/10.1007/s42114-021-00229-w.

[5] H. Jiang, H.Y. Sun, Density-functional theory, Quantum Chem. Age Mach. Learn. (2022) 27–65. https://doi.org/10.1016/B978-0-323-90049-2.00002-0.

[6] K.A. Baseden, J.W. Tye, Introduction to Density Functional Theory: Calculations by Hand on the Helium Atom, J. Chem. Educ. 91 (2014) 2116–2123. https://doi.org/10.1021/ed5004788.

[7] What is Density Functional Theory?, in: Density Funct. Theory, 2009: pp. 1–33. https://doi.org/https://doi.org/10.1002/9780470447710.ch1.

[8] A. Zangwill, Hartree and Thomas: the forefathers of density functional theory, Arch. Hist. Exact Sci. 67 (2013) 331–348. https://doi.org/10.1007/s00407-013-0114-4.

[9] R. Haunschild, A. Barth, B. French, A comprehensive analysis of the history of DFT based on the bibliometric method RPYS, J. Cheminform. 11 (2019) 1–15. https://doi.org/10.1186/s13321-019-0395-y.

[10] K. Capelle, A bird's-eye view of density-functional theory, Brazilian J. Phys. 36 (2006) 1318–1341. https://doi.org/10.1590/s0103-97332006000700035.

[11] C. Kittel, Introduction to Solid State Physics, 8th edition, Wiley Sons, New York, NY. (2004).

[12] SCHRODINGER Erwin An Undulatory Theory of the Mechanics of Atoms and Molecules. Phys. Rev. 28, 1049 - Published 1 December 1926.

[13] E. Engel, R.M. Dreizler, Density Functional Theory Theoretical and Mathematical Physics, 2011.

[14] C. Woodward, Electronic Structure Methods Based on Density Functional Theory, Fundam. Model. Met. Process. (2018) 478–488. https://doi.org/10.31399/asm.hb.v22a.a0005429.

[15] E.J. Liberman, Air force institute of technology, (2015).

[16] P.J. Knowles, M. Schütz, H.-J. Werner, Ab Initio Methods for Electron Correlation in Molecules, 2000.

[17] computational-physics.pdf, (n.d.).

[18] S.Belbey. Études théoriques des propriétés fondamentales des composés à base de métaux de transition Mastère. Université de M'sila, (2021).

[19] Wijesooriya.K, Naval postgraduate, Security. (2017) 1–55. https://apps.dtic.mil/sti/pdfs/AD1046101.pdf.

[20] Advanced Theoretical Chemistry (Simons). (2021, April 8). University of Utah.

[21] S.Ullah. Theoretical characterization of grapheneand other 2D materials, Federal University of Juiz de Fora, January 22,2020.1–9.

[22] S. Ali, Colour Centres in 2-D hexagonal Boron Nitride, (2019).

[23] S. Cottenier, S. Cottenier, Density Functional Theory and the Family of (L)APW-methods: a step-by-step introduction, 2004.

[24] N. Lucid, Advanced Theoretical Chemistry, (2015) 1–484.

[25] N. Shan, M. Zhou, M.K. Hanchett, J. Chen, B. Liu, Practical principles of density functional theory for catalytic reaction simulations on metal surfaces–from theory to applications, Mol. Simul. 43 (2017) 861–885. https://doi.org/10.1080/08927022.2017.1303687.

[26] J.P. Perdew, A. Zunger, Self-interaction correction to density-functional approximations for many-electron systems, Phys. Rev. B. 23 (1981) 5048–5079. https://doi.org/10.1103/PhysRevB.23.5048.

[27] K. Lejaeghere, G. Bihlmayer, T. Björkman, P. Blaha, S. Blügel, V. Blum, D. Caliste, I.E. Castelli, S.J. Clark, A. Dal Corso, S. De Gironcoli, T. Deutsch, J.K. Dewhurst, I. Di Marco, C. Draxl, M. Dułak, O. Eriksson, J.A. Flores-Livas, K.F. Garrity, L. Genovese, P. Giannozzi, M. Giantomassi, S. Goedecker, X. Gonze, O. Grånäs, E.K.U. Gross, A. Gulans, F. Gygi, D.R. Hamann, P.J. Hasnip, N.A.W. Holzwarth, D. Iuşan, D.B. Jochym, F. Jollet, D. Jones, G. Kresse, K. Koepernik, E. Küçükbenli, Y.O. Kvashnin, I.L.M. Locht, S. Lubeck, M. Marsman, N. Marzari, U. Nitzsche, L. Nordström, T. Ozaki, L. Paulatto, C.J. Pickard, W. Poelmans, M.I.J. Probert, K. Refson, M. Richter, G.M. Rignanese, S. Saha, M. Scheffler, M. Schlipf, K. Schwarz, S. Sharma, F. Tavazza, P. Thunström, A. Tkatchenko, M. Torrent, D. Vanderbilt, M.J. Van Setten, V. Van Speybroeck, J.M. Wills, J.R. Yates, G.X. Zhang, S. Cottenier, Reproducibility in density functional theory calculations of solids, Science (80). 351 (2016).

[28] N.W. Ashcroft, Solid state physics / Neil W. Ashcroft, N. David Mermin, Saunders College, Philadelphia (Pa.), 1976.

[29] E. Sjöstedt, L. Nordström, D.J. Singh, Alternative way of linearizing the augmented plane-wave method, Solid State Commun. 114 (2000) 15–20.

[30] J.M. Wills, M. Alouani, P. Andersson, A. Delin, O. Eriksson, O. Grechnyev, Linear Muffin-Tin Orbital Method, Full-Potential Electron. Struct. (2010) 35–46.

[31] V.O. Lume, October 1975, Weatherwise. 28 (1975) 276–283. https://doi.org/10.1080/00431672.1975.9931783.

[32] C.A.B. Set, Chapter 3 The (L) APW + lo Method, (n.d.).

[33] D.J. Singh, Introduction to the LAPW Method, Planewaves, Pseudopotentials LAPW Method. (1994) 35–43. https://doi.org/10.1007/978-1-4757-2312-0_4.

[34] L. Vitos, H.L. Skriver, B. Johansson, J. Kollár, Application of the exact muffin-tin orbitals theory: The spherical cell approximation, Comput. Mater. Sci. 18 (2000) 24–38. https://doi.org/10.1016/s0927-0256(99)00098-1.

[35] O. Krogh Anderson. Leniar Method in Band Theory. In: The Electronic Structure of Complex Systems Department of Electrophysics, Technical University, Lyngby, Denmark.

[36] L.M. Wienk, D.J. Singh, The Linearized Augmented Planewave Scintillators for Radiation Detection, (2014).

[37] F. Bultmark, Distorted Space and Multipoles in Electronic Structure Calculations, 2009.

[38] P. Blaha, K. Schwarz, G. Madsen, D. Kvasnicka, J. Luitz, WIEN2k, 2011.

[39] M. Aichhorn, L. Pourovskii, V. Vildosola, M. Ferrero, O. Parcollet, T. Miyake, A. Georges, S. Biermann, Dynamical mean-field theory within an augmented plane-wave framework: Assessing electronic correlations in the iron pnictide LaFeAsO, Phys. Rev. B - Condens. Matter Mater. Phys. 80 (2009) 1–17. https://doi.org/10.1103/PhysRevB.80.085101.

[40] S. Blügel, G. Bihlmayer, Full-Potential linearized augmented planewave method, Comput. Nanosci. 31 (2006) 85–129.

[41] P. Blaha, The FP-LAPW and APW + lo methods Overview of DFT concepts, (n.d.).

[42] P. Blaha, K. Schwarz, P. Sorantin, S.B. Trickey, Full-potential, linearized augmented plane wave programs for crystalline systems, Comput. Phys. Commun. 59 (1990) 399–415.

[43] K. Schwarz, P. Blaha, Solid state calculations using WIEN2k, Comput. Mater. Sci. 28 (2003) 259–273.

[44] T. Van Mourik, M. Bühl, M.P. Gaigeot, Density functional theory across chemistry, physics and biology, Philos. Trans. R. Soc. A Math. Phys. Eng. Sci. 372 (2014).

[45] K. Schwarz, P. Blaha, DFT Calculations for Real Solids, 2017.

CHAPTER III

Results and discussions

III.1. Introduction

The aim of this chapter, that is divided into two main sections, is to investigate the electronic properties, such as the band structure and density of states, and the semiconductor properties, such as the lattice parameter **a** and **c**, of the semiconductor material **h-BN** in both bulk **3D** and **2D** forms in the first part. And doing a comparative study with material **GaN**, and analyzing and interpreting the difference results obtained when we have changed the **Ga** atom by **B** atom in the second part. To conduct this study, the **WIEN2K** code was utilized, which is based on the linearized augmented plane wave (LAPW) method that employs the density functional theory (DFT). The exchange and correlation potential were determined using several approximations, including the LDA, GGA approximations.

III.2. Bibliographic reminder

✓ The Muffin-Tin spheres are used to describe the potential well in the crystal lattice, and their radius is an important parameter in the approximation, and are given in atomic units (Bohr radius) or in Angstrom (A°)**[1]**.

✓ The cut-off parameter $R_{K\,max}$ is used in the Muffin-Tin approximation to ensure the convergence of the energy eigenvalues. $R_{K\,max}$ is the average radius of the Muffin-Tin spheres, and K_{max} is the norm of the largest wave vector used for the plane wave expansion of the eigenfunctions. The wave functions in the interstitial region have been increased in the plane waves with a cut-off $R_{K\,max}$ to obtain the convergence of the energy eigenvalues**[2,3]**.

✓ The number of K-points considered in the Brillouin zone is an important parameter in the electronic structure calculations of solids. The Brillouin zone is a uniquely defined primitive cell in reciprocal space, which has all the symmetries of the point group of the reciprocal lattice**[4,5]**.

III.3. Details of Calculation

The calculation with Wien2k is able to generate the ground-state charge density, occupations, Fermi level, and so on.

The electronic structure calculation code WIEN2K was used to perform the calculations in this thesis. WIEN2K is a DFT implementation of the linearized augmented plane wave method with total potential (FP-LAPW)**[6,7]**. The semi-relativistic calculations were conducted by neglecting the spin-orbit effect **[6]**.The FP-LAPW method is one of the most accurate methods for performing electronic structure calculations for crystals. To determine the exchange-correlation potential, two approximations were used in our work which are:

1- The local Density Approximation (LDA) parameterized by Pedrew and Wang.
2- The Generalized Gradient Approximation (GGA) parameterized by Pedrew, Berke, and Erenzerhof **[8,9]**.

A. PART ONE: studying the properties of h-BN

Hexagonal Boron-Nitride h-BN

- HCP lattice, ABAB stacking
- Four atoms per cell, B and N (16 electrons)
- Lattice constants: a = 4.736 (a.u), c/a = 3.06

We have chosen for the compound h-BN in 3D and 2D the following convergence parameters indicated in the following table:

Table (III.1): Our choice of parameters included in the calculation for the compound h-BN in (3D) and (2D).

Compound	Approximation	$R_{MT_{min}} \times K_{max}$	K Points	R_{MT} (B)	R_{MT} (N)
h-BN (3D)	GGA	9	1200	1.23	1.36
	LDA	9	1200	1.23	1.36
h-BN (3D) Super-cell	GGA	9	1200	1.23	1.36
	LDA	9	1200	1.23	1.36
h-BN (2D) Super-cell (1x1x1)	GGA	7	200	1.29	1.43
	LDA	7	200	1.29	1.43
h-BN (2D) Super-cell (2x2x1)	GGA	7	200	1.29	1.43
	LDA	7	200	1.29	1.43
h-BN (2D) Super-cell (3x3x1)	GGA	7	200	1.29	1.43
	LDA	7	200	1.29	1.43

III.4. Crystal structure and electronic configuration of h-BN (3D) and h-BN (2D) material

III.4.1. Electronic configuration

Electronic configuration refers to the arrangement of electrons around the nucleus of an atom or molecule. It describes how electrons are distributed in atomic orbitals, including shells, sub-shells, and orbitals within the atom, so the electronic structure of the material h-BN is as follows:

Table (III.2): the electronic configuration of Boron-Nitride (BN).

Element	Number of electros Z	Electronic Configuration
B	5	[He] $2s^2 2p^1$ $1s^2 2s^2 2p^1$
N	7	[He] $2s^2 2p^3$ $1s^2 2s^2 2p^3$

III.4.2. Crystal structure of Boron-Nitride in (3D) and (2D)

h-BN crystallizes in the hexagonal crystal system and belongs to the space group by the following:

h-BN in 3D: $P6_3/mmc$, (n=194), Super-cell 1x1x1: P1.

h-BN in 2D:

- Super-cell 1x1x1: P-6m2, (n=187).
- Super-cell 2x2x1: P-6m2, (n=187).
- Super-cell 3x3x1: P-6m2, (n=187).

The Figures below shows the crystal structure of Boron-Nitride in 3D and 2D:

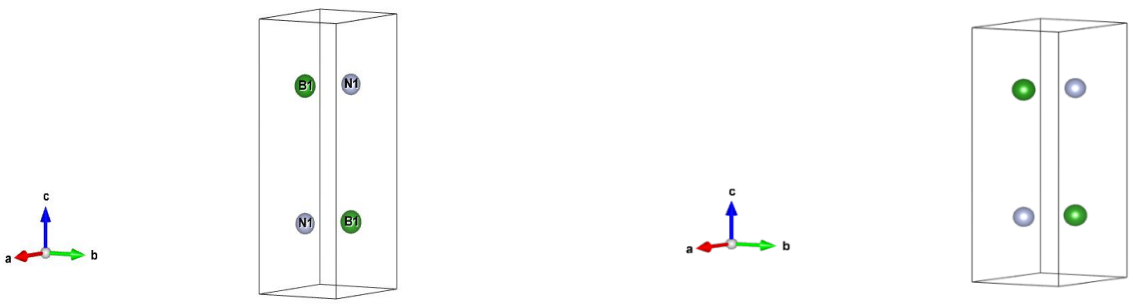

Figure (III.1): The crystal structure of Boron-Nitride h-BN in 3D.

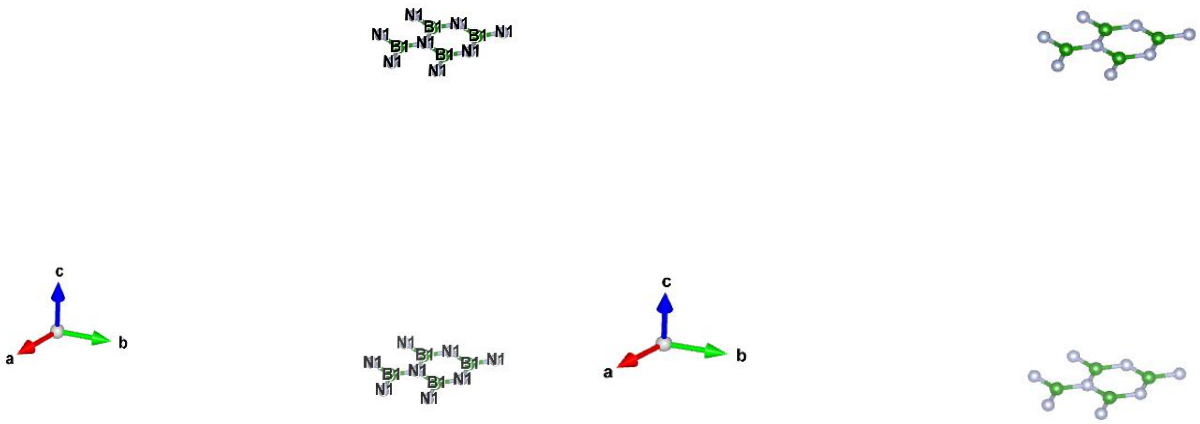

(a)

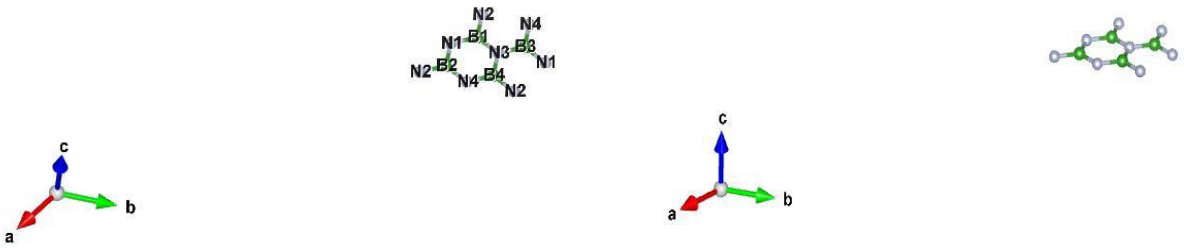

(b)

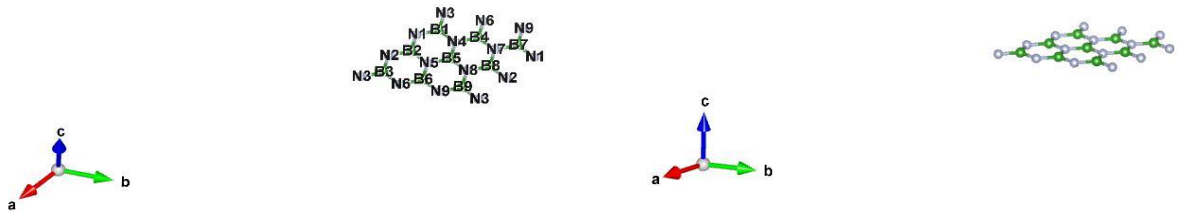

(c)

Figure (III.2): The crystal structure of Boron-Nitride h-BN in 2D:

(a):is h-BN(2D)-super-cell (1x1x1). **(b):** is h-BN(2D)-super-cell (2x2x1).

(c): is h-BN(2D)-super-cell (3x3x1).

h-BN crystallizes in the hexagonal system and belongs to the $P6_3/mmc$ space group. The structure is two-dimensional and consists of two BN sheets stacked together. The basic unit of h-BN is a honeycomb structure formed by the alternately arranged B and N atoms in a two-dimensional plane **[10]**. The length of the liaison between B and N in h-BN is approximately 3.07 Å **[11]**, and in h-BN, each atom of N is sp2 bonded in-plane to three atoms of B, and each atom of B is sp2 bonded in-plane to three atoms of N **[10].**

III.5. Structural properties

Structural properties refer to the physical and chemical properties of a material that are determined by its microscopic arrangement of atoms and molecules. The relationship between the structure and properties of materials is important in designing new materials in a rational way **[12]**.

To evaluate the structural properties of the two-dimensional (2D) and three-dimensional (3D) h-BN compound dimensions (3D) as: theoretical lattice parameters, the modulus of compressibility (β), and its derivative with respect to pressure (β') from the fundamental equilibrium state, the total energy obtained E_{min} is extrapolated, and the energy values thus obtained are then interpolated by the Murnaghan (1944)**[13,14]**.

$$E(V) = E_0 + \frac{\beta}{\beta'(\beta'+1)}\left[V\left(\frac{V_0}{V} - V_0\right)\right] + \frac{\beta}{\beta'}(V - V_0) \qquad \textbf{(III.1)}$$

Where:

E_0 : is the total energy.

V_0 : is the volume at equilibrium.

β : the modulus of compressibility.

The modulus of compressibility is determined at the minimum of the E(V) curve by the relation:

$$\beta = V\frac{\partial^2 E}{\partial V^2} \qquad \textbf{(III.2)}$$

β' : The derivative of the modulus of compressibility:

$$\beta' = \frac{\partial \beta}{\partial P} \qquad \text{(III.3)}$$

III.5.1. Optimization Curves

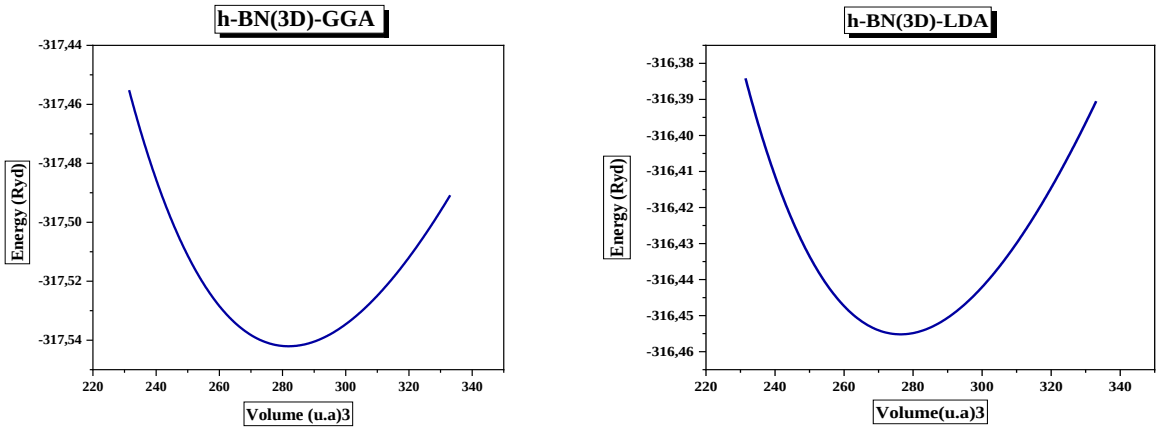

Figure (III.3): (a): The variation of energy as a function of volume for h-BN (3D) calculated by GGA and LDA.

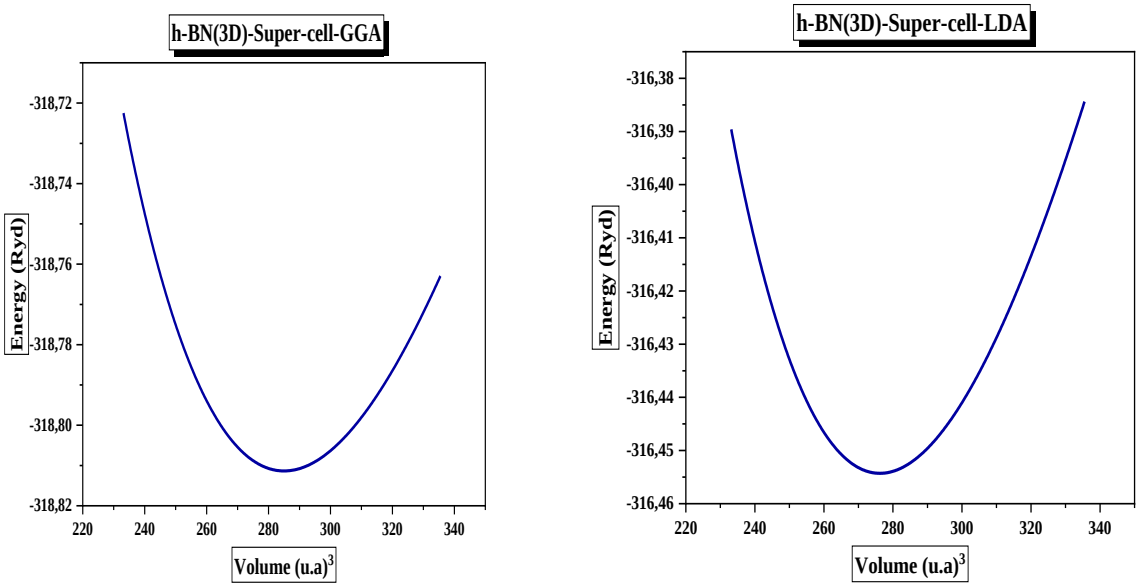

Figure (III.3): (b): The variation of energy as a function of volume for h-BN(3D)-Super-cell calculated by GGA and LDA.

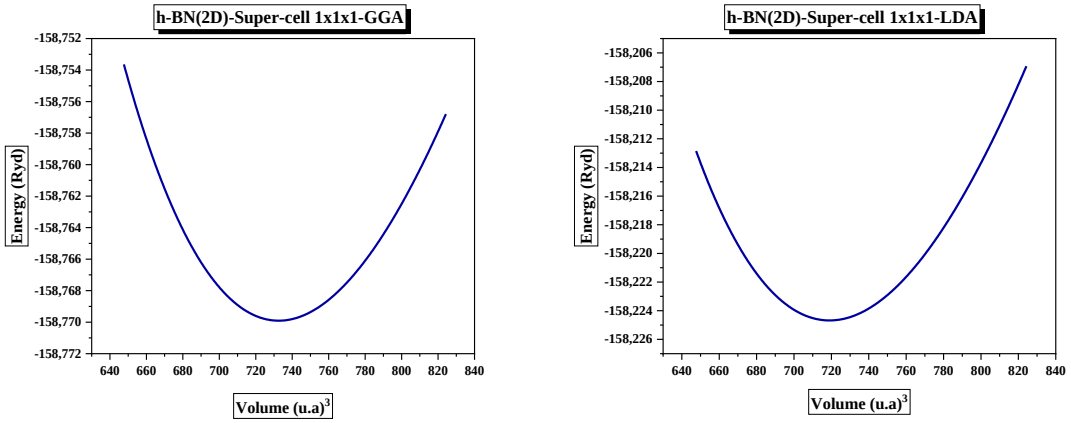

Figure (III.4): (a): The variation of energy as a function of volume for h-BN (2D)-Mono calculated by GGA and LDA.

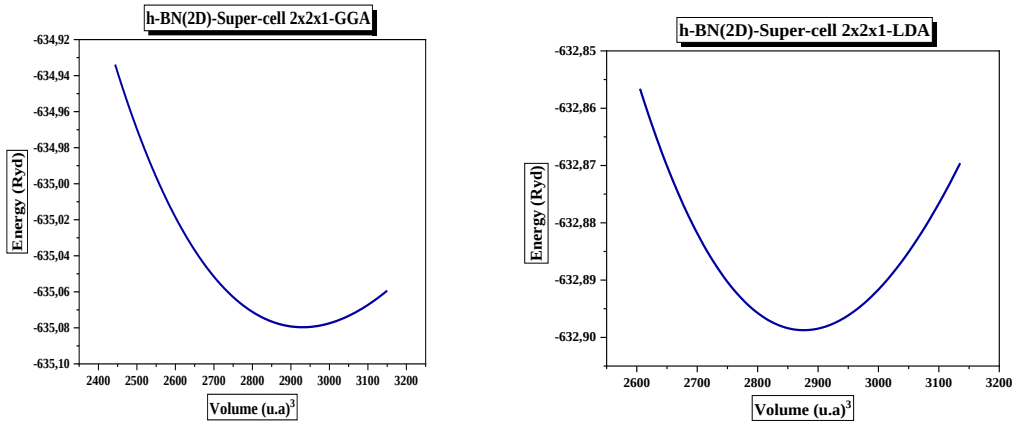

Figure (III.4): (b): The variation of energy as a function of volume for h-BN (2D)-Sup2x2x1 calculated by GGA and LDA.

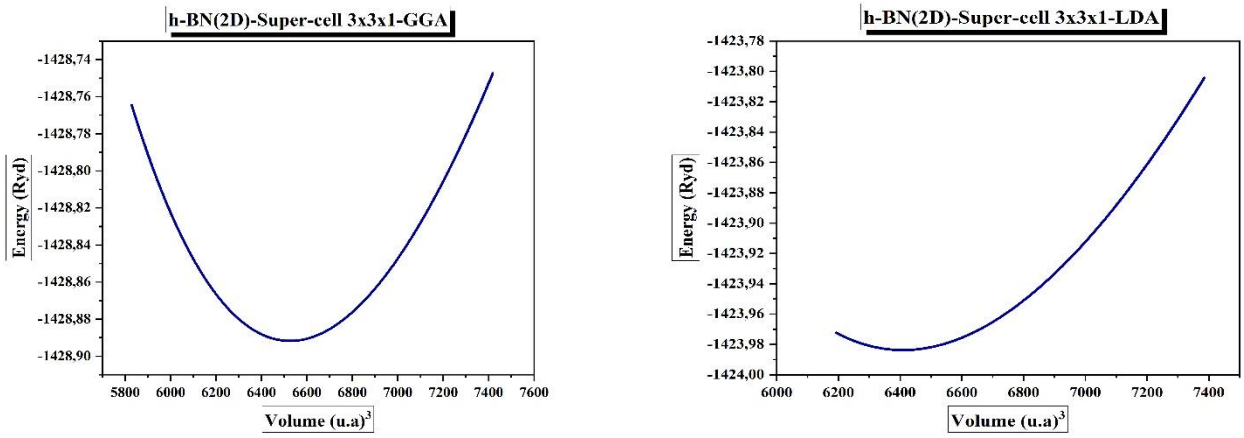

Figure (III.4): (c): The variation of energy as a function of volume for h-BN (2D)-Sup3x3x1 calculated by GGA and LDA.

III.5.2. Table of Structural Properties

In the table below we put the structural properties of the material h-BN in 3D and 2D:

Table (III.3): the structural properties of h-BN (3D) and h-BN(3D)-Super-cell Murnaghan.

Compound	Parameters	GGA	LDA	Theoretical value	Relative error (%)	
					GGA	LDA
h-BN (3D)	a (Å)	2.50	2.48	2.50	0	-0.008
	c (Å)	7.68	7.74	7.68	0	0.007
	c/a	3.06	3.11	3.06	0	0.016
	β (GPa)	209.8244	218.3702	-	-	-
	β’	3.6010	3.5720	-	-	-
	E_{min}	-317.542097	-316.455241	-	-	-
	V_0	281.8920	276.3942	-	-	-
h-BN (3D) Super-cell	a (Å)	2.51	2.49	2.51	0	-0.007
	c (Å)	7.78	7.67	7.70	0.01	-0.003
	c/a	3.09	3.08	3.06	0.009	0.006
	β (GPa)	204.4518	218.3721	-	-	-
	β’	3.5976	3.5634	-	-	-
	E_{min}	-318.811394	-316.454335	-	-	-
	V_0	284.9883	276.2662	-	-	-

In the table (III.3) we have brought all the values of structural properties at the equilibrium such as the lattice parameters **a**, **c** and the ratio **c/a**, the modulus of compressibility and its first derivative, the minimum total energy and the volume by using the GGA and LDA approximations. Also, we have included the theoretical values in the table to make the comparison easy and clear.

- **For h-BN (3D) structure**

As shown in the table above we note that relative error in **GGA=0** is higher than relative error in **LDA=-0.008**, but GGA gives results better than LDA approximation in lattice parameters.

We note can also note that the modulus of compressibility β in GGA= 209.8244 (GPa), its value is less than it is in LDA= 218.3702 (GPa).

And the value of volume in GGA is higher than the one in LDA.

- **For h-BN (3D)-Super-cell structure**

From the table we can be observed that the relative error in GGA=0 is greater than LDA=-0.008, but GGA approximation gives much closer results than LDA.

the modulus of compressibility β in GGA= 204.4518 (GPa), its value is less than it is in LDA= 218.3721 (GPa).

When comparing the h-BN(3D) structure with h-BN(3D)-Super-cell, it can be said that the values of the lattice parameters remained almost constant with a slight change in volume, modulus of compressibility and the total energy.

Table (III.4): the structural properties of h-BN (2D) Super-cell (1x1x1) (2x2x1) Murnaghan.

Compound	Parameters	GGA	LDA	Theoretical value	Relative error (%)	
					GGA	LDA
h-BN (2D) Super-cell (1x1x1)	a (Å)	2.51	2.49	2.50	0.004	-0.004
	c (Å)	19.97	19.86	20.00	-0.002	-0.007
	c/a	7.96	7.97	8.00	-0.005	-0.003
	β (GPa)	40.2837	41.8208	-	-	-
	β’	3.5967	3.5631	-	-	-
	E_{min}	-158.769910	-158.224682	-	-	-
	V_0	732.5699	719.0633	-	-	-
h-BN (2D) Super-cell (2x2x1)	a (Å)	2.51	2.47	2.50	0.004	-0.012
	c (Å)	19.97	19.86	20.00	-0.002	-0.007
	c/a	7.95	8.04	8.00	-0.006	0.005
	β (GPa)	40.3118	41.8842	-	-	-
	β’	3.6088	3.5099	-	-	-
	E_{min}	-635.079634	-632.898744	-	-	-
	V_0	2930.1428	2876.2970	-	-	-

Table (III.5): the structural properties of h-BN (2D) Super-cell (3x3x1) Murnaghan.

Compound	Parameters	GGA	LDA	Theoretical value	Relative error (%)	
					GGA	LDA
h-BN (2D) Sup 3x3x1	a (Å)	2.51	2.48	2.50	0.004	-0.008
	c (Å)	19.90	19.78	20.00	-0.492	-1.094
	c/a	7.93	7.97	8.00	-0.008	-0.003
	β (GPa)	42.3202	43.7890	-	-	-
	β'	3.5329	3.4029	-	-	-
	E_{min}	-1428.891776	-1423.983679	-	-	-
	V_0	6526.4158	6408.6914	-	-	-

Tables (III.4) and (III.5)

- **For h-BN (2D) structure**

  It can be seen that relative error in **GGA=0.004** is highest than **LDA=-0.004**.

  To conclude we can say that GGA is better suited than LDA for the calculation of structural properties in 2D.

  For the modulus of compressibility is visibly clear that in GGA is higher than LDA. Specifically:

  In h-BN(2D)-Super-cell 1x1x1: β (GGA)= 40.2837 (GPa), β (LDA)= 41.8208 (GPa).

- **For h-BN (2D)-Super-cell 2x2x1 structure**

  As the table above shows, the relative error in **LDA=-0.012** is less than the relative error in **GGA=0.004**. Hence

- **For h-BN (2D)-Super-cell 3x3x1 structure**

  We also note that the values given by the **LDA=-0.008** approximation are less than the values given by the **GGA=0.004** approximation.

Now, the value of the modulus of compressibility in the two structures is close because both structures are in two-dimensional. However, in the Super-cell 3x3x1 structure the modulus is slightly larger than that of the Super-cell 2x2x1 structure.

In Super-cell 2x2x1: β (GGA)= 40.3118 (GPa), β (LDA)= 41.8842 (GPa).

In Super-cell 3x3x1: β (GGA)= 42.3202 (GPa), β (LDA)= 43.7890 (GPa).

III.6. Electronic properties

The electronic properties of a material are important because they allow us to analyze and understand the nature of the bonds that form between different elements of the material. These properties include band structures, charge densities, and densities of states. The behavior of electrons within materials determines their magnetic, thermal, optical, and electrical properties.

III.6.1- Band Structure

Band structure is a representation of the allowed electronic energy levels of solid materials. It describes the range of energy levels that electrons may have within a solid, as well as the ranges of energy that they may not have (called band gaps or forbidden bands). The energy of adjacent levels is so close together that they can be considered as a continuum, an energy band. The band structure is often used to determine whether a material is a conductor, semiconductor, or insulator **[15].**

The energy gap defined by the difference between the maximum of valence band and the minimum of conduction band.

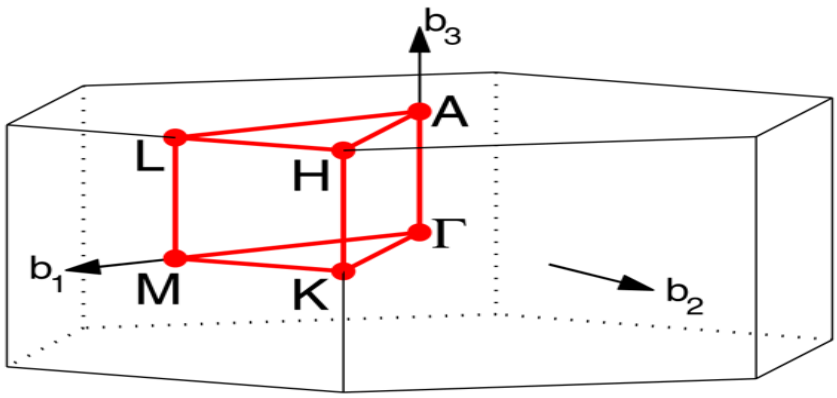

Figure (III.5): The first Brillouin zone of Boron-Nitride h-BN.

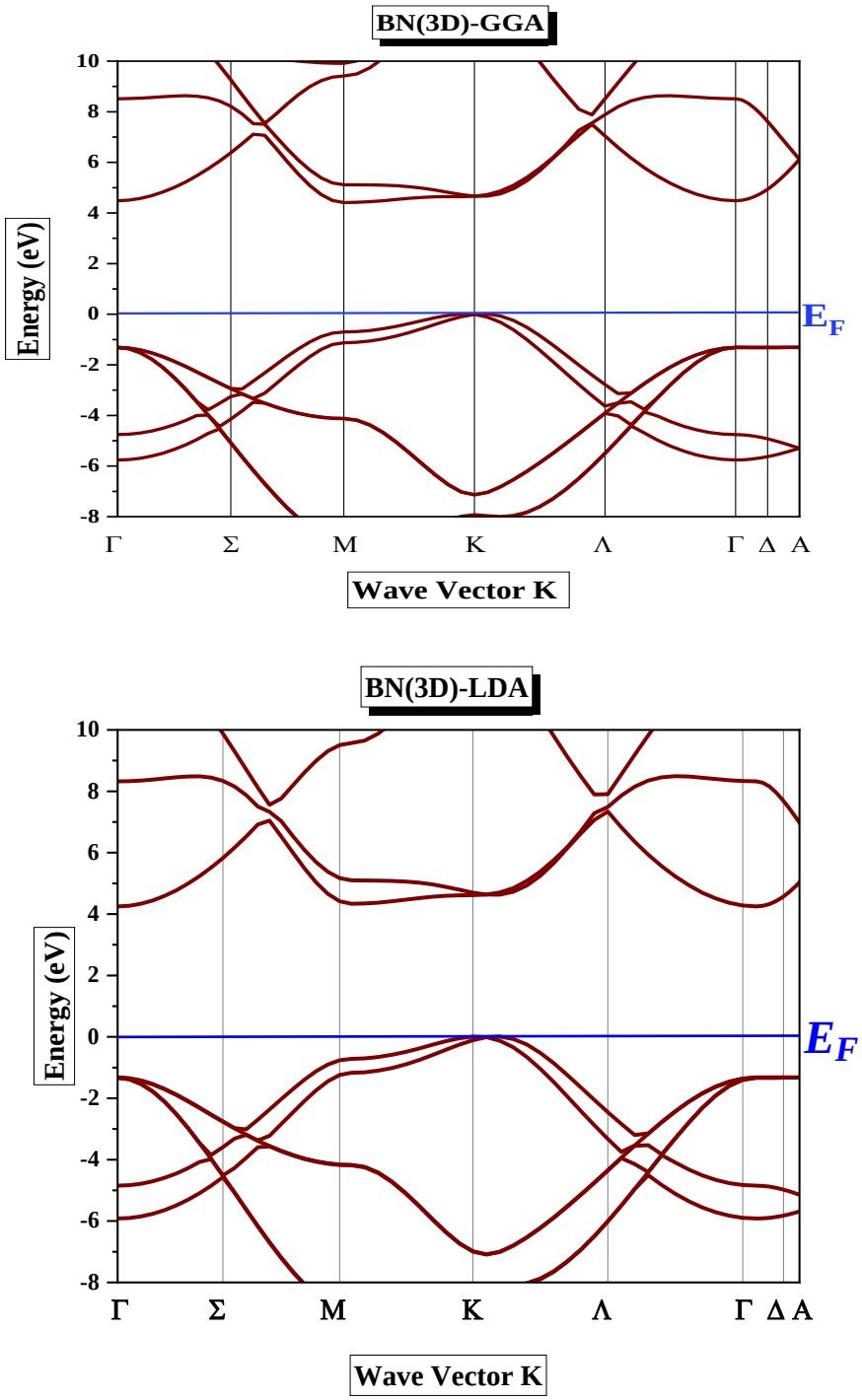

Figure (III.6): Band structure of h-BN (3D) in GGA and LDA.

- The Figure (III.6): represent electronic band structure of h-BN in bulk according to the directions of Brillouin zone associated with the ground state. As illustrated in the diagram of Figure (III.6), the compound h-BN has a maximum limit in valence band (VBM) and a minimum limit in conduction band (CBM) located at the point **(M→K)**

it is mean that we have an insulator with indirect gap, in both approximations **GGA** and **LDA**.

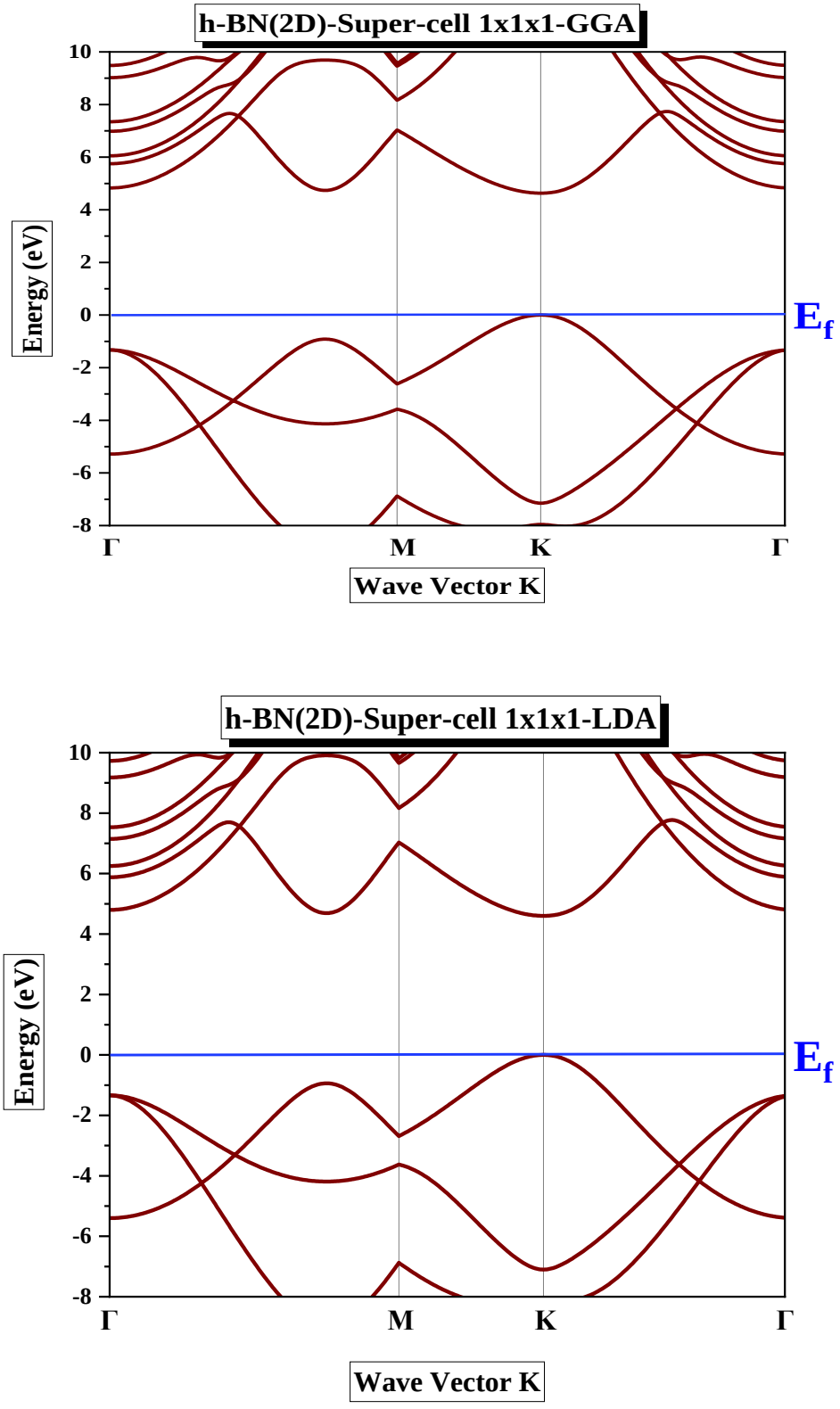

Figure (III.7): Band structure of h-BN (2D) super-cell (1x1x1) in GGA and LDA.

- The Figure (III.7): shows also the electronic band structure of h-BN in 2D (super-cell 1x1x1) and we conclude that it has a maximum limit in point K and a minimum limit in point K also **(K→K)**, that is mean we have an insulator with direct gap, in **GGA** and **LDA**.

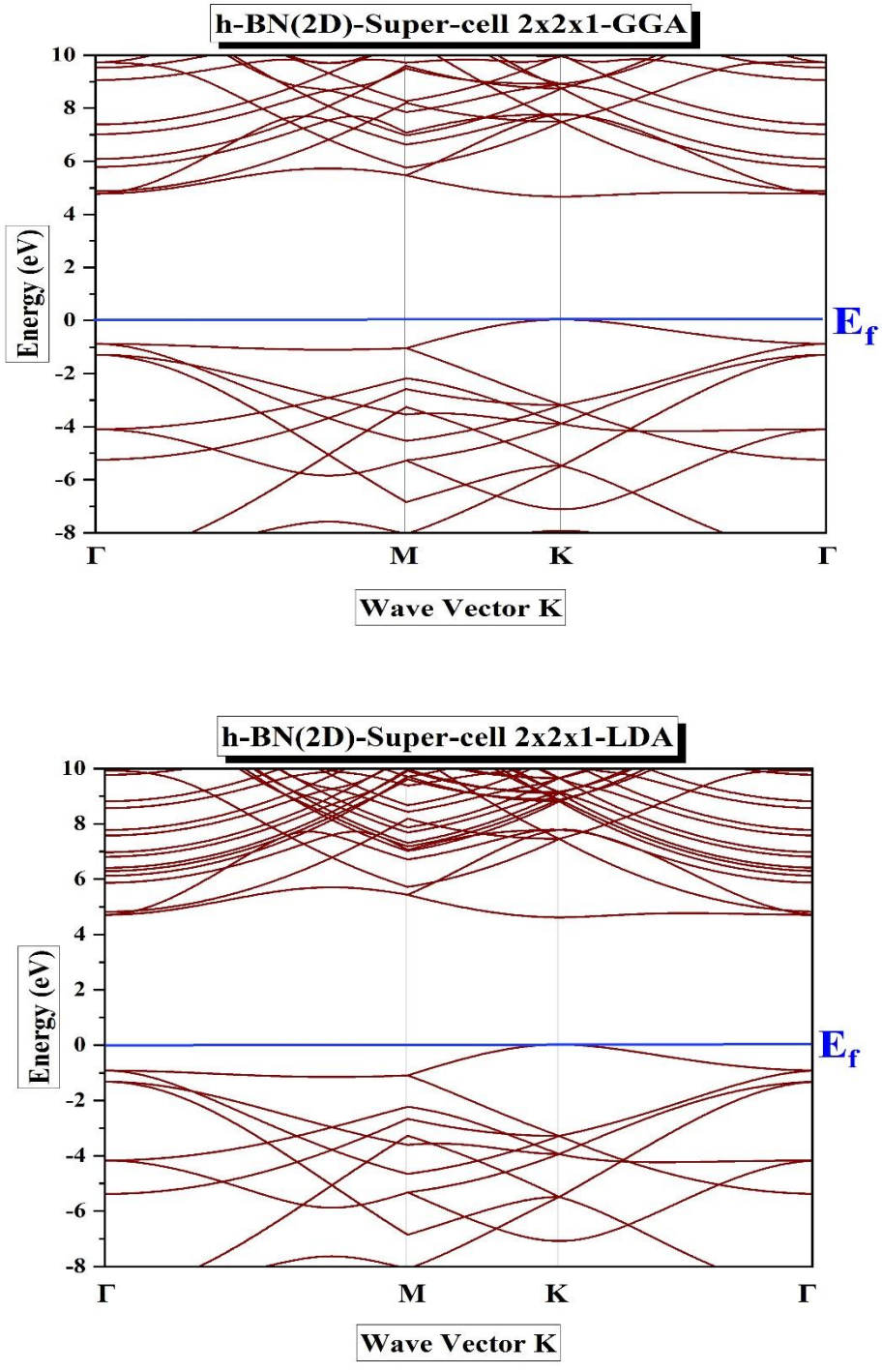

Figure (III.8): Band structure of h-BN (2D)-Super-cell (2x2x1) in GGA and LDA.

- The Figure (III.8): in this figure the material h-BN in 2D super-cell 2x2x1 is visibly clear that it has a maximum value at K point and a minimum value at K point **(K→K)**, So we conclude that we have an insulator with direct gap in **GGA** and **LDA**.

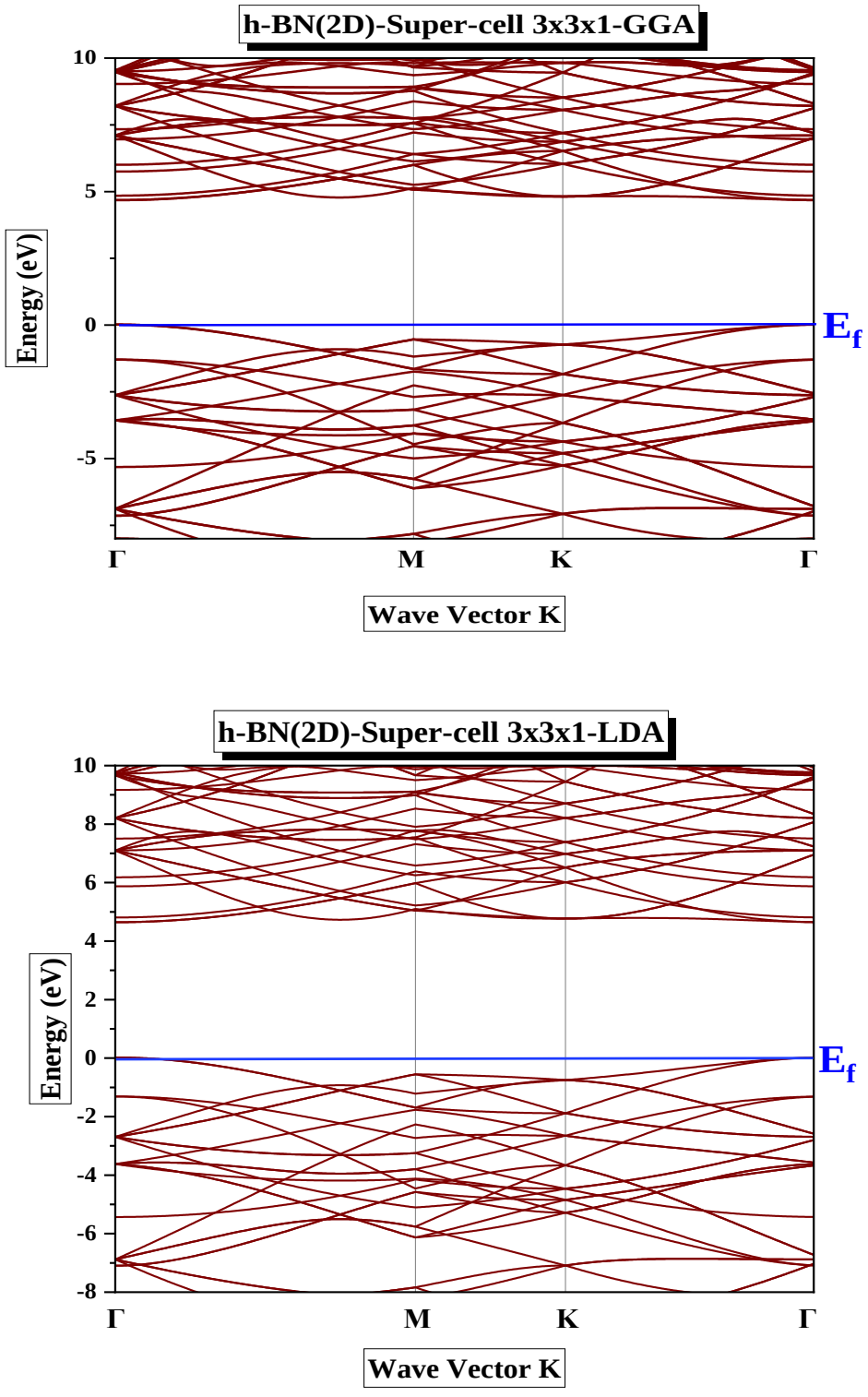

Figure (III.9): Band structure of h-BN (2D)-Super-cell (3x3x1) in GGA and LDA.

- The Figure (III.9): in this case we observe that we have a maximum value at **Γ** point and a minimum value at **Γ** point **(Γ→Γ)**, so, the nature of compound h-BN in super-cell (3x3x1) is an insulator with direct gap.

Table (III.6): Energy gap values in 3D and 2D dimensions Super-cell 1x1x1, Super-cell 2x2x1 and 3x3x1 calculated with GGA and LDA.

Material	E_g (eV)	
	GGA	LDA
h-BN (3D)	4.413	4.248
h-BN (2D) Super-cell 1x1x1	4.632	4.602
h-BN (2D) Super-cell 2x2x1	4.698	4.638
h-BN (2D) Super-cell 3x3x1	4.696	4.662

From table (III.6) we can see that the GGA approximation gives slightly higher values than the LDA approximation. And we notice that the values in 3D are less than the ones in 2D. So, we conclude that the energy gap can increase in the 2D structures.

III.6.2- Density State

The density of states (DOS) is a crucial physical quantity that helps in understanding the electronic band structure. Most transport properties of conductive solids depend on the DOS. The DOS provides the partial densities of states that describe the structure of chemical bonds between atoms in a crystal or molecule.

As shown in the figures below:

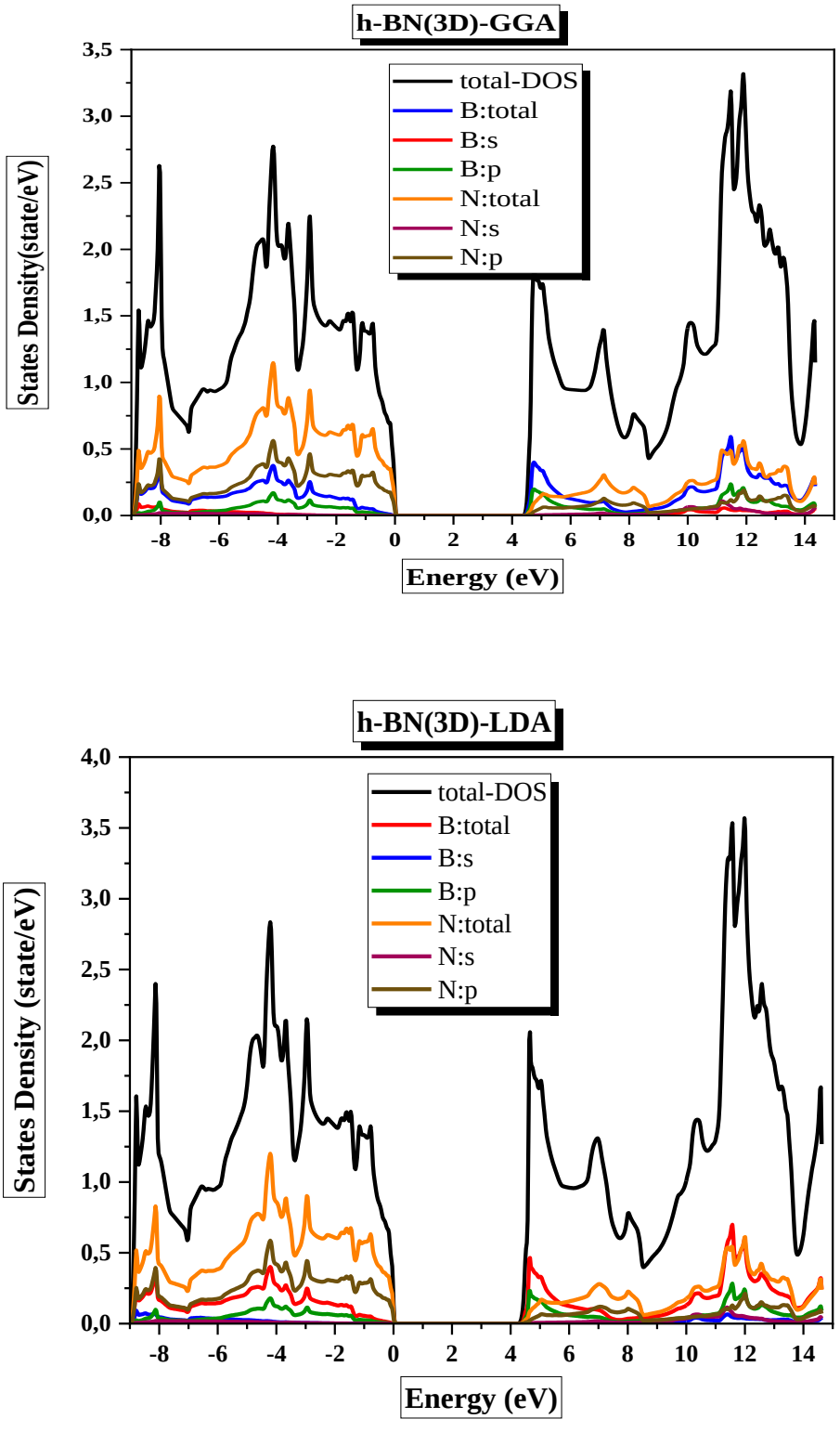

Figure (III.10): The density states of h-BN in (3D) for GGA and LDA.

The Figure (III.10) represent density states of h-BN in 3D calculated by GGA and LDA:

- The energetic zone (-8.8 eV and -6.9 eV) is mainly due to the **p** orbitals of **Nitrogen** and a slight contribution of **Boron s** orbitals.
- The energetic zone (-6 eV until 0 eV) is mainly dominated by **p** orbital of **N** and **p** orbitals of **B**.
- Above the Fermi level (4.68 eV – 8.5 eV) density state is made of a mixture of the orbital **p** of **N** and **p** of **B**.
- From (8.6 eV – 14 eV) there is a mixture of the **p** orbitals from **Boron** and **Nitrogen**, with a low turnout of the **s** orbitals of **Boron** and **Nitrogen**.

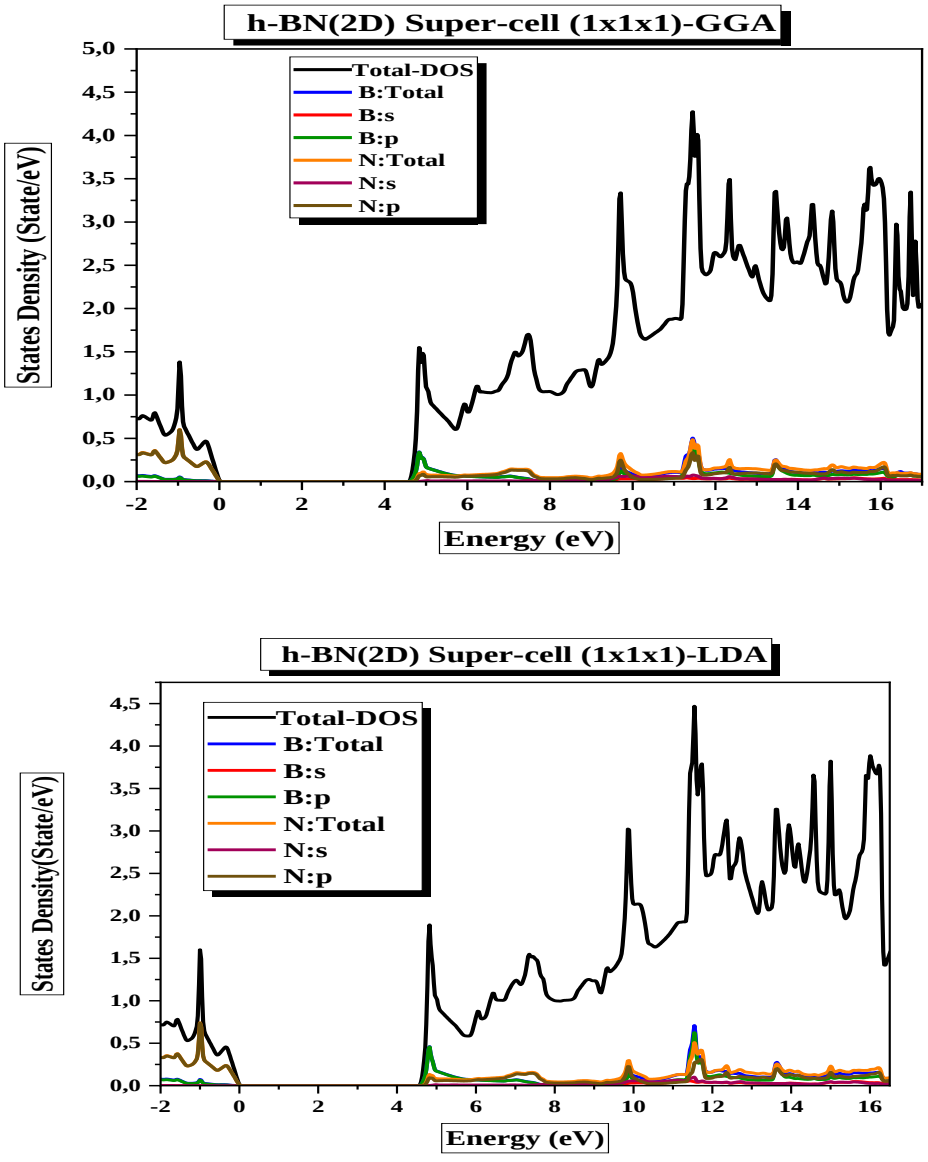

Figure (III.11): The density states of h-BN in (2D) for GGA and LDA.

The Figure (III.11) above define the density state of h-BN in (2D)-Super-cell (1x1x1) calculated by GGA and LDA approximation:

- The first energetic zone from (-2 eV until 0 eV), is completely dominated by the **p** orbitals of **Nitrogen** with a very weak contribution of **p** orbitals of **Boron**.
- Above Fermi level (4.70 eV – 8 eV) the largest contribution is from orbital **p** of **B**, hence the orbital **p** of **N** and a weak contribution of **s** orbital of **N** with total lack of orbital **s** of **B**.
- The energetic zone (8 eV – 17 eV) the orbital **p** of **Nitrogen** contributes a high percentage compared to the **p** orbital of **Boron**, and we note a small equal contribution between the **s** orbitals of **Boron** and **Nitrogen**.

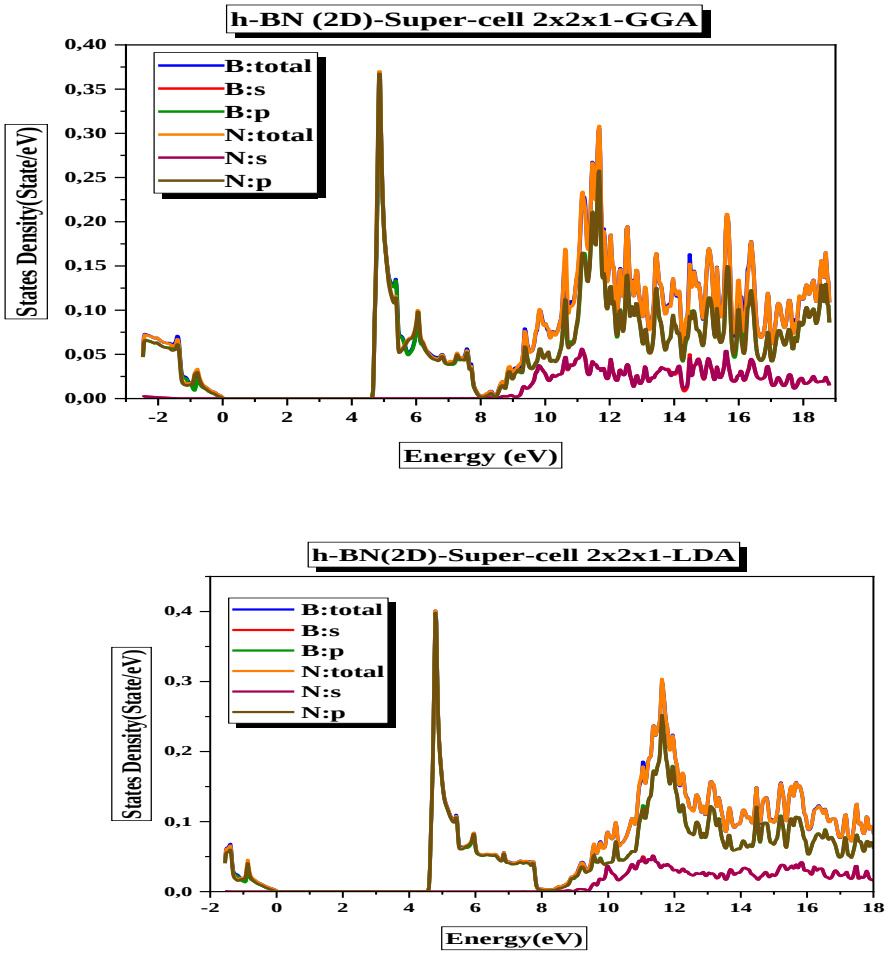

Figure (III.12): The density states of h-BN in (2D) Super-cell 2x2x1 for GGA and LDA.

The Figure (III.12) above define the density state of h-BN in (2D)-Super-cell (2x2x1) calculated by GGA and LDA approximation:

- The first energetic zone from (-2 eV until 0 eV), it can be said that there is an equal contribution for each of the two atoms **N** and **B**.
- Above Fermi level (4.54 eV – 8 eV) the contribution remains equal between orbitals **s** and **p** of **Boron** and **Nitrogen**.
- The energetic zone (8 eV – 18 eV) the orbital **p** of **Nitrogen** and of **Boron** contributes a high percentage compared to the **s** orbital of **both atoms**, and we note a small equal contribution between the **s** orbitals of **Boron** and **Nitrogen.**

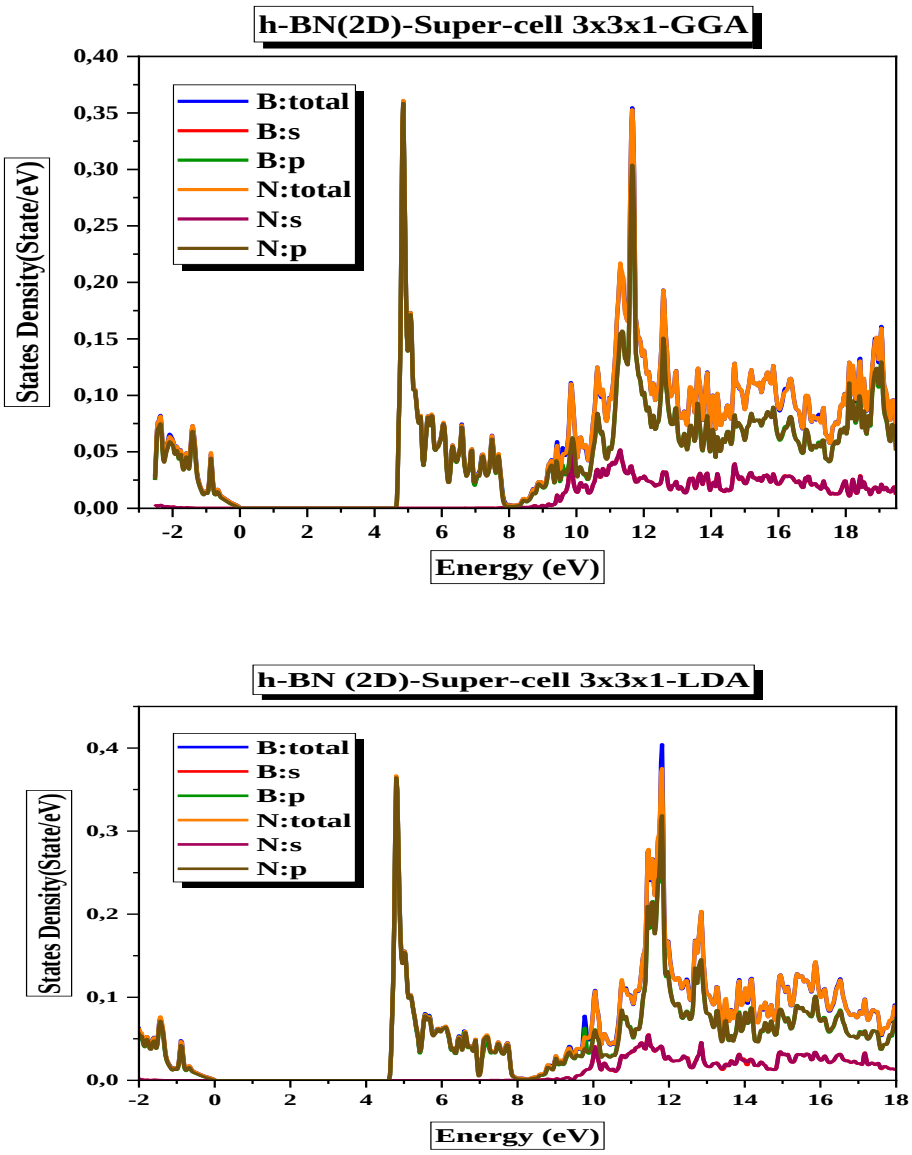

Figure (III.13): The density states of h-BN in (2D) Super-cell 3x3x1 for GGA and LDA.

The Figure (III.13) above define the density state of h-BN in (2D)-Super-cell (3x3x1) calculated by GGA and LDA approximation:

- The first energetic zone from (-2 eV until 0 eV), in this field, the contribution of the **p** orbital of **N** and **B** is predominant, while the **s** orbital of both atoms is almost non-existent.
- Above Fermi level (4.60 eV – 8 eV) the largest contribution is from orbital **p** of **B** and **N**. Also, we note the absence of contribution of orbital **s**.
- The energetic zone (8 eV – 18 eV) the orbital **p** of **Nitrogen** and **Boron** contributes a high percentage compared to the **s** orbital of both of them, and we note a small equal contribution between the **s** orbitals of **Boron** and **Nitrogen**.

B. PART TWO: Comparative study between Boron-Nitride and Gallium-Nitride

In this part we are going to change the atom B by Ga and see if there is a change of properties of materials.

III.7. Structural Properties

Table (III.7): the structural properties of h-BN (3D) and GaN (3D) Murnaghan.

Compound	Parameters	GGA	LDA	Theoretical value	Relative error (%)	
					GGA	LDA
h-BN (3D)	a (Å)	2.50	2.48	2.50	0	-0.008
	c (Å)	7.68	7.74	7.68	0	0.007
	c/a	3.06	3.11	3.06	0	0.016
	β (GPa)	209.8244	218.3702	-	-	-
	β'	3.6010	3.5720	-	-	-
	E_{min}	-317.542097	-316.455241	-	-	-
	V_0	281.8920	276.3942	-	-	-
GaN (3D)	a (Å)	3.21	3.15	3.21	0.187	-1.7
	c (Å)	5.24	5.14	5.24	-0.016	-1.88
	c/a	1.62	1.62	1.63	-	-
	β (GPa)	188.5501	203.8233	-	-	-
	β'	4.5864	4.7670	-	-	-
	E_{min}	-7989.050507	-7983.077148	-	-	-
	V_0	-	-	-	-	-

From the table (III.7) above we pick up the information follows:

1- We note that the lattice parameter **a** of **h-BN** is smaller than lattice parameter of **GaN**.
2- The value of lattice parameter **c** in **h-BN** is big than the **GaN**.
3- The modulus of compressibility β (GGA)= 209.8244 (GPa), β (LDA)= 218.3702 (GPa) in **h-BN** is bigger than the modulus of compressibility β (GGA)= 188.5501 (GPa), β (LDA)= 203.8233 (GPa) in **GaN**.
4- The total energy in **h-BN** is higher than the one in **GaN**.

At the end we conclude that GGA gives results mush closer to the theoretical values than the LDA approximation in 3D structures.

Table (III.8): the structural properties of h-BN (2D) and GaN (2D) Murnaghan.

Compound	Parameters	GGA	LDA	Theoretical value	Relative error (%)	
					GGA	LDA
h-BN (2D)	a (Å)	2.51	2.49	2.50	0.004	-0.004
	c (Å)	19.97	19.86	20.00	-0.002	-0.007
	c/a	7.97	7.97	7.97	0	0
	β (GPa)	40.2837	41.8208	-	-	-
	β'	3.5967	3.5631	-	-	-
	E_{min}	-158.769910	-158.224682	-	-	-
	V_0	732.5699	719.0633	-	-	-
GaN (2D)	a (Å)	6.37	6.31	6.32	0.82	-0.014
	c (Å)	14.72	14.72	14.72	0	0
	c/a	2.31	2.33	2.32	-0.004	0.004
	β (GPa)	31.3991	33.6404	-	-	-
	β'	4.1890	4.6662	-	-	-
	E_{min}	-15977.753753	-15965.771839	-	-	-
	V_0	-	-	-	-	-

From the table (III.8) above:

1- The value of lattice parameter **a** still big in **GaN** than **h-BN**, but we find the opposite in lattice parameter **c** where it is bigger in **h-BN** than **GaN**.
2- The modulus of compressibility β (GGA)= 40.2837 (GPa), β (LDA)= 41.8208 (GPa) in **h-BN** still bigger than the modulus of compressibility β (GGA)= 31.3991 (GPa), β (LDA)=33.6404 (GPa) in **GaN**.
3- The total energy of **GaN** is less than the one of **h-BN**.

By looking to the relative error values, we can conclude that LDA gives better results in 2D structures.

III.8. Electronic Properties

III.8.1- Band Structure

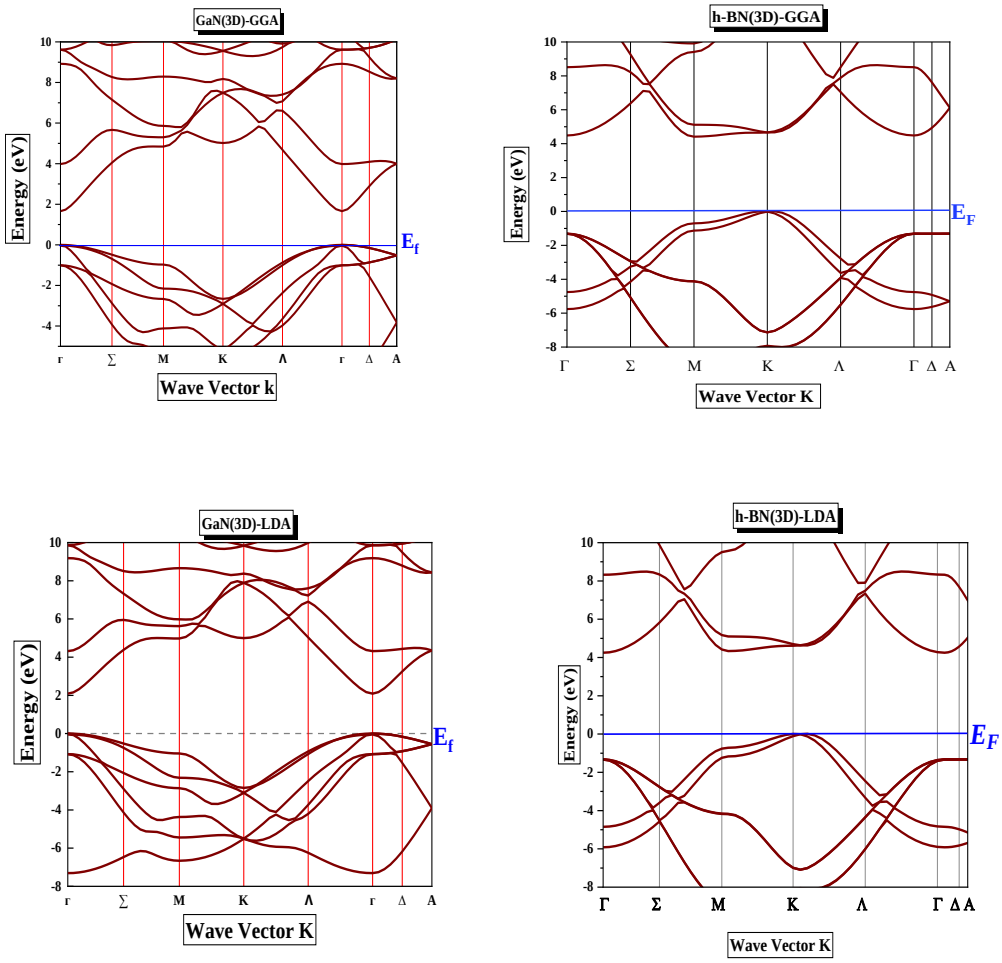

Figure (III.14): Band structure of h-BN and GaN in (3D) in GGA and LDA.

From the figure (III.14) we can see that GaN has a maximum limit in valence band (VBM) and a minimum limit in conduction band (CBM) located at the point **(Γ→Γ)**, it is mean that we have semiconductor with direct gap, in both approximations **GGA** and **LDA**.

And h-BN has a maximum limit in valence band (VBM) and a minimum limit in conduction band (CBM) located at the point **(M→K)** it is mean that we have an insulator with indirect gap, in both approximations **GGA** and **LDA**.

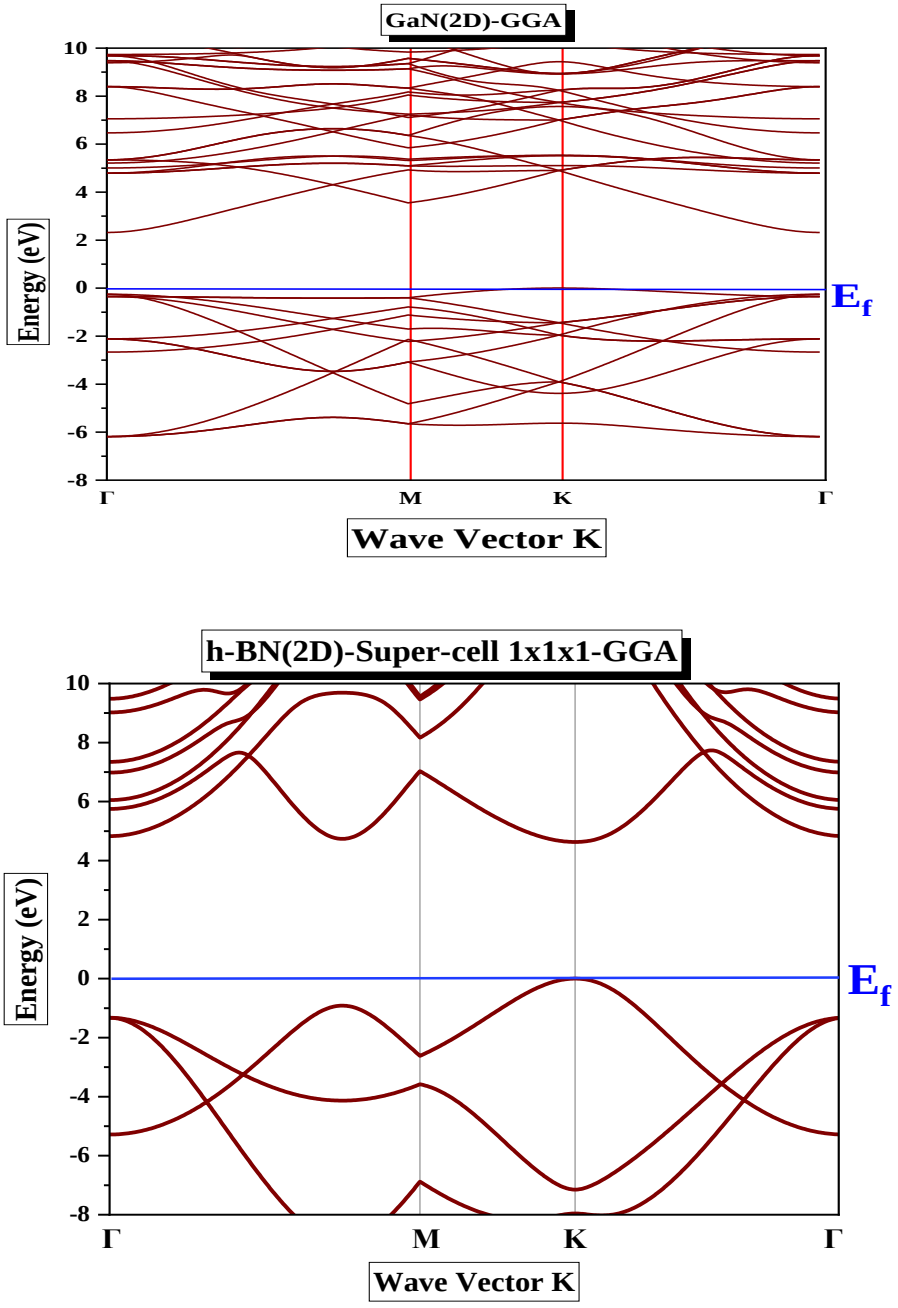

Figure (III.15): (a) Band structure of h-BN and GaN in (2D) in GGA.

From the figure (III.15) (a) we can see that GaN has a maximum limit in point **K** and a minimum limit located at the point **Γ**, **(K→Γ)**, it is mean that we have semiconductor with indirect gap in **GGA**.

As illustrated in the same figure h-BN has a maximum limit in point **K** and a minimum limit in point **K** also **(K→K)**, that is mean we have an insulator with direct gap, in **GGA**.

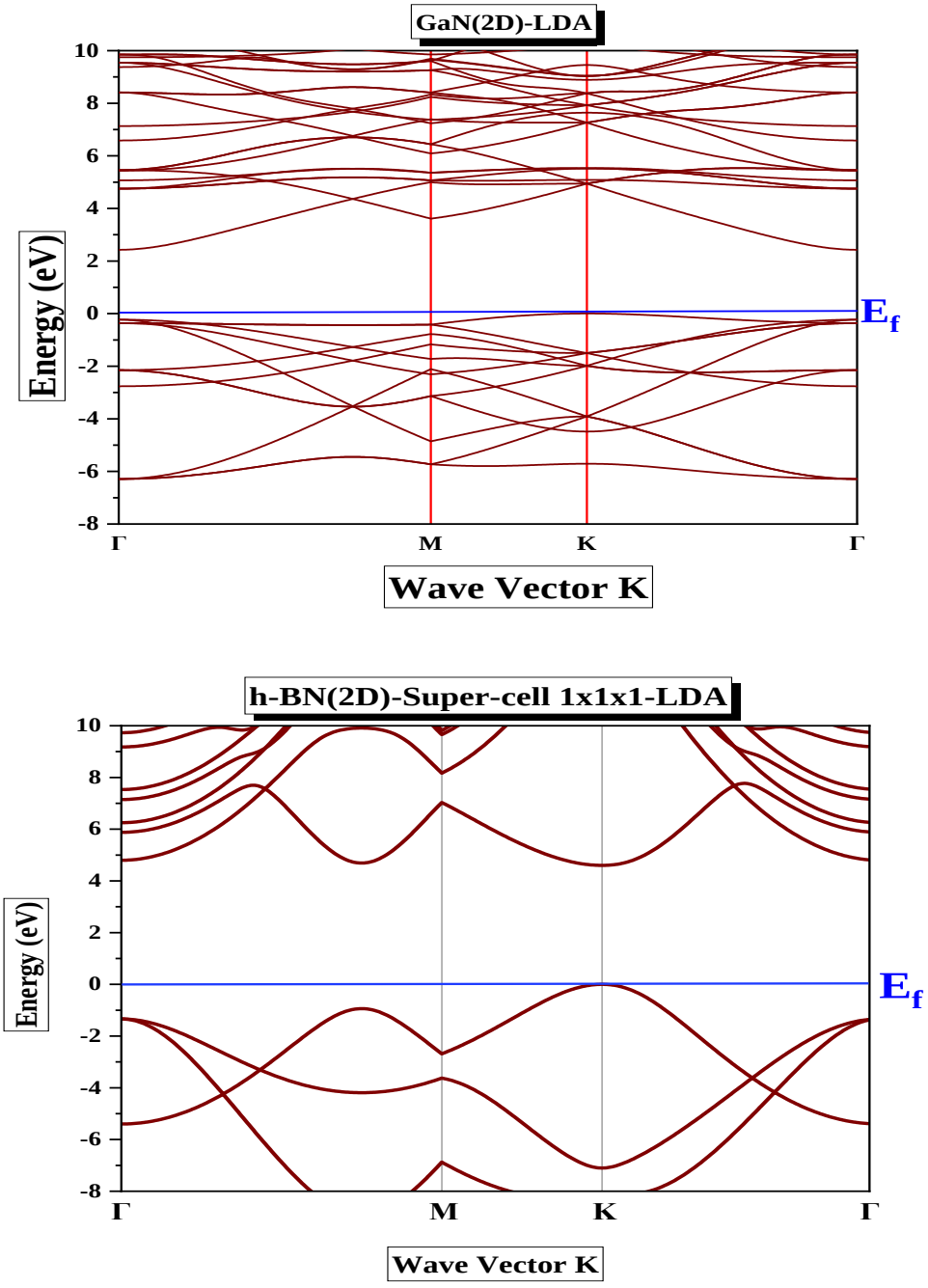

Figure (III.15): (b) Band structure of h-BN and GaN in (2D) in LDA.

From the figure (III.15) (b) we note that GaN has a maximum limit in point **K** and a minimum limit located at the point **Γ**, **(K→Γ)**, it is mean that we have semiconductor with indirect gap, and h-BN has a maximum limit in point **K** and a minimum limit in point **K** also **(K→K)**, that is mean we have an insulator with direct gap, in **LDA**.

Table (III.9): Energy gap values in 3D and 2D dimensions of GaN and h-BN calculated with GGA and LDA.

Compound		E_g (eV)	
		GGA	**LDA**
h-BN	**(3D)**	4.413	4.248
	(2D)	4.632	4.602
GaN	**(3D)**	1.661	2.091
	(2D)	2.397	2.501

From the table (III.9) above we note that GaN in both structures 3D and 2D have a semiconducting nature, and h-BN in 3D and 2D have an insulating nature.

III.8.2- Density State

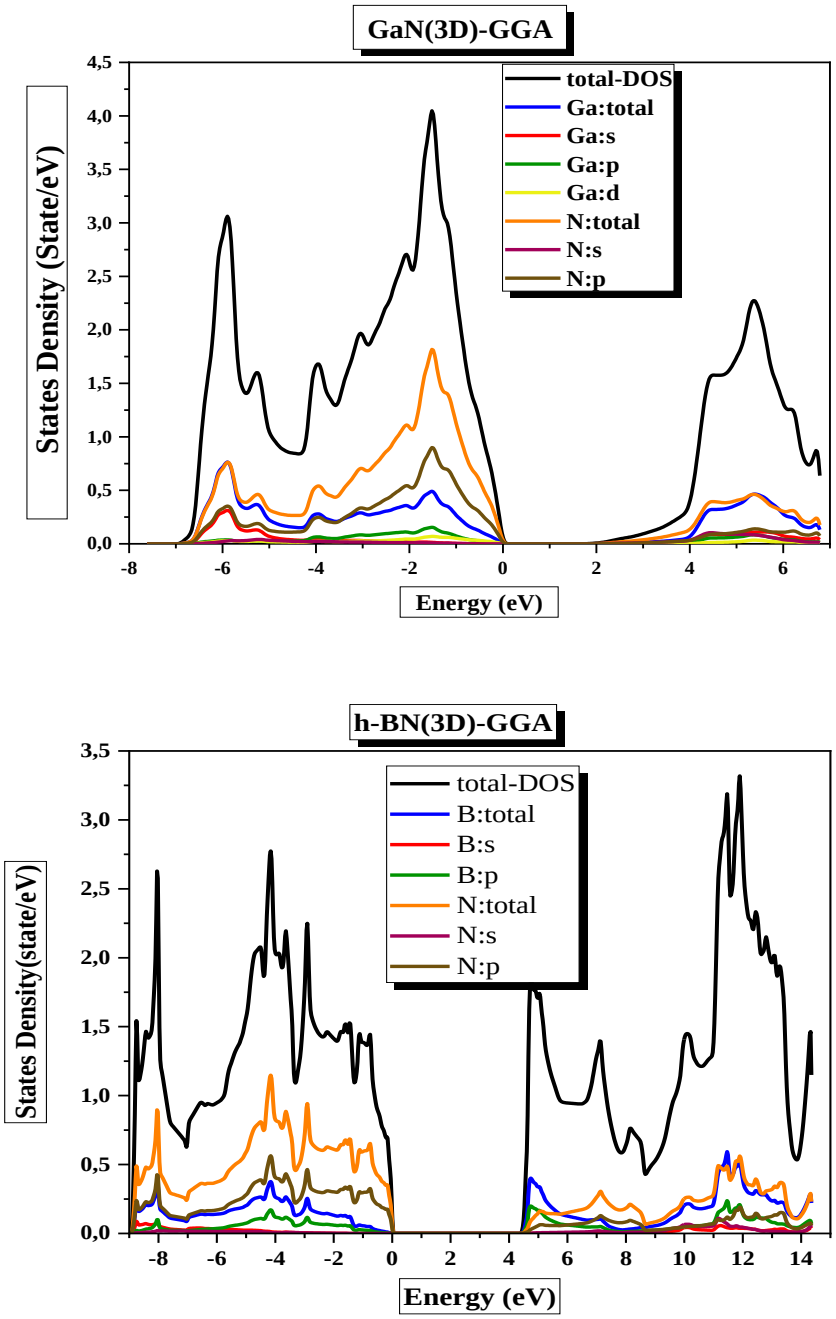

Figure (III.16): (a): The density states of GaN and h-BN in (3D) for GGA.

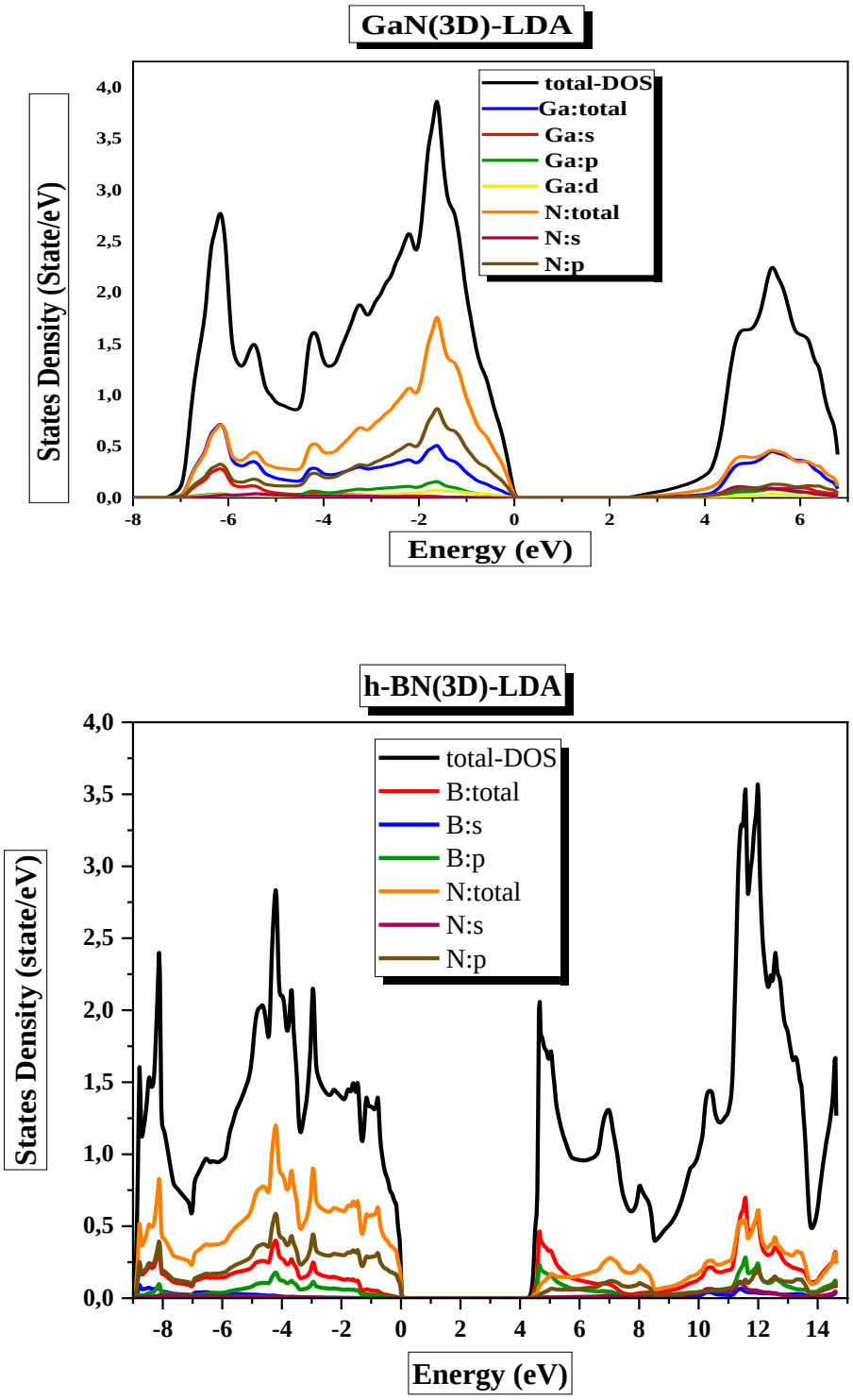

Figure (III.16): (b): The density states of GaN and h-BN in (3D) for LDA.

As depicted in the figure (III.16) (a) and (b):

- The energetic zone (-7 eV to 0 eV) is mainly due to the **p** orbitals of **Nitrogen** and a slight contribution of **Boron s** orbitals in h-BN and in GaN is mainly dominated by the **Nitrogen** p-orbital and the **Gallium** p-orbital.

So, the contribution has changed from orbital **s** in **Boron** to the orbital **p** when we put **Gallium**.

- Above the Fermi level (4 eV until 7 eV) is mainly dominated by **p** orbital of **N** and **p** orbitals of **B** in h-BN, and in **Gallium-Nitride**, is dominated mainly by the N p-orbital and the Ga s-orbital, with a small contribution from the Ga p-orbital.

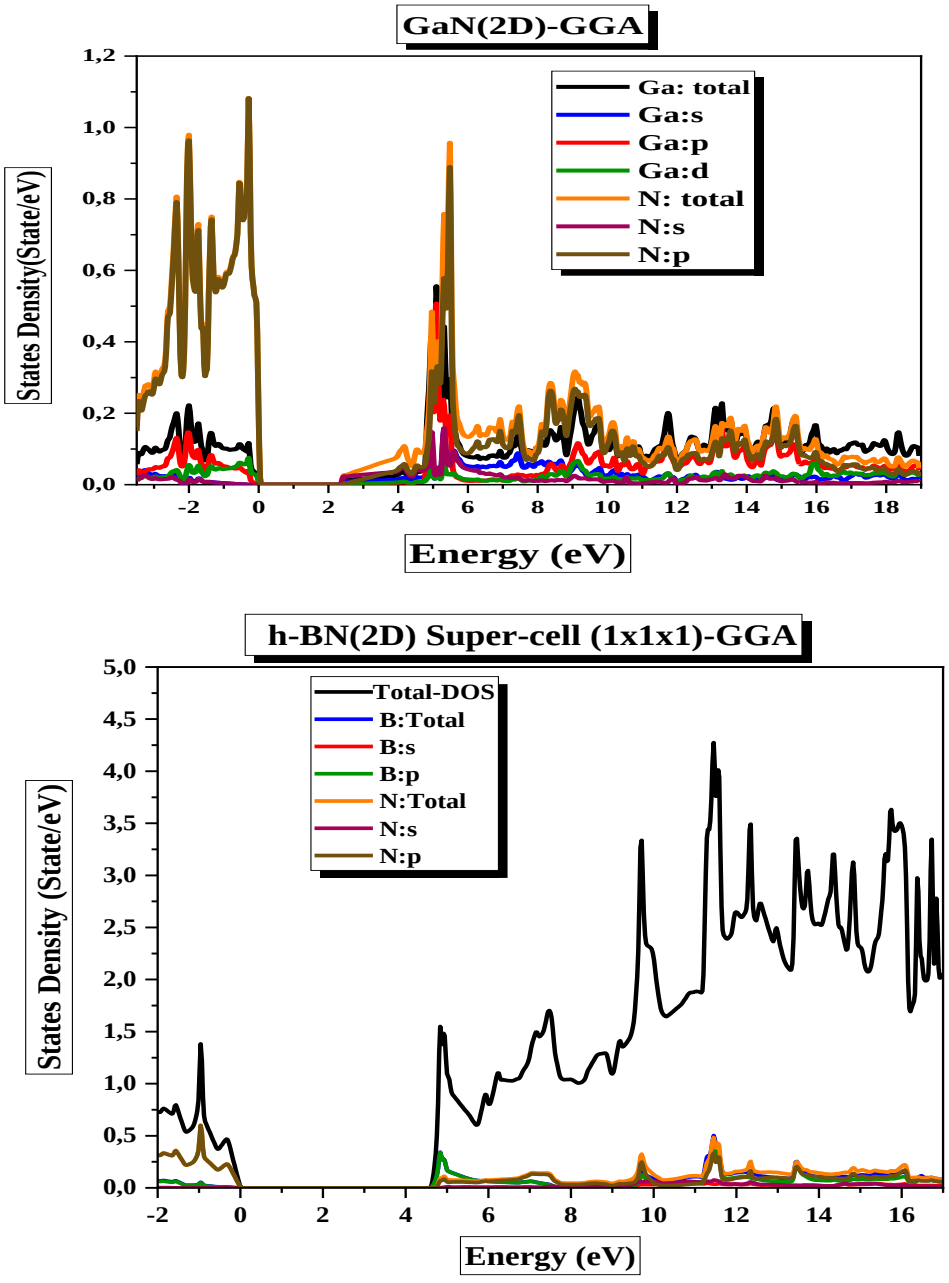

Figure (III.17): (a): The density states of GaN and h-BN in (2D) for GGA.

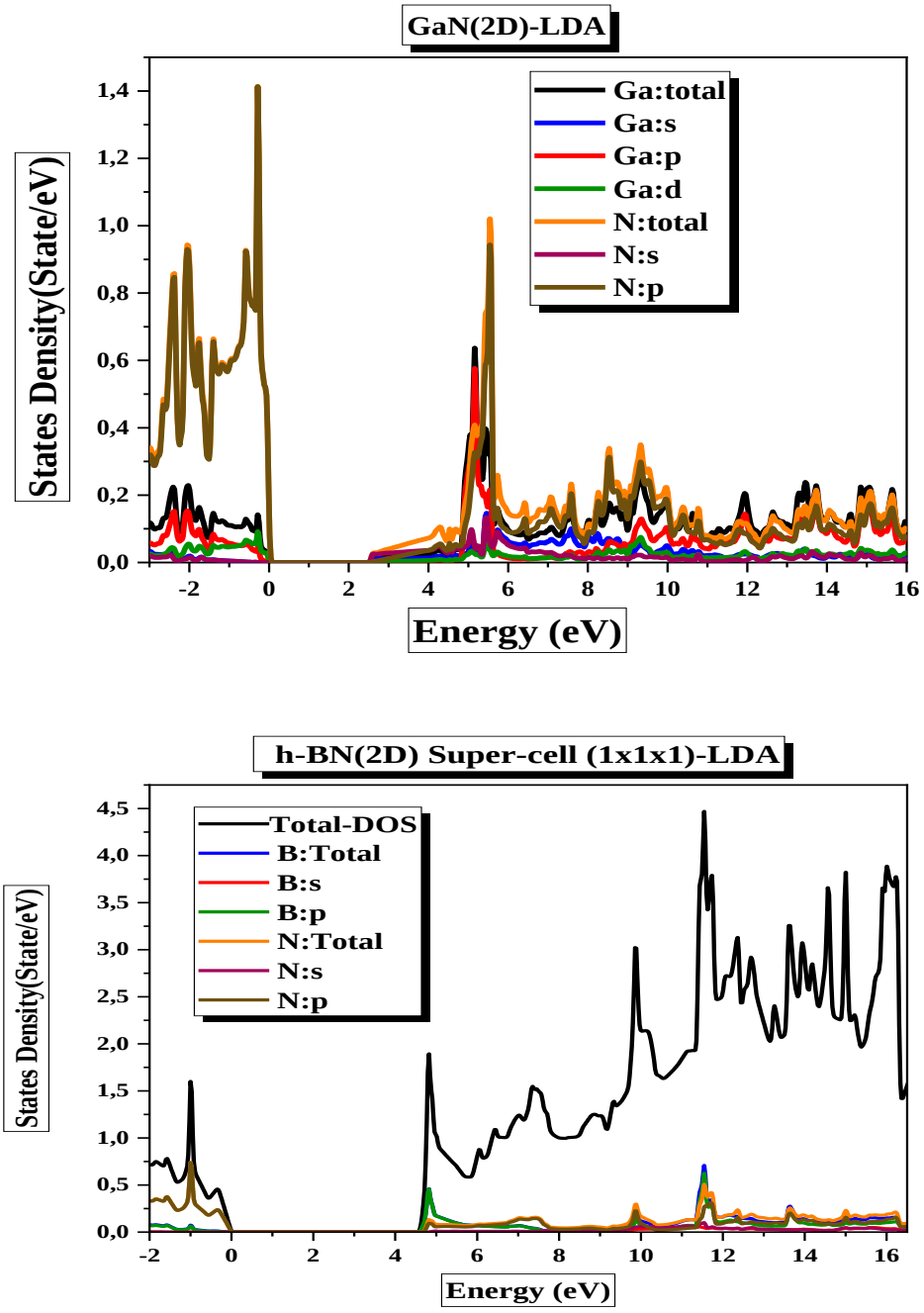

Figure (III.17): (b): The density states of GaN and h-BN in (2D) for LDA.

As clarified in the figure (III.17) (a) and (b):

- The first energetic zone from (-2 eV until 0 eV), is completely dominated by the **p** orbitals of **N** with a very weak contribution of **p** orbitals of **B** in the Boron-Nitride, and in the Gallium-Nitride is mainly controlled by the **p** orbital of **N** and the **p** and **d** orbitals of **Ga**.

- Above Fermi level (4.70 eV – 6 eV) the largest contribution is from orbital **p** of **B**, hence the orbital **p** of **N** and a weak contribution of **s** orbital of **N** with total lack of orbital **s** of **B**, in the other compound GaN, in this interval we can say that it is largely controlled by the p orbital of N, the p orbital of Ga with a small contribution from the d orbital of Ga and the appearance of s orbital of N.
- The next energetic zone (6.8 eV – 8 eV) the contribution in h-BN is still from orbital **p** of **B** and the orbital **p** of **N** and a weak contribution of **s** orbital of **N** with reduction of orbital **s** of **B**. At the same area in GaN, is mainly dominated by the **p** orbital of **N**, and the **s** orbital of **Ga** with a small contribution from **p** of **Ga**.
- The energetic zone (8 eV – 17 eV) the orbital **p** of **Nitrogen** contributes a high percentage compared to the **p** orbital of **Boron**, and we note a small equal contribution between the **s** orbitals of **Boron** and **Nitrogen**. On the other hand, in the material GaN we note that is mainly dominated by the **N p**-orbital and the **Ga p**-orbital, with a small contribution from the **Ga s**-orbital.

References

[1] P. Vajeeston, Theoretical Modeling of Hydrides Theoretical Modeling of Hydrides Department of Physics University of Oslo, (2016).

[2] A. Kissavos, Development and application of Muffin-Tin Orbital based Green's function techniques to systems with magnetic and chemical disorder, 2006.

[3] S. Cottenier, Density Functional Theory and the Family of (L)APW-methods: a step-by-step introduction, 2013.

[4] P. Kratzer, J. Neugebauer, The Basics of Electronic Structure Theory for Periodic Systems., Front. Chem. 7 (2019) 106. https://doi.org/10.3389/fchem.2019.00106.

[5] J. Chen, Z. Xu, Y. Chen, Chapter 1 - Introduction of density functional theory, in: J. Chen, Z. Xu, Y.B.T.-E.S. and S. of S.M. Chen (Eds.), Elsevier, 2020: pp. 1–12. https://doi.org/https://doi.org/10.1016/B978-0-12-817974-1.00001-6.

[6] A. Cheriet, S. Khenchoul, L. Aissani, B. Lagoun, M. Zaabat, A. Alhussein, First-principles calculations to investigate structural, magnetic, electronic and elastic properties of full-Heusler alloys Co2MB (M=V, Mn), Solid State Commun. 337 (2021) 114426. https://doi.org/https://doi.org/10.1016/j.ssc.2021.114426.

[7] K. Schwarz, P. Blaha, DFT Calculations for Real Solids, 2017. https://doi.org/10.1002/9783527691036.hsscvol5022.

[8] R. Peverati, D.G. Truhlar, Exchange − Correlation Functional with Good Accuracy for Both Structural and Energetic Properties while Depending Only on the Density and Its Gradient, (2012).

[9] J. Toulouse, Review of approximations for the exchange-correlation energy in, (2022) 1–65.

[10] J. Wang, F. Ma, M. Sun, Graphene, hexagonal boron nitride, and their heterostructures: properties and applications, RSC Adv. 7 (2017) 16801–16822. https://doi.org/10.1039/c7ra00260b.

[11] D.-H. Kim, H.-S. Kim, M.W. Song, S. Lee, S.Y. Lee, Geometric and electronic structures of monolayer hexagonal boron nitride with multi-vacancy, Nano Converg. 4 (2017) 13. https://doi.org/10.1186/s40580-017-0107-0.

[12] J. Korbmacher, G. Schiemer, What Are Structural Properties?†, Philos. Math. 26 (2018) 295–323. https://doi.org/10.1093/philmat/nkx011.

[13] V.G. Tyuterev, N. Vast, Murnaghan's equation of state for the electronic ground state energy, Comput. Mater. Sci. 38 (2006) 350–353. https://doi.org/10.1016/j.commatsci.2005.08.012.

[14] Z. Cancarevic, Prediction of not-yet-synthesized solids at extreme pressures, and the development of algorithms for local optimization on ab-initio level, (2006). http://elib.uni-stuttgart.de/opus/volltexte/2007/2894/.

[15] L.K. Lamontagne, Band structures and the meaning of the wave vector k, Lect. Notes. 1 (2018) 7–8.

General Conclusion

General Conclusion

The unique structural and electronic properties of hexagonal boron nitride (h-BN) make it a promising material for a variety of industrial applications. It has a hexagonal lattice structure similar to graphene, with boron and nitrogen atoms alternately arranged in a honeycomb pattern. h-BN is distinguished by its high thermal stability, superior chemical inertness, wide bandgap, and exceptional electrical insulating properties.

1-Structural and electronic properties of Boron Nitride:

The hexagonal lattice structure of h-BN confers notable mechanical stability and a planar surface that is conducive to the manufacture of devices. The present study reveals that the characteristics of h-BN undergo a transformation, exhibiting a softening behaviour in two dimensions. This inference is drawn from the observed values of compressibility modulus, which decrease from 209.8244 in three dimensions to 40.2837 in two dimensions.

The three-dimensional structure of h-BN exhibits an indirect band gap as determined by the GGA and LDA approximations. The two-dimensional h-BN compound exhibits a direct gap as determined by the GGA and LDA approximations.

Based on our investigation, it has been determined that h-BN exhibits a substantial bandgap, measuring 4.413 eV in three dimensions and 4.632 eV in two dimensions, thereby rendering it a highly effective insulator. The aforementioned characteristic makes it suitable for deployment in scenarios where electrical isolation holds paramount importance.

2-Comparative study with GaN:

Gallium Nitride (GaN) is a wide-bandgap semiconductor material that is widely utilised in various industries. Although h-BN and GaN exhibit distinctive characteristics, they exhibit notable distinctions with respect to their constitution, crystalline arrangement, and practical uses.

- h-BN is composed of Boron and Nitrogen atoms, whereas GaN is composed of Gallium and Nitrogen atoms.
- h-BN has a hexagonal lattice structure, whereas GaN's crystal structure is either cubic (Wurtzite) or hexagonal (Zinc blende).

- Bandgap: h-BN has a wide bandgap (approximately 4.632 eV), making it an insulator, whereas GaN has a narrower bandgap (approximately 2.397 eV), making it an optoelectronic-compatible semiconductor.
- The GaN compound possesses a direct gap in 3D and an indirect gap in 2D, whereas the h-BN compound has an indirect gap in 3D and a direct gap in 2D.
- The primary applications of h-BN include thermal management, protective coating, high-voltage devices, and dielectric materials. In contrast, Gallium Nitride (GaN) is utilised in various optoelectronic devices such as light-emitting diodes (LEDs) and lasers, high-power electronic devices including transistors and diodes, and wireless communication systems.
- Conductivity: h-BN is an electrical insulator, whereas GaN exhibits both electrical and exceptional thermal conductivity (in doped form).
- So, the distinct properties of h-BN and GaN make them suited for diverse industrial applications. It is optimal for high-temperature environments, protective coatings, and dielectric materials due to h-BN's exceptional thermal stability, chemical inertness, and electrical insulation properties. GaN, with its reduced bandgap and high electrical and thermal conductivity, is an excellent semiconductor material.

Abstract

Due to their distinctive structural and electronic properties, two-dimensional (2D) and three-dimensional (3D) materials, specifically hexagonal boron nitride (h-BN) and gallium nitride (GaN), have garnered significant attention. These materials' diverse properties make them promising candidates for a wide range of applications, including electronics, optoelectronics, and beyond. h-BN and GaN have distinct structural features. h-BN is composed of a hexagonal lattice of alternate boron and nitrogen atoms, producing a 2D honeycomb structure with a large bandgap. In contrast, GaN has a cubic or hexagonal crystal structure with strong covalent bonds between gallium and nitrogen atoms in its 3D bulk form. These structural differences are a factor in their distinct material properties. In terms of its electronic properties, h-BN is an insulator due to its wide bandgap. This property, in conjunction with its exceptional thermal and chemical stability, makes h-BN appropriate for use as a dielectric material, protective coating, or substrate for a variety of electronic devices. In contrast, GaN has a relatively narrow bandgap, making it an outstanding electronic transport semiconductor. This quality enables its application in high-power and high-frequency electronic devices, such as LEDs, lasers, and power amplifiers. In addition, the 2D structure of h-BN imparts additional intriguing electronic properties. h-BN exhibits distinct quantum confinement effects and intense electron-electron interactions, resulting in phenomena such as excitons and plasmons, due to its atomically thin structure. These characteristics make h-BN applicable for quantum optics and nanophotonics applications. In addition, the integration of h-BN and GaN in heterostructures or hybrid material systems allows for the combination of their unique properties. These composite structures allow for the engineering of band alignments, interface states, and electronic transport, paving the way for the creation of novel devices with enhanced functionality and performance. h-BN and GaN, in both their 2D and 3D forms, have remarkable structural and electronic properties. For the design and fabrication of advanced electronic and optoelectronic devices, it is vital to comprehend and exploit these properties. Further exploration and research of these materials holds great potential for propelling technological advancements in a variety of disciplines.

Keywords: Nanomaterials, 2D and 3D materials, h-BN, structural and electronic properties, DFT, FP-LAPW.

ملخص

المواد ثنائية الأبعاد (2D) والثلاثية الأبعاد (3D)، وتحديدًا نتريد البورون السداسي (h-BN) ونتريد الجاليوم (GaN)، قد لفتت انتباهًا كبيرًا بسبب خصائصها الهيكلية والإلكترونية الفريدة. تتميز هذه المواد بخصائص متنوعة تجعلها مرشحات مثالية لتطبيقات مختلفة، تتراوح بين الإلكترونيات والإلكترونيات الضوئية وما بعدها. من الناحية الهيكلية، تتميز h-BN وGaN بخصائص مختلفة. يتكون h-BN من شبكة سداسية مكونة من ذرات البورون والنيتروجين المتناوبة، وتشكل هذه الذرات هيكل العسل ثنائي الأبعاد مع فجوة طيفية كبيرة. بالمقابل، يتبنى GaN هيكل بلوري مكعب أو سداسي في الشكل الثلاثي الأبعاد، مع روابط تساهمية قوية بين ذرات الجاليوم والنيتروجين. تساهم هذه الاختلافات الهيكلية في تباين خصائص المواد. من حيث الخصائص الإلكترونية، يتمتع h-BN بفجوة طيفية واسعة، مما يجعله عازلاً. تجعل هذه الخاصية، بالإضافة الى استقرارها الحراري والكيميائي الممتاز، h-BN مناسبة لتطبيقات كمادة عازلة، وطلاء واقي، أو قاعدة لأجهزة إلكترونية مختلفة.

بالمقابل، يتمتع GaN بفجوة طيفية نسبياً ضيقة، مما يجعله نصف موصل بخصائص نقل إلكتروني ممتازة. تمكن هذه الخاصية استخدامه في أجهزة إلكترونية عالية الطاقة والتردد، مثل الصمامات الثنائية الباعثة للضوء والليزرات ومضخمات الطاقة. وبالإضافة إلى ذلك، فإن طبيعة h-BN ثنائية الأبعاد تدخل خصائص إلكترونية مثيرة للاهتمام. نظرًا لطبيعتها الرقيقة جدًا، تظهر h-BN تأثيرات الحصر الكمي والتفاعلات الإلكترونية القوية الفريدة، مما يؤدي إلى ظواهر مثل الإثارات والبلازمونات. تفتح هذه الخصائص إمكانيات لا حصر لها لـ h-BN في التطبيقات التي تنطوي على البصريات الكمية والنانوفوتونيات. بالإضافة إلى ذلك، فإن دمج h-BN وGaN في هيكل مختلط أو كنظام مواد هجين يوفر فرصًا لدمج خصائصهما المميزة. تمكن هذه الهياكل الهجينة من هندسة توازنات الفجوات، وحالات الواجهة، والنقل الإلكتروني، مما يوفر طرقًا لتطوير أجهزة جديدة ذات أداء ووظائف محسنة. وفي الختام، فإن h-BN وGaN، سواء في أشكالهما ثنائية وثلاثية الأبعاد، يتمتعان بخصائص هيكلية وإلكترونية مذهلة. فهم واستغلال هذه الخصائص أمر حاسم لتصميم وتصنيع الأجهزة الإلكترونية والإلكترونيات الضوئية المتقدمة. وتحمل استكشاف وبحث هذه المواد الكثير من الوعود لدفع التطورات في مجالات التكنولوجيا المختلفة.

كلمات مفتاحية : المواد النانوية ، المواد ثنائية وثلاثية الأبعاد ، نتريد البورون السداسي (h-BN) ، الخصائص الهيكلية والخصائص الإلكترونية ، FP-LAPW، DFT.

Résumé

En raison de leurs propriétés structurales et électroniques distinctives, les matériaux bidimensionnels (2D) et tridimensionnels (3D), en particulier le nitrure de bore hexagonal (h-BN) et le nitrure de gallium (GaN), ont fait l'objet d'une attention particulière. Les diverses propriétés de ces matériaux en font des candidats prometteurs pour un large éventail d'applications, y compris l'électronique, l'optoélectronique et au-delà. Le h-BN et le GaN ont des caractéristiques structurales distinctes. Le h-BN est composé d'un réseau hexagonal d'atomes de bore et d'azote alternés, produisant une structure 2D en nid d'abeille avec une large bande interdite. En revanche, le GaN a une

structure cristalline cubique ou hexagonale avec de fortes liaisons covalentes entre les atomes de gallium et d'azote dans sa forme 3D en masse. Ces différences structurales sont à l'origine de leurs propriétés matérielles distinctes. En termes de propriétés électroniques, le h-BN est un isolant en raison de sa large bande interdite. Cette propriété, associée à son exceptionnelle stabilité thermique et chimique, fait du h-BN un matériau diélectrique approprié, un revêtement protecteur ou un substrat pour toute une série de dispositifs électroniques. En revanche, le GaN a une bande interdite relativement étroite, ce qui en fait un excellent semi-conducteur de transport électronique. Cette qualité lui permet d'être utilisé dans des dispositifs électroniques à haute puissance et à haute fréquence, tels que les DEL, les lasers et les amplificateurs de puissance. En outre, la structure 2D du h-BN lui confère d'autres propriétés électroniques intéressantes. Le h-BN présente des effets de confinement quantique distincts et des interactions électron-électron intenses, qui donnent lieu à des phénomènes tels que les excitons et les plasmons, en raison de sa structure atomiquement fine. Ces caractéristiques rendent le h-BN applicable à l'optique quantique et aux applications nanophotoniques. En outre, l'intégration du h-BN et du GaN dans des hétérostructures ou des systèmes de matériaux hybrides permet de combiner leurs propriétés uniques. Ces structures composites permettent l'ingénierie des alignements de bandes, des états d'interface et du transport électronique, ouvrant ainsi la voie à la création de nouveaux dispositifs dotés de fonctionnalités et de performances améliorées. Le h-BN et le GaN, sous leurs formes 2D et 3D, présentent des propriétés structurales et électroniques remarquables. Pour la conception et la fabrication de dispositifs électroniques et optoélectroniques avancés, il est essentiel de comprendre et d'exploiter ces propriétés. La poursuite de l'exploration et de la recherche sur ces matériaux offre un grand potentiel pour propulser les avancées technologiques dans une variété de disciplines.

Mots clés : Nanomatériaux, matériaux 2D et 3D, h-BN, propriétés structurales et électroniques, DFT, FP-LAPW.